Stony Brook University

The Interconnected Network of ESCRT and Non-ESCRT Cellular Proteins Required for Retroviral Release

A Dissertation Presented

by

Gisselle Nilda Medina

To

The Graduate School

in Partial Fulfillment of the

Requirements

for the Degree of

Doctor of Philosophy

in

Molecular Genetics and Microbiology

Stony Brook University

August 2008

Stony Brook University

The Graduate School

Gisselle Nilda Medina

We, the dissertation committee for the above candidate for the

Doctor of Philosophy degree,

Hereby recommend acceptance of this dissertation

Dr. Carol A. Carter, Professor, Molecular Genetics and Microbiology

Dr. Patrick Hearing, Professor, Molecular Genetics and Microbiology

Dr. James Bliska, Professor, Molecular Genetics and Microbiology

Dr. Suzanne Scarlata, Professor, Physiology and Biophysics, Stony Brook

This dissertation is accepted by the Graduate School

Lawrence Martin

Dean of the Graduate School

Abstract of the Dissertation

The interconnected network of cellular proteins ESCRT and non-ESCRT required for retroviral release

By

Gisselle Nilda Medina

Doctor in Philosophy

in

Molecular Genetics and Microbiology

Stony Brook University

2008

The structural polyprotein, Gag, drives the assembly and release of retroviruses from the plasma membrane of cells and its expression alone is sufficient for the formation of virus-like particles (VLPs). Trafficking and membrane targeting of Gag requires a series of events that are directed by the interaction between cellular proteins and regions in Gag known as L domains, however the precise mechanism is not well understood. The functionally exchangeable L domains in the Gag protein of the human retrovirus, HIV-1, and the related avian retrovirus, ASV, bind Tsg101 and Nedd4, respectively. Tsg101 and Nedd4 function in endocytic sorting and trafficking of cargo proteins typically destined for degradation. In the first part of my thesis, I determined if the cellular factors were functionally exchangeable as a means of determining whether HIV and ASV use the same trafficking pathway. The results obtained by using dominant negative forms of Tsg101, Nedd4, and Vps4, an ATPase that regulates their availability, suggest that HIV-1 and ASV use different pathways, even though they both utilize the endocytic machinery. In particular, covalently linking Tsg101 to an ASV Gag L domain mutant ablated the

requirement for Nedd4 for Gag release, but budding occurred through a different membrane region.

The second part of my thesis examines the involvement of non-endocytic factors such as Sprouty2, in the release of HIV-1 Gag. Spry2 modulates ESCRT-mediated trafficking pathways of EGFR and requires binding to phosphatidylinositol 4,5-biphosphate [$PI(4,5)P_2$] to exert its function. In this study, I found that depletion of endogenous Spry2 inhibited VLP production as did expression of a C-terminal fragment of the Spry2 protein, specifically by sequestering Gag into intracellular vesicles. Furthermore, a Spry2 mutant lacking the only conserved sequences in the N-terminal domain relieved the inhibitory effects. Interestingly, a mutant of Spry2 that had no detectable effect on WT Gag release promoted release of a Gag mutant lacking a functional Tsg101 binding site. Examination of cells by confocal microscopy revealed that wild type-Spry2 co-localized with $PI(4,5)P_2$ in complexes that were resistant to cold Triton X-100 extraction. In contrast, the Spry2 variant failed to co-localized with $PI(4,5)P_2$.

Dedication Page

This Dissertation is dedicated to my mother Gladys.

Con aguja e hilo

cosió nuestros caminos,

y aunque con mucho frío

nunca olvidó abrigarnos

para darnos calor y abrigo.

Con bordados y encajes,

decoró nuestras vidas,

y con patrones consisos,

guió los diseñ̃os de su perfecta confección.

Gracias Mamá

Table of Contents

List of Figures

List of Abbreviations

AAA	ATPases associated with diverse cellular activities
AIDS	acquired immunodeficiency syndrome
AIP1	ALG-2 (apoptosis linked gene 2) interacting protein 1
AP-2	adaptor protein 2
ASV	avian sarcoma virus
BLV	bovine leukemia virus
CA	capsid
CHMP	charged multivesicular body proteins
CypA	cyclophilin A
DNA	deoxyribonucleic acid
Eap	ELL associated proteins
EGFR	epidermal growth factor receptor
EIAV	equine infectious anemia virus
ESCRT	endosomal sorting complex required for transport
GLUE	Gram-like, ubiquitin binding on Eap45
HECT	homologous to E6-AP C-terminus
HIV-1	human immunodeficiency virus type 1
Hrs	hepatocyte growth factor regulated substrate
HTLV	human T cell leukemia virus
IN	integrase
LDI-1	late domain interacting protein 1
MA	matrix
MAPK	mitogen activated protein kinase
MHR	major homology region
MLV	murine leukemia virus
MVB	multivesicular body
NC	nucleocapsid
Nedd4	neuronal precursor cell expressed developmentally downregulated 4
$PI(4,5)P_2$	phosphatidyl inositol (4,5) bisphosphate
PI3P	phosphatidylinositol 3-phosphate
PR	protease
RNA	ribonucleic acid
RSV	rous sarcoma virus
RT	reverse transcriptase
RTK	receptor tyrosine kinase
Tsg101	tumor susceptibility gene 101
UEV	ubiquitin E2 variant
UIM	ubiquitin interactive motif
VLP	virus like particles
Vps	vacuolar protein sorting
WT	wild type

Acknowledgements

Many people have helped me in the course of this research. I would like to thank my advisor, Dr. Carol Carter, for the great academic support she has given me while working on this project and has given me the confidence to welcome the challenges that research offers. I am also very grateful to each member of my thesis committee, Dr. Patrick Hearing, Dr. James Bliska and Dr. Suzanne Scarlata for their help and suggestions.

I am very grateful to all members of the Carter Lab for their help, advice, assistance, and for being an extended family during the time we shared here at Stony Brook University. In special I would like to thank to Dr. Lorna Ehrlich who has given great advices not only about science but also about life in general.

I would like to thank my family, for their constant encouragement, love and support throughout my time in graduate school. Especially, I would like to thank my Mother for being such a good friend and for providing me with example that everything is possible when we put our minds into it.

I also would like to thank the Department of Molecular Genetics and Microbiology which has provided a great atmosphere to work at, make good friends and exchange ideas. I would like to thank every person in this department for making it such a wonderful place to be at.

CHAPTER 1: Introduction

Retroviruses

Retroviruses belong to the viral family *Retroviridae* that are characterized by sharing a common virion structure, replicative strategy and genetic composition (23). The genome of these viruses is linear, single stranded, and of positive polarity. Retroviruses maintain their genetic information in the form of ribonucleic acid (RNA) and through the use of the viral RNA-directed DNA polymerase (reverse transcriptase, RT) are capable of producing deoxyribonucleic acid (DNA) from RNA. Subsequently, with the viral enzyme integrase (IN), their genomes can be integrated into the host chromosome establishing a latent infection. Retroviral infection does not lead to death of the host cell. The cell can survive the infection, continue to divide and become permanently virus producing. This clever strategy makes this group of viruses one of the most fascinating pathogens to study, and learn not only their strategies to successfully establish latent infection, but also to understand the mysterious cellular processes that accompany a viral infection.

One of the most intensively studied retrovirus is the human immunodeficiency virus (HIV), the causative agent of AIDS (Acquired Immunodeficiency Syndrome) responsible for the current pandemic. HIV is divided into two major subtypes, HIV-1 and HIV-2. HIV-1 is the virus that was originally discovered and it is more virulent, relatively easily transmitted, and the cause of the majority of HIV infections globally. In contrast, HIV-2 is less transmittable than HIV-1 (113). The work in this thesis, when referring to the human retrovirus, is referring to the subtype HIV-1. HIV-1 is divided into

different groups M (major), O (outlier) and N (new). Among HIV-1 group M strains, there are nine genetic subtypes (A-D, F-H, J and K), six subtypes (A1, A2, A3 and A4 and F1 and F2), thirty-seven circulating recombinant forms and a variety of unique recombinant forms (86). This viral diversity is contributed by three factors: i) the viral replication rate, which in vivo is very rapid, generating an estimated 10^{10} virions per day in an infected individual (52); ii) the RT that copies viral RNA into DNA, which is error-prone, introducing on average one substitution per genome per replication round; and, iii) recombination which is due to the fact that two RNA molecules are packaged into the virion alternately, generating a mosaic DNA genome. The crossover frequency ranges from seven to thirty per replication round. The diversity of HIV-1 genetic forms makes this virus the most genetically variable of human pathogens and therefore poses a difficult challenge for prevention and treatment programs.

All retroviruses encode three major proteins: *gag*, which codes for the internal structural proteins of the virion; *pol*, which encodes the enzymatic functions of the virus; and *env*, which codes for the virion envelope glycoproteins (128). However, more complex retroviruses can contain accessory genes. HIV, which belongs to the lentiviruses genus, encodes six additional genes *vif, vpr, nef, tat, rev* and *vpu.* These accessory genes regulate and coordinate viral gene expression, and some also have additional roles.

Retrovirus life cycle

A simple diagram of a retrovirus life cycle is depicted in Figure 1. The initial step in retrovirus infection is the binding of the viral envelope glycoproteins, g120 and gp41, to specific cellular receptors on the surface of the cell. HIV-1 can recognize macrophages

or T cells bearing the CD4 receptor and a co-receptor CCR5 (macrophages) or CXCR4 (T cells). The binding of the viral glycoprotein (gp120) to a CD4 receptor exposes a variable region in the viral protein that allows the interaction with the co-receptor, triggering conformational changes of gp120 and gp41 that ultimately lead to the fusion of the viral and host membranes. The entry of HIV-1 into the cell takes place through plasma membrane regions enriched in lipid rafts because gp120 only binds to receptors that are found in lipid rafts (107). After fusion of the viral envelope with the membrane of the host cell, the viral core is released into the cytosol where it disassembles. Core disassembly is characterized by dissociation of capsid protein which forms the core shell and release of the reverse transcription complex into the cytosol. Subsequently, the viral RNA is converted into double stranded linear DNA by the viral reverse transcriptase. In the case of HIV-1, this process is initiated in the cytoplasm and completed in the nucleus. Upon completion of reverse transcription, the complex becomes integration-competent and is termed the preintegration complex (PIC). The PIC protects viral DNA from degradation and facilitates its integration into the host cell chromosome (89). Following nuclear import, the linear DNA becomes integrated into the host cell chromosome through the action of the viral integrase enzyme. Viral transcripts are then transported from the nucleus to the cytoplasm where they are translated or packaged. The viral Gag polyprotein ensures proper assembly and release through the plasma membrane. Depending on the cell type, virus assembly takes place at the plasma membrane or in endosomal vesicles. Virus particles are budded as immature particles containing a spherical shell of structural proteins underneath a host-derived membrane. Immature

Figure 1. HIV-1 life cycle. **A**) The initial step involves the interaction between a virion and a host cell, which is mediated by the viral glycoprotein gp120/gp41, the cellular receptor CD4, and a cellular co-receptor (CCR5or CXCR4 on macrophages or T cells, respectively). **B**) A conformational change in the glycoproteins occurs and triggers virus-cell membrane fusion, releasing the core into the cytoplasm. **C**) Reverse transcription is initiated in the cytoplasm within the core structure. **D**) Nuclear import of the viral genome in the PIC allows the integration of viral DNA into the host chromosome. **E**) Viral transcripts are then transported from the nucleus to the cytoplasm where they are translated or packaged. **F**) The cytoplasmically translated Gag and Gag-Pol polyproteins are then localized to the cell membrane as are the Env proteins which are translated at the endoplasmic reticulum and transported to the plasma membrane through the secretory pathway. **G**) Assembly of Gag and Gag-Pol polyproteins occurs at the plasma membrane to form an immature virion which begins to bud from the plasma membrane. **H**) As budding occurs, the virion undergoes maturation forming the infectious particle.

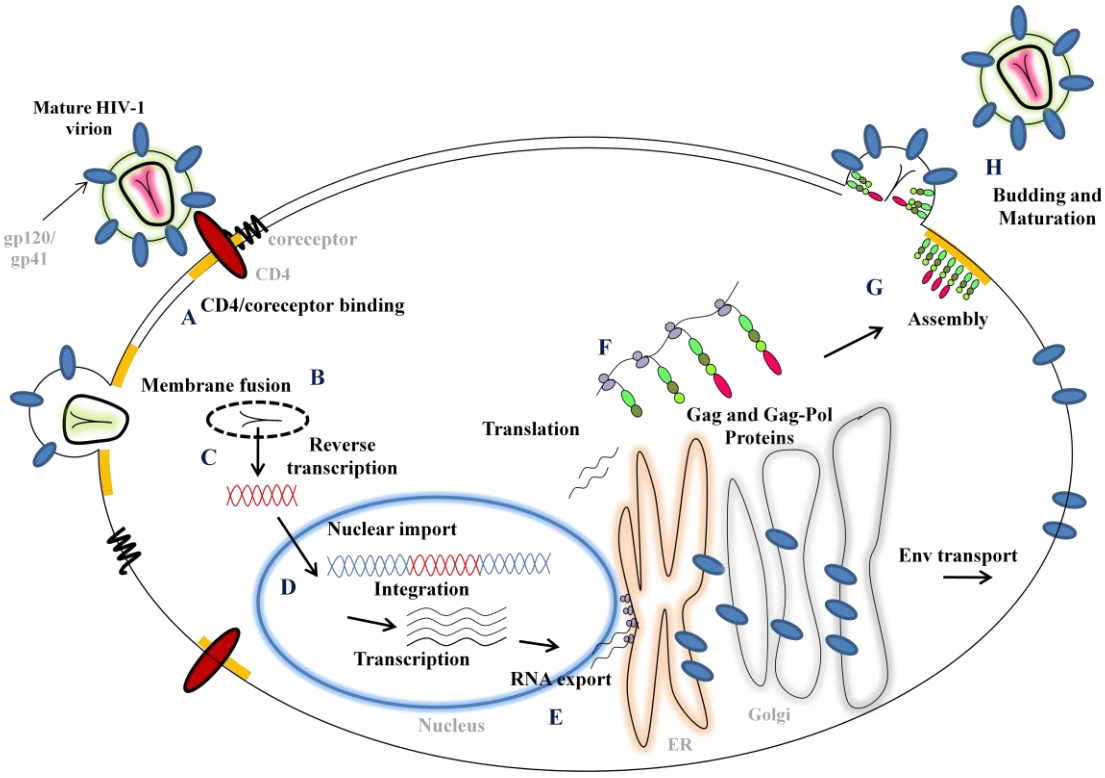
Mature HIV-1
virion
gp120/
gp41
coreceptor
CD4
A
CD4/coreceptor binding
Membrane fusion
B
C
Reverse
transcription
Nuclear import
D
Integration
Transcription
RNA export
Nucleus
E
Translation
F
Gag and Gag-Pol
Proteins
G
Assembly
H
Budding and
Maturation
Env transport
ER
Golgi

particles lack the central cone-like core that characterizes the mature particle. Immature virions subsequently undergo a maturation step which involves rearrangement of the structural proteins, condensation to form an inner core, and conversion of the virus particle into an infectious virion.

Gag Protein

A successful viral infection is ultimately marked by the assembly and release of progeny virus particles. This complex process is driven by the multidomain Gag protein (Figure 2). Gag expression alone is sufficient for the assembly and release of non-infectious, virus like particles [VLPs (122)]. Gag is synthesized as a polyprotein precursor on free ribosomes in the cytoplasm. Typically, for every 10-20 Gag molecules made, one molecule of a Gag-Pol fusion protein is synthesized. This is due to an infrequent frame-shifting event occurring just upstream of termination codons in the *gag* gene that results the ribosomes to shift from the gag reading frame into the pol reading frame (56). Interaction (I) domains in Gag permit the Gag and Gag-Pol molecules to remain associated (35). This permits the same mechanism that targets the Gag precursor to the site of virion assembly also to direct the Gag-Pol precursor. A large number of Gag molecules are needed to form the virion structure; however, the enzymes encoded in the *pol* gene, protease (PR), reverse transcriptase (RT), and integrase (IN), are needed in smaller numbers since they carry out catalytic functions.

Gag Domains

Figure 2. Schematic diagram of the proteins encoded in the gag and pol genes of HIV-1 and ASV retroviruses. All Gag proteins have in common MA, CA, and NC sequences and other cleavage products. In the case of **A**) HIV-1, on the N-terminus is a myristate group, which along with a stretch of basic residues located in MA, forms a bipartite motif that facilitates membrane binding. Note the absence of a myristate group in ASV-Gag **B**); in this case, membrane binding is facilitated through the ionic interactions alone. In the CA region, a Major Homology Region is conserved in both retroviruses. The spacer peptides, p1, p2 (HIV), and p10 (ASV) aid in the processing of Gag but their precise function is not known. The NC region binds to and packages the viral genome through two conserved zinc finger domains. Late (L) domains located in p6 (HIV) or p2b (ASV) regions are involved in the late stages of budding. These domains contain specific sequences that allow the interaction with cellular proteins. This schematic is not to scale and does not represent the actual sizes of Gag and Pol.

A. HIV-1

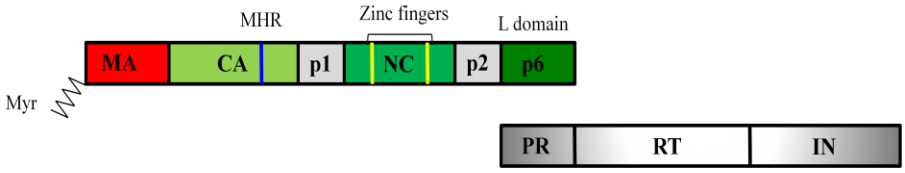
MHR
Zinc fingers
L domain
MA
CA
p1
NC
p2
p6
Myr
PR
RT
IN

B. ASV


MA
p10
CA
NC
PR
p2a
p2b
L domain
RT
IN

During or shortly after virus budding from the host cell, the viral protease (PR) cleaves Gag into mature Gag proteins matrix (MA), capsid (CA), nucleocapsid (NC), and p6. PR-mediated Gag processing leads to virus maturation by inducing a major transformation in virion structure which can be morphologically detected in the electron microscope. The MA remains associated with the plasma membrane but CA condenses and forms a shell around the viral RNA/NC complex. The cleavage of Gag also generates spacer peptides but their precise function remains to be elucidated.

The different regions in Gag that have been identified orchestrate the major steps in virus assembly and release. The MA domain is responsible for targeting Gag to the plasma membrane. In the case of HIV-1 Gag, this association is typically through a bipartite motif consisting of an N-terminal, covalently attached myristic acid moiety added co-translationally and a highly basic domain in MA. The interaction of this domain with the plasma membrane is proposed to be mediated by a myristyl switch (118, 147) which consists of the myristate adopting either an exposed or a sequestered conformation (1). Recent findings indicate that the MA domain of HIV-1 Gag specifically binds to plasma membrane phospholipids, in particular PI(4,5)P2 (20, 101, 116) and this binding is proposed to trigger the myristic acid moiety to be exposed, providing the stable association with the plasma membrane. In the case of other retroviruses that do not have a myristoylated MA domain, such as the avian sarcoma virus (ASV), membrane binding is mediated exclusively by ionic interactions (25).

The CA domain of Gag plays an important role in the assembly of the virus and in early postentry steps during viral replication. The CA domain forms the “core” in the mature virion, and this is what is released into the cytoplasm of a newly infected cell to

start a new cycle of viral replication (35, 118). The mature CA protein provides structural stability to the virion by encapsidating the viral RNA-protein complex. In the case of HIV-1, the N-terminus of the CA protein functions in virion maturation and incorporation of the cellular protein cyclophilin A (CypA). The C-terminus of CA forms a dimerization domain that contributes to Gag-Gag interactions. In this region there is a conserved sequence among different genera of retroviruses known as the major homology region [MHR (139)]. This region is essential for CA structure and mutations within it result in defects in assembly, maturation and infectivity (28, 79, 110). The CA domain is also a target of cellular factors that regulate retroviral infectivity. For instance, the CA domain of HIV-1 directly interacts with CypA, a cellular protein that is incorporated into the virion through interactions with a proline-rich region in the N-terminal region of the CA domain (11, 34, 77, 129). CypA is a cytosolic protein that catalyzes the *cis-trans* isomerization of proline residues and has been shown to enhance viral infectivity (34). The specific role of CypA in HIV-1 remains unknown, however recent findings suggest that CypA modulates retroviral restriction activity (76).

Directly downstream of the CA domain is the NC domain or I domain, a highly basic region whose role is to promote Gag-Gag multimerization, RNA binding and encapsidation (12, 22, 35, 118, 137). Other aspects of the virus life cycle that are influenced by the NC domain include genomic RNA dimerization, membrane binding, reverse transcription and annealing (35). Mutations in the NC basic residues cause defects in Gag-viral RNA interaction and thus in assembly and budding (12, 22, 137). The NC domain contains two zinc finger motifs that are highly conserved among retroviruses and are required for RNA binding (118). RNA binding facilitates

localization and concentration of Gag monomers to promote Gag assembly. Recent studies showed that mutations in the NC zinc fingers have an effect in Gag trafficking, resulting in a strong intracellular Gag retention and a decrease in virus production (32, 38).

L domains

The determinant of virus release in retroviral Gags is encoded by a sequence motif called the Late (L) domain which functions late in assembly and stimulate the release of virus particles from the plasma membrane (8). Three classes of motifs have been defined in viral L domains (Figure 3); these bear the core sequence: Pro-Thr/Ser-Ala-Pro [P (T/S) AP], Pro-Pro-X-Tyr (PPXY), or Tyr-Pro-X-Leu (YPXL). The first evidence that suggested the presence of a region in Gag that was necessary for virus release arose from the observation that truncation of the p6 domain at the C-terminus of HIV-1 Gag inhibited virus production at a late stage in the assembly and release process (37). This phenotype was characterized by the accumulation of tethered virions at the plasma membrane as observed by electron microscopy. Subsequent studies that analyzed HIV-1 p6 revealed that a highly conserved region with the consensus sequence P(T/S)AP was responsible for the budding and release activity of p6 (53, 142). In the case of ASV Gag, a mutational analysis of this protein revealed that the small peptide p2b, located between the MA and p10 as shown in Figure 2, plays an important role in virus particle production (140). Later studies suggested the presence of PPXY motifs in other retroviruses such as Mason–Pfizer monkey virus [M-PMV(144)], murine leukemia virus

Figure 3. Viral Late budding or "L" domains. Examples of L-domain motifs from diverse retroviruses are shown. A single or double recognizable motif is present within a short linear sequence. HIV-1 contains a PTAP and the auxiliary LYPXL motif late domains while ASV encodes a PPPY sequence as its late domain. Similar motifs in the Gag proteins encoded by HTLV, MLV and EIAV retroviruses are shown.

HIV-1	PE**PTAP**PEE…..YPLASLYPXXLFG
ASV	TASA**PPPY**RID
HTLV	DPQIP**PPPY**VE**PTAP**QV
MLV	LLTED**PPPY**RID
EIAV	TPQTQL**YPDL**SEIK

[MLV(146)], human T-cell leukemia virus [HTLV-1(10, 49, 67, 135)], and bovine leukemia virus [BLV(136)] that facilitated virus budding. These findings led to new investigations, examining the role of these motifs in the structural proteins of other simple enveloped viruses. Different studies concluded that PTAP and/or PPXY motifs participate in the budding of filoviruses (47), rhabdoviruses (24, 48) and arena viruses (105). Different L domain motifs, YPXL and YP(LXX)n, was identified for the retrovirus equine infectious anemia virus [(EIAV; Figure 3) (18, 104, 111)]. A related sequence is found in HIV-1 p6 region and, in certain contexts, this motif can provide some L domain activity to HIV-1 (81, 125).

L Domains and Cellular Proteins

A series of observations by different groups suggested that L domains display positional independence and functional exchangeability (24, 69, 104, 142, 145) and led to the idea that L domains were sites of interactions with cellular factors. The PTAP, PPXY and YXXL motifs were found to interact with different proteins that participate in the sorting of cellular cargo in the endosome.

Endosomes are responsible for separating proteins that will be recycled from those that will be degraded in lysosomes (Figure 4). Cellular proteins that are not recycled back to the trans-Golgi network or the plasma membrane are delivered to late endosomes and lysosomes (39). Proteins destined for degradation are incorporated into intralumenal vesicles that bud from the limiting membrane inwards, away from the

Figure 4. Illustration of the endocytic sorting pathway. Signaling receptors (e.g., EGFR) that need to be downregulated are internalized and then ubiquitinated by an E3 ubiquitin ligase protein such as Nedd4. Monoubiquitination signals the endocytosis of the cellular receptor and the ubiquitin moiety is recognized by a series of cellular proteins that are part of the ESCRT complex (e.g., Tsg101). Deubiquitination events in combination with the disassembly of ESCRT complexes from the endosomal membrane causes the formation of intralumenal vesicles, *i.e*., biogenesis of the MVB. The MVB fuses with the lysosome where degradation of cellular cargo occurs. Degradation may also occur in proteasomes. Those receptors that are not ubiquitin-targeted for degradation will recycle back to the plasma membrane.

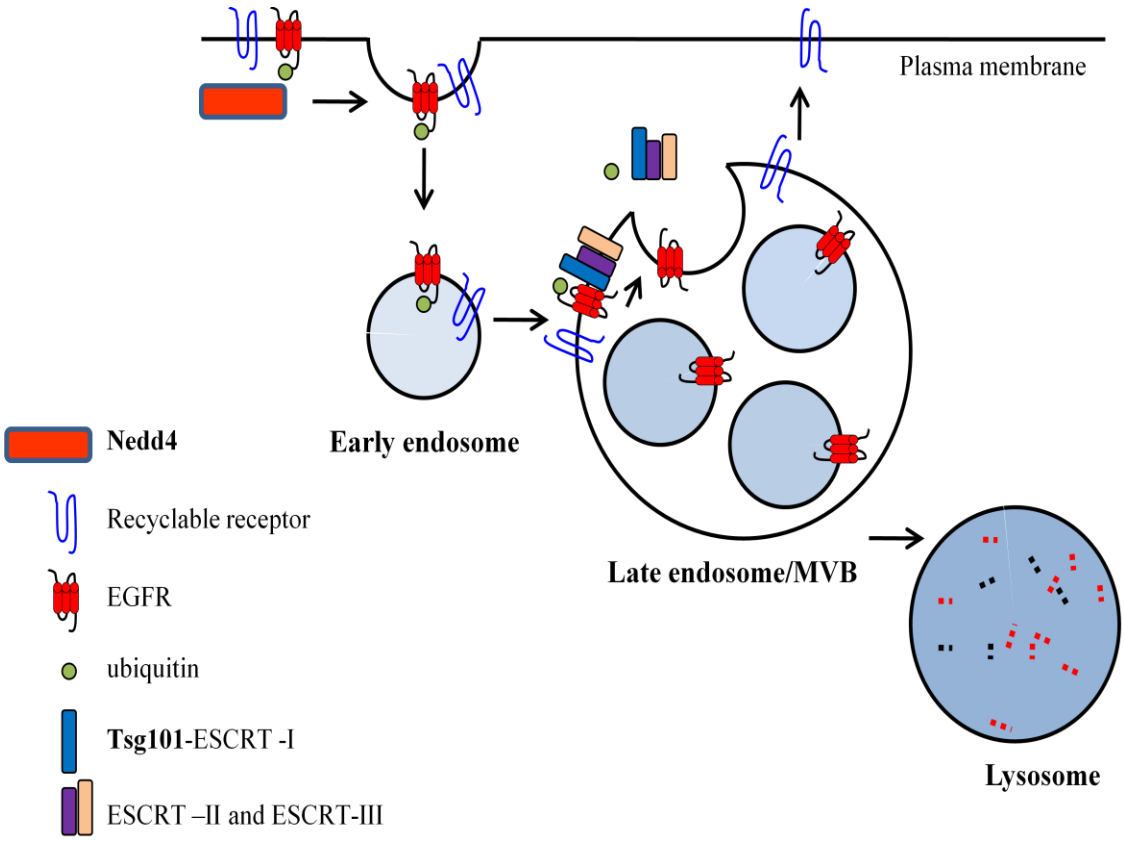
Plasma membrane
Early endosome
Late endosome/MVB
Lysosome
Nedd4
Recyclable receptor
EGFR
ubiquitin
Tsg101-ESCRT -I
ESCRT –II and ESCRT-III

cytoplasm, forming multivesicular bodies (MVBs). Fusion of MVBs with lysosomes initiates the degradation of the intralumenal vesicles and their contents. Targeting of protein cargo into this degradative pathway is highly regulated and depends on posttranslational modification by ubiquitin. Specifically, monoubiquitination serves as a signal for entry of proteins into the MVB pathway. Both MVB vesicle formation and sorting of ubiquitinated cargo depends on the *e*ndosomal *s*orting *c*omplex *r*equired for *t*ransport (ESCRT) which is a group of conserved proteins that are recruited to the endosome. In a similar way, retroviral Gag proteins mimic host cell proteins that normally recruit ESCRT complexes and divert these complexes to sites of viral particle assembly to enable the topologically equivalent budding of cellular and nascent virion membranes away from the cytoplasm, leading to release of viral particles into the extracellular environment. In this section I will describe in detail the interaction of the retroviral L domains of HIV-1 (PTAP) and ASV (PPXY)-Gag and their interaction with cellular proteins that participate in the sorting of cellular cargo mediated by the ESCRT machinery.

The PTAP L domain was shown to bind the cellular protein Tsg101. Specifically, our lab established that Tsg101 interacted with the p6 region of HIV-1 Gag both *in vitro* and in the cytoplasm of transfected cells by doing yeast two hybrid analysis and co-immunoprecipitation, respectively (133). Furthermore, another group established that depleting the endogenous levels of Tsg101 by siRNA markedly impaired HIV-1 virus production (26, 36). Tsg101 is a protein involved in the recognition and sorting of cellular endosomal cargo as illustrated in Figure 4 (5, 58) and is a component of the ESCRT-I complex. Tsg101 was originally identified in a random RNA knockout screen

for tumor suppressor genes (70). Its expression is tightly regulated and therefore overexpression leads to transformation (71) and can contribute in the progression of breast cancer (100). This protein has also been implicated in genome stability, mitotic spindle formation (143), gene transcription, regulation of ubiquitination events (71, 127) and recently in cytokinesis (15, 92) . However, in the context of virus budding, Tsg101 is important because it participates in the sorting of endocytic cargo and specifically in the process of intralumenal vesicle formation at an endosomal compartment which, as noted above, shares similarities with the process of virus budding. As shown in Figure 5, Tsg101 is a multidomain protein composed of an N-terminal ubiquitin E2 variant (UEV) domain (residues 1-145) which displays significant sequence similarity to E2 ubiquitin conjugases but is unable to catalize ubiquitin transfer as it lacks the active site cysteine (63, 109). This domain not only binds to ubiquitin or ubiquitinated proteins (58) but also binds the HIV-1 PTAP L domain (36, 133). In addition, Tsg101 has a proline rich region (residues ~146-215), a predicted coiled-coil region (residues ~240-311), and a predicted helical C-terminal domain that is highly conserved (residues ~330-390). These regions are responsible for interacting with other components of the ESCRT-1 complex and also provide an autoregulatory mechanism that controls its stability (31, 87).

L domains characterized by the PPPY motif have been shown to interact with the Neuronal precursor cell-expressed developmentally downregulated 4 (Nedd4) family of cellular E3 ubiquitin ligases. Specifically, Nedd4 binds to the p2b region of the RSV Gag protein and is required for release of the virus-like particles (VLPs) assembled by Gag (60, 132). Like Tsg101, Nedd4 is also implicated in endocytic processes. Nedd4 ubiquitinates several plasma membrane proteins and provides the major signal for sorting

Figure 5. Schematic illustrations of Tsg101 and Nedd4 showing the putative domain structures and binding partners. **A**. Schematic illustration of Tsg101 showing the amino acid numbering scheme and approximate interaction sites of known binding partners. At its N-terminus the UEV domain contains sequences that can bind to ubiquitin and PTAP motifs such as the motif in HIV-1 Gag. It also contains a Pro (proline rich) region; CC (coiled-coil) region; SB (steadiness box) region. Vps28, a member of ESCRT-1 binds in the SB region. Vps37, another member of ESCRT-1, bind to Tsg101 through the CC region. **B.** Schematic diagram showing the structural organization of a mammalian Nedd4 E3 ubiquitin ligase family member. The C2 domain translocates the protein to the membrane upon calcium binding. Family members contain two to four WW domains that are known to bind substrate proteins containing PY motifs. ASV Gag contains a PY motif in its L domain. The catalytic cysteine within the HECT domain is responsible for ubiquitin ligation.

A. Tsg101

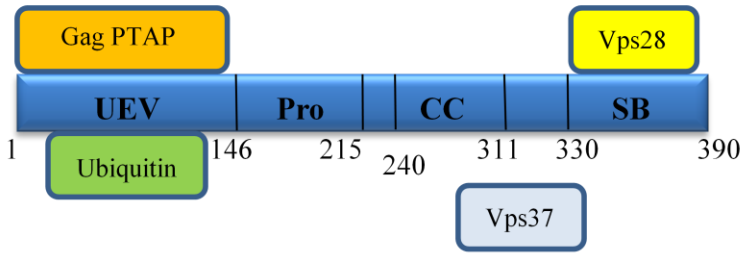

B. Nedd4

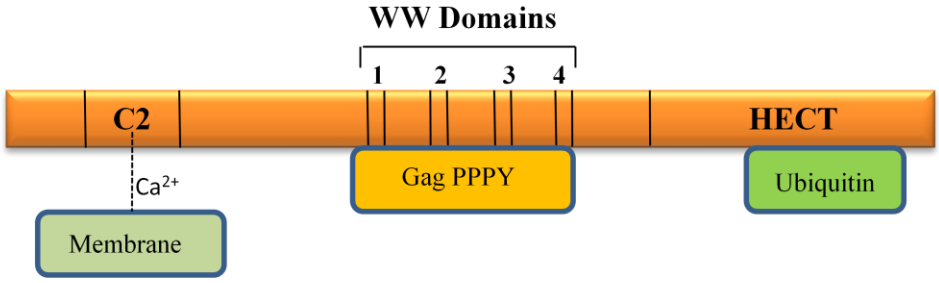

proteins into MVBs (57, 80). Nedd4 and Nedd4-related proteins are conserved from yeast to mammals and are defined by a similar domain organization (Figure 5B). All contain a C2 domain at the N-terminus; are known to interact with a variety of phospholipids and proteins (93); and are thought to function in protein localization and trafficking. The two to four WW domains present in the middle of the protein are modules consisting of approximately 35 amino acids and named for the presence of two conserved tryptophan residues spaced 20-22 amino acids apart that mediate substrate recognition [reviewed in (78, 126)], primarily by recognizing PPXY motifs. The HECT domain at the C-terminus of the protein provides the catalytic function for the ubiquitination of target proteins. Briefly, the mechanism involves the initial binding of an ubiquitin-conjugated E2 enzyme to the HECT domain with subsequent thiol-ester exchange to transfer the ubiquitin moiety from the E2 to the catalytic cysteine in the E3. Transfer of ubiquitin then occurs to either a target protein, or to another ubiquitin molecule, to form a polyubiquitin chain. In both situations, the ubiquitin is transferred from the E3 catalytic cysteine to a lysine side-chain ε-amino group forming an isopeptide bond (106, 119).

In the case of the YXXL motif, it has been shown that the cellular proteins AP-2 and AIP-1/ALIX can be recruited to sites of EIAV Gag viral budding (111, 125) by a direct interaction with the L domain in the p9 region of Gag. Similarly, a YP(LXX)n motif found downstream of the PTAP sequence in HIV-1 Gag can also recruit AIP-1/ALIX but does not act in the same manner as the motif in EIAV Gag since the interactions of ALIX with p6 (HIV) or p9 (EIAV) are regulated by context-dependent factors (66). Nevertheless, ALIX also participates in endosomal sorting and protein

trafficking by interacting with Tsg101 and other components of the ESCRT machinery. Clearly, all the L domain binding proteins, Tsg101, ALIX and Nedd4, have extensive interaction with other components of the MVB sorting machinery and thus provide a way to recruit all the factors that make the "budding machinery" necessary for efficient viral egress.

The ESCRT cellular machinery

Four ESCRT complexes have been described and are thought to function sequentially in trafficking of cellular cargo, at least in yeast. (54, 64) The ESCRT-0 complex contains the proteins hepatocyte growth factor-regulated substrate (Hrs) and signal-transducing adaptor molecule (STAM). ESCRT-0 binds directly to the endosome by interacting with the lipid phosphatidylinositol 3-phosphate (PI3P) and recruits the ESCRT-I (59, 75, 90). The ESCRT-I is composed of four subunits, Tsg101, Vps28 and Vps37 and the recently identified Mvb12 (91, 99), in both yeast and humans. The Vps28 subunit of ESCRT–I recruits ESCRT-II(64). The ESCRT–II forms the bridge between ubiquitinated cargo, the endosomal membrane, and the ESCRT–I and –III complexes (4). It is composed of Eap30, Eap45, and Eap20. Eap45 contains a pleckstrin homology (PH) domain variant called a "GLUE" domain, which binds to phosphoinosites and ubiquitin (51, 123). ESCRT-II binds proteins that compose ESCRT-III complex. The ESCRT-III is composed of several homologous, highly charged subunits that contain charged and predicted coiled-coil regions (3). Four subunits, CHMP2A-B, CHMP6, CHMP3 and CHMP4, form a large and tightly membrane-bound assemblage. ESCRT-III binds the

Figure 6. Schematic showing the functions of endosomal sorting complex required for transport (ESCRT) and ESCRT-related proteins in endosomal sorting of ubiquitinated membrane proteins (cargo). Ubiquitinated cargo is recognized by ESCRT-0 complex by binding of the ubiquitin-interactive motif (UIM) in Hrs. This protein is anchored to the endosomal surface by an interaction between the FYVE motif in Hrs and PI(3)P in the endosomal membrane. Cargo is then transferred to the ESCRT-I complex, which is recruited via Tsg101's UEV domain. ESCRT-II is recruited by the Vps28-Eap45 interaction; ESCRT-III is recruited to the endosomal membrane by its interaction with lipids. In the final steps of sorting, ubiquitins are removed from cargo by the deubiquitinating enzyme (DUB) AMSH, and the ESCRT complexes are dissociated by the ATPase activity of Vps4.

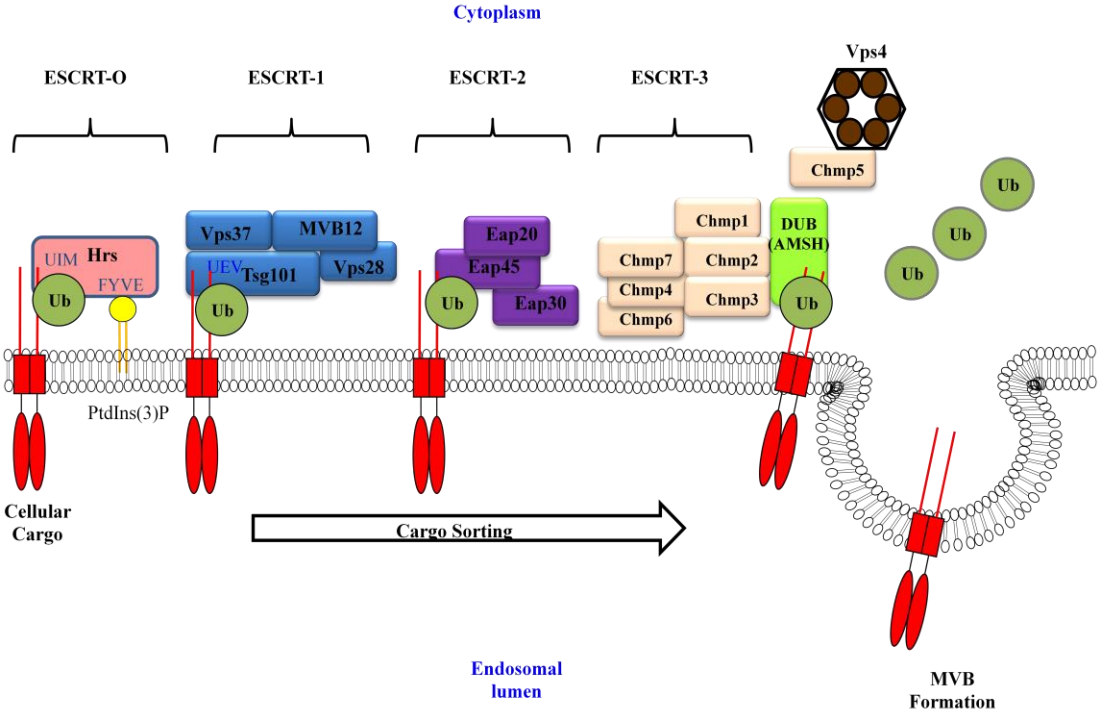
Cytoplasm
ESCRT-O
ESCRT-1
ESCRT-2
ESCRT-3
Vps4
Chmp5
Ub
Ub
Ub
Chmp1
DUB
(AMSH)
Chmp7
Chmp2
Chmp4
Chmp3
Chmp6
Ub
Vps37
MVB12
Eap20
Eap45
UEV
Tsg101
Vps28
Ub
Ub
Eap30
UIM
Hrs
FYVE
Ub
PtdIns(3)P
Cellular
Cargo
Cargo Sorting
Endosomal
lumen
MVB
Formation

ATPase Vps4 to finally induce the deformation of the membrane, drive the invagination and fission of intralumenal vesicles into MVBs, and facilitate disassembly of the ESCRT complexes on the MVB limiting membrane (6, 7). Interestingly, ALIX bridges Tsg101 of ESCRT-1 with CHMP4B of ESCRT-III. As HIV Gag can bind both Tsg101 and ALIX, it does not require ESCRT-II function (65). Based on biochemical analysis of the ESCRT complexes in yeast, a model for the function of the ESCRT proteins in this pathways has been proposed [reviewed in (54)] and described in Figure 6.

Sprouty2, a regulator of ESCRT-mediated EGFR trafficking

The ESCRT cellular machinery is targeted by regulatory proteins that have a negative impact in the process of cellular cargo degradation. The best example for this kind of regulation is mediated by proteins that belong to the Sprouty (Spry) family. The Spry family of proteins are a highly conserved group of negative modulators that have been shown to participate in the downregulation of receptor tyrosine kinases (RTKs) by targeting the endocytic machinery (61, 62).

The founding member of the family, *Drosophila* Spry (dSpry), was initially described as an antagonist of Breathless, the insect equivalent of the fibroblast growth factor receptor (FGFR) which mediates branching of the *Drosophila* trachea (41). Four orthologs of dSpry have been identified in mammals (Spry1-4). Of these, Spry2 exhibits the highest level of homology to the ancestral gene and a great amount of studies have linked Spry2 to the modulation of epidermal growth factor receptor (EGFR) signaling and trafficking (115). Other RTKs that have been shown to be modulated by Spry2

Figure 7. Schematic of the four mammalian Sprouty proteins. The conserved carboxyl-terminal cysteine rich region, responsible for membrane targeting to $PI(4,5)P_2$ is shown in yellow; black bars indicate putative SH3-binding sequence (PxxP). Y indicates the conserved tyrosine residue locate in the amino terminal end. This residue undergoes phosphorylation in response to receptor tyrosine kinase stimulation

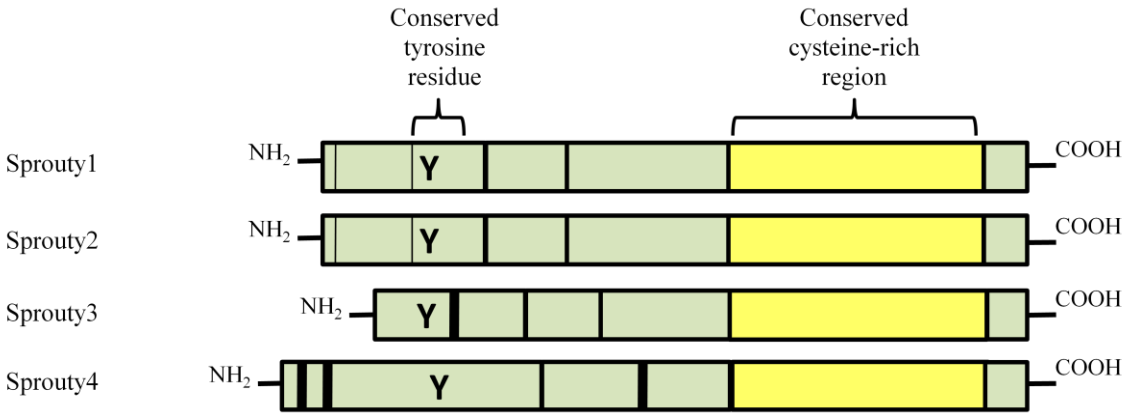
Conserved
tyrosine
residue
Conserved
cysteine-rich
region
Sprouty1
Sprouty2
Sprouty3
Sprouty4
NH2
COOH
Y

include FGFR, the vascular endothelial growth factor receptor (VEGFR) and the hepatocyte growth factor receptor [HGF (55, 68)]. Signals that are derived from RTK, such as EGFR, are transduced by downstream signaling molecules (e.g., Grb2, Sos, Ras, Raf, etc), which lead to the activation of the mitogen-activated protein kinase (MAPK). This signaling event is essential for different cellular processes such as growth differentiation and migration.

As illustrated in Figure 7, Spry proteins contain a much conserved cysteine-rich region present at the carboxyl terminus of all mammalian Spry proteins. This region is important for the translocation of Spry to the plasma membrane by its interaction with phosphatidylinositol-4,5-bisphosphate [$PI(4,5)P_2$ (72, 73)]. Outside the cysteine rich region, at the amino terminal site, a conserved tyrosine residue mediates the interaction of Spry with signaling molecules that contain Src-homology-2 (SH2) domains. However, outside of this region, sequence divergence is observed in all Spry homologs. This might explain their complex and diverse mode of action that has been observed (13, 19, 40, 61, 84).

The modulation of EGFR signaling and trafficking by Spry2 is complex. As illustrated in Figure 8, Spry2 can have a negative or positive effect on EGFR signaling. One way of positively modulating EGFR signaling is by Spry2's interaction with the E3 ubiquitin ligase Cbl. Upon EGF induction, Spry2 undergoes phosphorylation on its tyrosine residue. This phosphorylation site functions as binding site for the SH2 domain of Cbl (33, 115). As this SH2 domain is required for Cbl to interact with the activated form of the EGFR, the binding of Spry2 recruits Cbl away from the EGFR and prevents

Figure 8. Schematic diagram illustrating the EGFR signaling pathway and modulation by Spry **A.** Upon activation of EGFR, various tyrosine residues become phosphorylated on the cytosolic tail of the receptor and they become targets of both positive and negative regulatory proteins bearing intrinsic SH2 domains. The SH2 domain on Cbl binds directly to one of the phosphorylated tyrosine residues on EGFR. Cbl functions as an E3 ubiquitin ligase where it tags the EGFR for ubiquitination, endocytosis and destruction via the intracellular endosomal system. A positive signal, by which the Ras/MAP kinase pathway gets activated, is initiated by the binding of the Grb2 SH2 domain to tyrosine residues on EGFR. The signal gets transduced leading to cellular growth and differentiation. **B**. When Spry2 is expressed in activated cells it tranlocates to the plasma membrane, by binding to free $PI(4,5)P_2$, and becomes phosphorylated. The two tyrosine-phosphorylated sites on EGFR and Spry2 compete for binding to the SH2 domain of Cbl. This prevents EGFR downregulation and the net result of this is the failure of EGFR to submit to endocytosis and destruction, allowing the Ras/MAP-kinase signal to be sustained. Spry2 can also negatively regulate the EGFR signaling by recruiting the adaptor molecule Grb2 or by directly interacting with Raf. Adapted from Guy et al. (40)

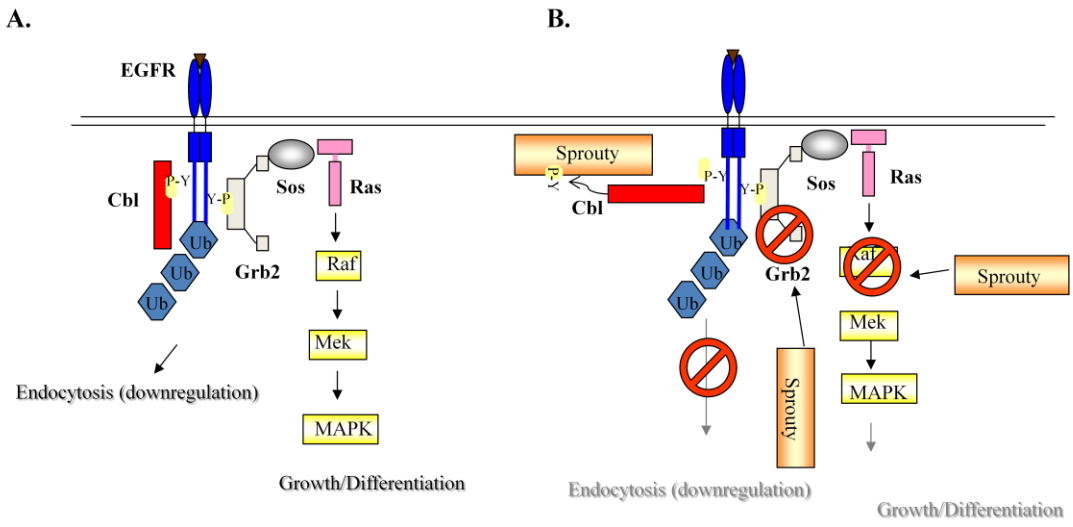
A.
EGFR
Cbl
P-Y
Y-P
Sos
Ras
Ub
Ub
Ub
Grb2
Raf
Mek
MAPK
Endocytosis (downregulation)
Growth/Differentiation
B.
Sprouty
Cbl
P-Y
Y-P
Sos
Ras
Ub
Ub
Ub
Grb2
Raf
Sprouty
Mek
MAPK
Sprouty
Endocytosis (downregulation)
Growth/Differentiation

its ubiquitination and internalization which leads to a sustained MAPK signaling. On the contrary, Spry2 can negatively regulate EGFR by interacting with adaptor molecules that participate in transducing the signal from the plasma membrane. One of these adaptor molecules is Grb2(46), which prevents the activation of Ras, and therefore inhibiting the transduction of the signal.

Spry2 functions in preventing ubiquitination of cellular cargo (e.g., EGFR) and the recent observation that Spry2 can modulate the interaction of ESCRT proteins, specifically the association between Hrs (ESCRT-0) and Tsg101 [(ESCRT-I)(62)], suggests that Spry2 can positively regulate EGFR signaling by preventing cellular sorting in the MVB, which ultimately prevents degradation in the lysosome. This kind of regulation should provide an advantage to pathogens that utilize the ESCRT machinery. As noted above, HIV-1 Gag and ASV-Gag utilize the ESCRT machinery but are excluded from the lysosomal pathway. Instead Gag proteins can recruit this cellular machinery, assemble and exit the cell.

Focus of this thesis

Based on the observations described above, it is now apparent that MVB biogenesis and virus budding are topologically similar events and retroviral Gags, through their L domains, are hijacking the ESCRT machinery for trafficking and efficient release. However, the mechanism underlying the recruitment and utilization of these proteins by the different retroviruses is not clearly understood and the route that Gag follows before reaching its ultimate destination at the cell periphery still remains a

subject of debate. Moreover, while the linkage to the endocytic trafficking machinery of viruses with PTAP motifs in their Gag proteins is well documented, the mechanisms that links Nedd4 and viruses whose Gag proteins contain a PPPY motif is not clear. Understanding the specific pathways utilize by diverse retroviral Gag proteins is of great importance in order to find specific inhibitors that can block their trafficking to the plasma membrane and, therefore, provide novel strategies for treatment of infections caused by the human retrovirus HIV-1.

After describing Materials and Methods (Chapter Two), I investigate the dependence of the functionally exchangeable L domains of HIV-1 and ASV-Gag on Nedd4 and Tsg101, respectively, as a means of determining whether HIV-1 and ASV-Gag use the same trafficking pathways (Chapter 3). In Chapter Four, I explore in more detail the requirement of ASV Gag for Tsg101 and conclude that Tsg101 can substitute for Nedd4, the natural cellular protein binding partner for Gag, in promoting efficient budding but Tsg101 directs ASV Gag to a different membrane region for VLP assembly and release. In Chapter Five, I examine the role in Gag release of Sprouty2 (Spry2), a non-ESCRT protein that regulates trafficking of cell surface receptors to degradative compartments, a process that is directed by the ESCRT machinery. I conclude that Spry2 also regulates the trafficking and release of HIV Gag, and participates in directing Gag to the plasma membrane. Together, the studies described in Chapters Three, Four, and Five, and discussed in Chapter Six, provide interesting new information about the cellular pathways involved in retroviral trafficking and release.

CHAPTER 2: Materials and Methods

Plasmids

pCMV-HIV-1 *gag* encoding HIV-1 Gag C-terminally tagged with green fluorescent protein (Gag-GFP) has been previously described (50). Briefly, plasmid p55M1234, a Rev-independent full length *gag* gene clone, was used to amplify the Gag sequence by PCR to produce an EcoRI site at the 5' end and a BamHI at the 3' to allow the insertion into pEGFP-N1 (Clontech, Palo Alto, CA) in frame with the *gfp* gene. Site-directed mutation of the Gag PTAP motif to generate the construct P7L-Gag-GFP encoding a Gag with a non-functional late domain (LTAP) was constructed by using site-directed mutagenesis kit (Qiagen, Valencia, CA). The point mutation was sequenced to confirm the specified mutation. The plasmid ASV-Gag-GFP encodes the ASV Gag proteins minus the last six residues of NC and all of PR (132) fused to enhanced GFP in the pEGFP-N2 backbone. Construct Δp2b-Gag-GFP lacks the nucleotide sequence coding for the PPPPYV sequence within p2b as well as the last six residues of NC and all of PR. The pΔp2b-Gag-GFP sequence was amplified from p2036-Gag/Δp2b by PCR to produce a HindIII site at the 5'end and a KpnI site at the 3'end to allow for insertion into pEGFP-N2, with Gag placed in frame with GFP. DNA encoding ASV Gag -Δp2b-Tsg101 was constructed by doing a double digestion of p2036 (60) with KpnI and XbaI to remove the gfp coding region. Using PCR-based methods, a 5' KpnI site was introduced upstream of the start codon of ASV Gag-Δp2b. Additionally, a 3' HpaI site was introduced downstream of the ASV-Gag-Δp2b coding sequence. Similarly, a 5' HpaI and a 3' XbaI site were introduced upstream and downstream, respectively, of the full length coding

sequence of *tsg101*. Both PCR products were ligated to the KpnI and XbaI doubly digested p2036 vector DNA to produce p2036 ASV Gag-Δp2b-*tsg101*, in which Tsg101 is translationally fused in frame to the C-terminus of ASV-Gag-Δp2b. This strategy was also utilized to construct HIV-Gag-P7L-*tsg101* fusion construct and the ASV-Gag-Δp2b-*vps37C*, -Δp2b-*eap20*, and Δp2b-*chmp4B* constructs. Constructs encoding the human full length Tsg101 C-terminally tagged with myc (pLLEXP1-*tsg101*-myc) and Tsg101-myc deletion mutants including the pLLEXP1-*tsg101* N-term or C-term-myc or the pLLEXP-HA-*tsg101* have been described previously (71, 75). DNA encoding human *vps4*A or *vps4A*-E228Q was a gift of Dr. Sunquist [University of Utah (36)]. LDI-1 construct had been previously described (60). Briefly, LDI-1 was subcloned into the p2036 backbone with a HA tag at the N-terminus. KpnI and XbaI restriction sites were introduced by standard PCR techniques into the LDI-1construct at 5' and 3' ends, respectively, and used for subcloning into plasmid 2036.

Plasmid amplification and purification

Recombinant plasmids were propagated in *Escherichia coli* DH5α, c600, or MC1061/P3 in Luria Bertani (LB) medium containing either 50ug/ml of ampicillin, kanamycin or 25ug/ml of tetracycline at 37°C for about 12-16 hours. Isolation of plasmid DNA was performed by using the Endofree plasmid purification Maxi-prep kit (Qiagen, Valencia, CA) following the manufacturer's instruction. Endotoxin removal ensures high transfection efficiency by using the endotoxin removal buffer provided in the kit. Plasmid DNA yield was determined by spectrophotometry at 260nm and quantitative analysis on an agarose gel was performed.

Cell culture and transfection

Cos-1(African monkey kidney cells), 293/E (human embryonic kidney cells expressing the EBNA 1 protein of Epstein-Barr virus), DF-1(chicken embryo fibroblasts, or DF-1/RCAS/BP-A (chicken embryo fibroblasts constitutively expressing ASV) cells were grown in Dulbecco's modified Eagle medium [DMEM (GIBCO BRL-Invitrogen) supplemented with fetal bovine serum [5%, 10%, 10%, 10%, respectively (Hyclone, Inc)]. 293/E cells were supplemented with the antibiotic G418 (geneticin) for maintenance. For transfection experiments, cells were seeded to obtain 60% confluency in a 100mm tissue culture plate. Cells were grown at 37°C under 5% CO_2. Cells were transfected by using Fugene6 (Roche, Indianapolis, IN) transfection reagent according to the instructions of the manufacturer.

Preparation of cytoplasmic extracts and virus isolation

At 48 hours post-transfection, the cells were harvested by scraping (cell scraper 25cm-2 position blade from Sarstedt, Inc.) into cold Dulbecco's Phosphate-Buffered Saline (D-PBS) and collected by centrifugation at 3000 rpm for 10 min at 4°C. The pelleted cells were washed two times with cold D-PBS and allowed to swell in cold hypotonic buffer (10mM Tris-HCL (pH 7.4) and 1mM $MgCl_2$), containing protease inhibitors (Roche, Indianapolis, IN) and disrupted using a Dounce homogenizer with a type B pestle (40 strokes). The total lysate of approximately 1ml was spun for 10 min. at 1000x *g* at 4°C to remove unbroken cells, nuclei, and mitochondria, producing a total cytoplasmic fraction. For immunoprecipitation experiments, the cytoplasmic extract was cleared of large particulate material by spinning at 10,000x *g*. In order to isolate the virus-like particles

produced by Gag, the cell culture media from each plate was filtered through a 0.45µm filter and applied to a cushion of 20% sucrose in a centrifuge tube and then spun at 37,000 rpm for 90 min at 4°C (Beckman SW41 rotor). The pelleted VLPs were resuspended in 50µl of PBS and loading buffer at 4°C.

Protein detection

Proteins were separated by electrophoresis through 12.5% SDS-polyacrylamide gels. Following electrophoresis, the gels were transferred to nitrocellulose membranes and analyze by Western blotting. The membranes were blocked in 5% non-fat milk for 1 hour and then rinse three times with PBS-T (1% Tween). Shortly after the membranes were incubated with the primary antibody for 24 hours and rinsed. The corresponding secondary antibody was added at a 1:10,000 dilution in 5% non-fat milk dissolve in PBS-T and incubated for 1 hour at room temperature. Proteins were visualized by chemiluminescence using Lumi-light reagents (Roche, Indianapolis, IN) and measurements of relative protein levels were determined by densitometry using NIH Image software. Alternatively, when using secondary antibodies containing a fluorescent dye, the proteins were visualized by scanning the membrane with the Odyssey Infrared Imaging System and protein levels were quantified using the Odyssey software.

Antibodies

Tsg101 was detected by using either a monoclonal or polyclonal antibody (Santa Cruz Biotechnology, Santa Cruz, CA) at a 1:1000 dilution. Nedd4 proteins were detected with anti-Nedd4 polyclonal antibodies given by Dr. D Rotin (124). Anti-HA, anti-myc tagged proteins were detected by using either monoclonal or polyclonal antibodies from Sigma

(St. Lois, MO) at a 1:1000 dilution. GFP-tagged proteins were detected by using a monoclonal antibody from Clontech Laboratories (Mountain View, CA) at a 1:1000. For detection of ASV chimeric proteins an anti-AMV-MA (p19) monoclonal antibody was used, this antibody recognized the MA domain of ASV and was developed by David Boettiger and was obtained from the Developmental Studies Hybridoma Bank under the auspices of the NICHD and maintained by the University of Iowa, Department of Biological Sciences (Iowa City, IA). HIV chimeric proteins were detected using an anti-CA rabbit polyclonal antibody raised against a native form of the capsid protein (30).

Fluorescence microscopy

Cos-1 cells were used for fluorescence imaging due to the relatively high ratio of cytoplasm to nucleus, which facilitates the analysis of cellular trafficking events. These cells were grown to 40% confluency on large square coverslips (22x22mm) in six well plates in DMEM supplemented with fetal bovine serum and antibiotics (1% Streptomycin and Penicillin) and transfected as previously described (88). At 24 hours post-tranfection, the cells were washed twice with PBS and fixed in 3.7% formaldehyde (Fisher, Fairlawn, NJ) in PBS for 20 min. at room temperature on a rocking platform and covered with aluminum paper. Samples were then washed three times with PBS, for 5 min. each wash and permeabilized with 0.1% Triton-X 100 for 4 min. and washed three times again with PBS.

CHAPTER 3: Functionally exchangeable PPPY and PTAP L domains and ESCRT mediated trafficking pathways required for efficient release.

Summary

In this chapter I examined the dependence of the functionally exchangeable L domains of HIV-1 and ASV Gag on Nedd4 and Tsg101, respectively, as a means of determining whether HIV-1 and ASV-Gag use the same trafficking pathways. The functional exchangeability feature of L domains predicts that ASV Gag, containing a PPXY L domain, might share the same pathway as the one used by HIV Gag, containing a PT/SAP L domain. However, it is possible that the mechanism utilized by ASV Gag is independent of the pathway taken by a virus whose Gag contains a PTAP motif. One possible mechanism by which a Gag protein with the PPPY motif might be linked to the endocytic cellular machinery is through the interaction between the ubiquitin E2 variant Tsg101 and the E3 ubiquitin ligase Nedd4. The results of the study described in this chapter suggests that ASV Gag, like HIV Gag, utilizes the endocytic machinery and that Tsg101 and Nedd4 interact at steady state, providing a possible link for Nedd4 to the ESCRT cellular machinery. However, it was observed that a dominant negative (DN) mutant of Tsg101 had little effect on ASV Gag VLP release and a DN mutant of Nedd4 had little effect HIV Gag VLP release, indicating that the pathways used by HIV and ASV are not the same. Interestingly, although a C-terminal fragment of Tsg101 that inhibited the budding of HIV and murine leukemia virus (MLV), a retrovirus whose Gag protein contains both the PTAP and the PPPY motif, was not found to block ASV release, we found that the quality of the budding event was impacted. Examination by electron microscopy revealed double particles tethered to each other, indicating a defect

in particle-particle detachment. The results obtained in this study clearly support the notion that viruses lacking the PTAP motif can also utilize the cellular endocytic machinery. However, the way they access the machinery is apparently not through the interaction between Nedd4 and Tsg101. Nevertheless, our EM observations suggest that proper interaction between Tsg101 and Nedd4 might be necessary for efficient particle detachment.

***Specific Contribution**:* I designed and performed the experiments in Figures 2, 3, 5, and 6. The attached publication, Medina *et al*, 2005 in the Traffic Journal was provided by the copyright owner, Blackwell Munksgaard and permission has been granted for its use in this dissertation.

Traffic 2005; 6: 880–894
Blackwell Munksgaard

doi: 10.1111/j.1600-0854.2005.00323.x

The Functionally Exchangeable L Domains in RSV and HIV-1 Gag Direct Particle Release Through Pathways Linked by Tsg101

Gisselle Medina[1], Yongjun Zhang[2], Yi Tang[3], Eva Gottwein[1], Marcy L. Vana[2], Fadila Bouamr[1], Jonathan Leis[2] and Carol A. Carter[1,*]

[1]Departments of Molecular Genetics & Microbiology, State University of New York at Stony Brook, Stony Brook, NY 11794-5222, USA
[2]Microbiology & Immunology, Northwestern University Feinberg School of Medicine, Chicago, IL 60611, USA
[3]Children's Memorial Hospital, Chicago, IL 60614, USA
**Corresponding author: Carol A. Carter, ccarter@ms.cc.sunysb.edu*

The functionally exchangeable L domains of HIV-1 and Rous sarcoma virus (RSV) Gag bind Tsg101 and Nedd4, respectively. Tsg101 and Nedd4 function in endocytic trafficking, and studies show that expression of Tsg101 or Nedd4 fragments interfere with release of HIV-1 or RSV Gag, respectively, as virus-like particles (VLPs). To determine whether functional exchangeability reflects use of the same trafficking pathway, we tested the effect on RSV Gag release of co-expression with mutated forms of Vps4, Nedd4 and Tsg101. A dominant-negative mutant of Vps4A, an AAA ATPase required for utilization of endosomal sorting proteins that was shown previously to interfere with HIV-1 budding, also inhibited RSV Gag release, indicating that RSV uses the endocytic trafficking machinery, as does HIV. Nedd4 and Tsg101 interacted in the presence or absence of Gag and, through its binding of Nedd4, RSV Gag interacted with Tsg101. Deletion of the N-terminal region of Tsg101 or the HECT domain of Nedd4 did not prevent interaction; however, three-dimensional spatial imaging suggested that the interaction of RSV Gag with full-length Tsg101 and N-terminally truncated Tsg101 was not the same. Co-expression of RSV Gag with the Tsg101 C-terminal fragment interfered with VLP release minimally; however, a significant fraction of the released VLPs was tethered to each other. The results suggest that, while Tsg101 is not required for RSV VLP release, alterations in the protein interfere with VLP budding/fission events. We conclude that RSV and HIV-1 Gag direct particle release through independent ESCRT-mediated pathways that are linked through Tsg101–Nedd4 interaction.

Key words: Gag, HIV-1, L domain, Nedd4, RSV, Tsg101, Vps4

Received 24 June 2004, revised and accepted for publication 24 June 2005, published on-line 1 August 2005

All retroviruses have in common three genes, *gag*, *pol* and *env*, which specify the structural and enzymatic functions of the virus (1). The Gag protein, encoded in *gag*, is sufficient for the formation and release of virus-like particles (VLPs) from Gag-expressing cells. The determinant of viral maturation and release through the plasma membrane is the late (L) domain, originally defined in Rous sarcoma virus (RSV) and subsequently shown to be functional in HIV type-1 (HIV-1) (2–5) (reviewed in 6). Although highly conserved within retroviral subgroups, the L domains in different families vary in amino acid sequence. HIV-1 has a Pro-Thr-Ala-Pro (PTAP) sequence as its L-domain core; equine infectious anemia virus (EIAV) has a Tyr-Pro-Asp-Leu sequence; RSV, Mason–Pfizer monkey virus (MPMV) and Moloney murine leukemia virus (Mo-MLV) have a Pro-Pro-Pro-Pro-Tyr (PY motif) sequence; and human T-cell leukemia virus (HTLV) and other retroviruses have both PY and PTAP motifs (4,7–12). These motifs are also found in the unrelated rhabdo-, filo- and herpes-virus groups, where they are also implicated in membrane trafficking (13–17). In addition, these motifs exist in plasma membrane- and endosomal membrane-associated cellular proteins, where they similarly serve as docking sites for cellular proteins involved in diverse functions including endocytic trafficking (18–20).

The retroviral L domains are functionally exchangeable (21–24). This observation suggests that they might direct an interaction with common cellular machinery, and recent studies support this notion. The prototypic PTAP, PY and YXXL motifs were found to interact with different cellular proteins (10,19,25–31). Tsg101, a protein involved in recognition and sorting of cellular endosomal cargo (32,33), binds to the PTAP motif in the p6 domain of the HIV-1 Gag protein (25,27,28) and is required for VLP release (27). Nedd4, an ubiquitin (Ub)-ligating (E3) enzyme, binds to the PY motif in the p2b region of the RSV Gag protein and is similarly required for VLP release (26). Another cellular protein, AIP-1, binds the YXXL motif in EIAV Gag and an LXXL motif downstream of the PTAP sequence in HIV-1 Gag (31,34–36). To date, approximately 20 additional cellular proteins have been found involved in endocytic sorting complexes required for trafficking [ESCRT 0, 1, 2 and 3; (33,37–41)] in a network that participates in the release of HIV-1 and other retroviruses (31,42–47, reviewed in 48). The cellular proteins are orthologs of the yeast class-E proteins, which are known to be required for vacuolar protein sorting (Vps proteins) (49). These proteins exist mainly as soluble proteins or complexes that are sequentially recruited from the cytosol to endosomal compartments. Cellular cargo destined for

degradation, such as internalized ubiquitinated plasma membrane receptors undergoing downregulation, is transported to early 'sorting' endosomes through the action of Hrs (Vps27), a protein that binds the surface of early endosomes and recruits Tsg101 (50–55). Tsg101 induces the biogenesis of multivesicular bodies (MVBs) (40,56). Multivesicular bodies are carrier endosomes that contain the cargo within luminal vesicles due to the inward invagination of the regions on the endosomal membrane-bearing Hrs. The MVBs eventually fuse with lysosomes, resulting in exposure of cargo on the internal luminal vesicles to hydrolytic enzymes. Cargo destined to return to the plasma membrane (e.g. transferrin receptor) is transported to a different region on the early endosome and enters a recycling pathway. Afterwards, the cellular proteins involved in sorting are released from the endosome membrane into the cytoplasm for recycling through the action of members of the AAA family of ATPases, Vps4A and Vps4B (57).

While the linkage between Tsg101, the endocytic trafficking machinery and viruses with PTAP motifs is well documented, the mechanism that links Nedd4 and viruses with PY motifs to the machinery has been elusive. We previously reported that the L domain in RSV Gag interacts with endogenous Nedd4 proteins in primate COS-1 cells and human 293/E cells and with Nedd4-related proteins of avian origin, which we designated as L-domain-interacting proteins 1 and 2 (LDI-1, LDI-2; 26). L-domain-interacting protein-1 and LDI-2 lack the enzymatic [homologous to E6-AP carboxyl terminus (HECT)] domain but contain the N-terminal membrane-binding (C2) domain and the central PY-motif-binding WW domain. More recently, we identified the 3′-end of the gene encoding LDI-1 and determined that full-length (FL) LDI-1 has a C-terminal Ub ligase HECT domain similar to other Nedd4 family members (58). Some of the Gag proteins in the cytoplasm are modified, and mono- and di-ubiquitinylated forms of Gag are encapsidated. Modification is tightly correlated to efficient VLP release. We further demonstrated that a fragment of Nedd4 containing only the WW domain or a mutated FL Nedd4 protein containing an inactivating mutation in the catalytic site is a dominant-negative (DN) inhibitor of RSV Gag budding. The fact that Nedd4 proteins function as binding partners of the RSV L-domain, which is functionally exchangeable with the PTAP motif in HIV-1 Gag recognized by Tsg101, suggested that HIV-1 and RSV Gag might utilize the same trafficking pathway involving Tsg101 and Nedd4. Alternatively, the two Gag proteins might use Nedd4 and Tsg101 in pathways that are entirely separate but parallel, both pathways leading to particle release. Here, we show that release of VLPs assembled by RSV Gag was inhibited by a DN-interfering mutant of Vps4 that was previously shown to interfere with recycling of Tsg101 and to inhibit release of HIV-1, EIAV, Mo-MLV, MPMV and Ebola virus (10,12,17,27,41,47,59). We also show that Tsg101 interacted with both hemagglutinin (HA)-tagged LDI-1 and the endogenous Nedd4 proteins in COS-1 cells. Expression of HA-LDI-1 interfered with the Tsg101–Nedd4 interaction. Not surprisingly, HA-LDI-1 did not associate with HIV-1 Gag or interfere with its release. In contrast, Tsg101 and RSV Gag were found to co-localize, and the interaction required the Nedd4-binding site in Gag. Interestingly, co-expression with a Tsg101 protein lacking the N-terminal Ub E2-variant domain (UEV) in Tsg101 interfered with release of the Gag protein of Mo-MLV but had little or no effect on RSV Gag release. Intriguingly, however, the RSV VLPs were frequently detected in clusters that failed to detach from each other, suggesting that the Tsg101 mutant interfered with a Nedd4 function required for proper particle release. Thus, it appears that RSV and HIV-1 Gag direct particle release through ESCRT-mediated pathways that are independent but linked through Tsg101–Nedd4 interaction.

Results

A DN mutant of the AAA ATPase Vps4 inhibits release of RSV Gag

The Vps4 mutation used in this study contained an E228Q substitution, which prevents ATP hydrolysis (27). This mutant has been shown to suppress budding of HIV-1, Mo-MLV and other retroviruses (10,12,17,27,41,47,59), reflecting a requirement for a functional vacuolar-sorting pathway. To test the effect of the Vps4 mutant on RSV Gag release, we co-transfected different amounts of constructs encoding the wild-type (WT) Vps4 protein or the Vps4 substitution mutant with a constant amount of DNA-encoding RSV Gag containing a D37S mutation that inactivates PR (26). The use of the D37S mutant makes it easier to assess effects on release, as only the Gag precursor that directs productive particle formation is detected. Cell lysate and media fractions were prepared following labeling of the cells with ^{35}S-Met and Cys for 2.5 h. Viral proteins were immunoprecipitated from the media and cell-lysate fractions and separated using SDS–PAGE. As shown in Figure 1A, co-expression of RSV Gag with WT Vps4 (lanes 2 and 3) did not interfere significantly with release of VLPs into the media (upper panel), as compared with control cells expressing Gag alone (lane 1). No non-specific signals were detected in a mock-treated sample (lane 4). In contrast, co-expression with Vps4 E228Q (lanes 5 and 6) reduced release of RSV VLPs into the media (upper panel); the amount of $Pr76^{Gag}$ detected in the cell lysate (lower panel) was comparable with, or greater than, control levels. Comparisons of the signal of Gag in the media and lysate fractions, which reflect the efficiency of Gag budding, indicated that the level of Gag release was approximately threefold lower in the presence of the Vps4 mutant as compared with Vps4 WT (Figure 1B). To confirm the results of the budding assay, we examined the co-transfected cells by electron microscopy (EM). No particles were detected in the vicinity of mock-transfected

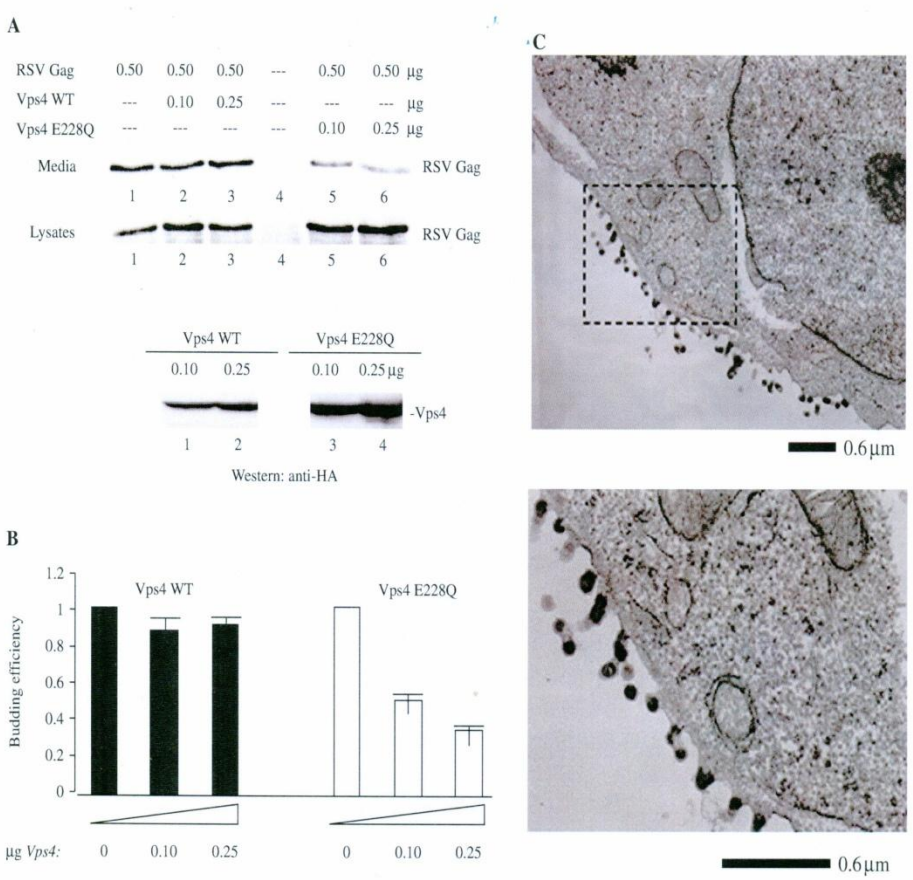

Figure 1: Co-expression of Rous sarcoma virus (RSV) Gag and Vps4. A) Effect on virus-like particle (VLP) release. Rous sarcoma virus $Pr76^{Gag}$ was expressed in 293/E cells (lane 1) in the presence of wild-type Vps4 (lanes 2 and 3) or Vps4 E228Q (lanes 5 and 6) and labeled with a mixture of 35S-Met and Cys for 2.5 h before harvesting at 48 h. Lane 4 is an untransfected control. The ratio of *vps4* : *gag* DNA (in µg) used for transfection were lanes 2 and 5, 0.2:1 and lanes 3 and 6, 0.5:1. Upper panel, VLP in media; Lower panel, Gag- and HA-tagged Vps4 in cell lysate. Proteins were detected by autoradiography. B) Semi-quantitative analysis of VLP release. The panel shows the ratio of the Gag signal in VLP isolated from the media to the Gag signal in cell lysates (VLP/cell lysate). C) Examination using electron microscopy (EM). Cells were prepared for thin section EM as described in *Materials and Methods*. The area outlined in the dashed rectangle is enlarged.

cells or cells transfected with DNA-encoding Vps4 WT (data not shown; cf. Figure 8A). In contrast, VLPs tethered to each other and to the cell were detected in samples co-transfected with RSV Gag and Vps4 E228Q (Figure 1C). This is similar to what is observed with RSV Gag containing an L-domain deletion; such budding structures were never observed following transfection of RSV Gag alone. The results indicate that release of RSV Gag requires proteins under the control of Vps4, as is the case for HIV-1 and other retroviral Gags, and suggest that, like them, RSV Gag uses components of the endocytic trafficking machinery.

HA-LDI-1 co-localizes with RSV Gag and blocks its release but does not affect HIV-1 Gag

If RSV and HIV-1 Gag share the same pathway for budding, a possible convergent point could be a potential interaction between Nedd4 and Tsg101. As noted above, Nedd4 is an Ub-ligating (E3) enzyme (60). The primary sequence and the three-dimensional structure of the N-terminal domain of Tsg101 are homologous to that of Ub-conjugating (Ubc; E2) enzymes (61–63). The sequence in Tsg101 is highly conserved and most closely resembles the subgroup of E2 enzymes that the Nedd4 family specifically recognizes (61). Hemagglutinin-tagged LDI protein,

comprised of the C2 and WW domains of avian Nedd4 with an N-terminal HA tag (26) (Figure 2, top), was first examined for association with RSV Gag in COS-1 cells using confocal microscopy (Figure 2, panels A–F). When expressed alone, RSV Gag-green fluorescent protein (GFP) exhibited dispersed, punctate fluorescence (panel A). Hemagglutinin-tagged LDI-1, expressed alone and detected by indirect immunofluorescence with mouse anti-HA antibody and a TRITC-tagged anti-mouse secondary antibody, was distributed throughout the cytoplasm (panel B). Following co-expression of Gag-GFP and HA-LDI-1 (panels C–E), the green (Gag, panel C) and red (HA-LDI-1, panel D)

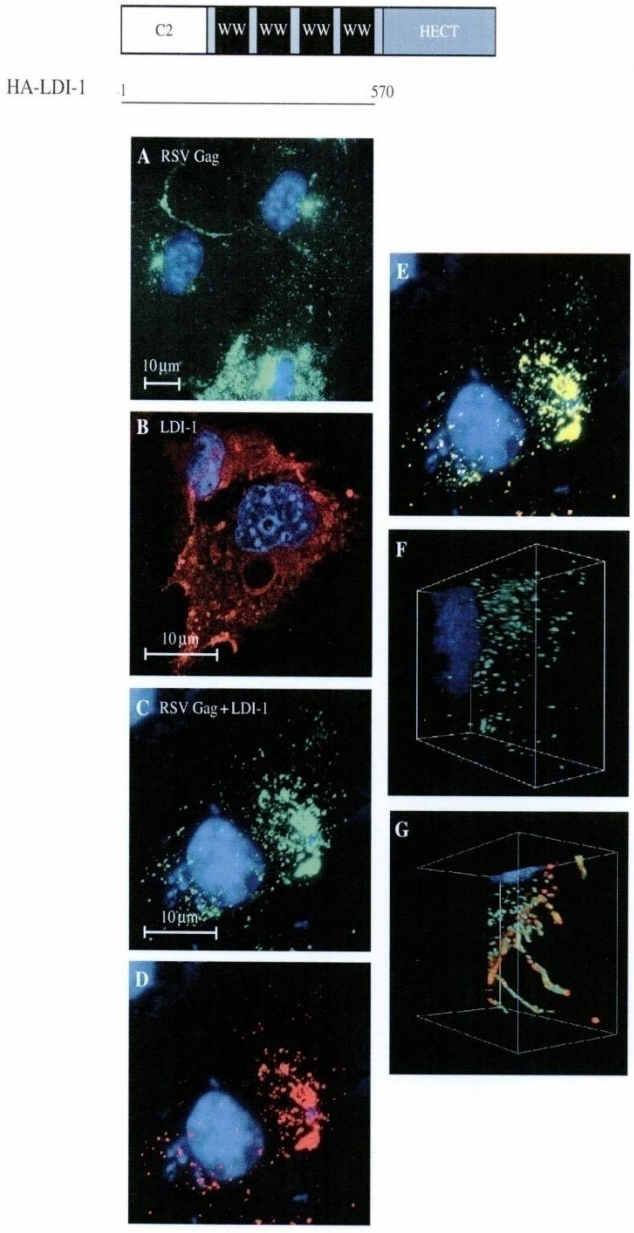

Figure 2: Confocal microscopy of cells co-expressing Rous sarcoma virus Gag-green fluorescent protein (RSV Gag-GFP) and hemagglutinin-L-domain-interacting protein (HA-LDI)-1. Top, Schematic drawing of the Nedd4-related fragment used in this study. COS-1 cells were transfected with DNA encoding RSV-GFP alone (panel A), LDI-HA alone (panel B), or RSV Gag-GFP (green) and HA-LDI-1 (red) (panels C–G). Panel E shows the merged Gag-GFP (panel C) and LDI-1 (panel D) images. Panels F and G: three-dimensional renderings of stacked *z* sections through cells expressing RSV Gag alone (panel F) or LDI-1 and RSV Gag (panel G). The LDI-1 protein was detected by indirect immunofluorescence using mouse anti-HA as primary antibody and rabbit anti-mouse tagged with TRITC as secondary antibody.

fluorescent signals were significantly mixed, as indicated by the yellow color (panel E). Similar results were obtained using 293 cells for fluorescence microscopy (not shown). The spatial relationship between RSV Gag-GFP and HA-LDI-1 was evident in a composite of 0.4-μ confocal images taken throughout the cell and rendered as a three-dimensional image (panels F and G). Here, co-localization is visualized as significant intermingling of the red and green fluorescent signals rather than the yellow color detected in the two-dimensional image. Rous sarcoma virus-green fluorescent protein fluorescence in the absence (panel F) and presence (panel G) of HA-LDI-1 expression is shown. This finding indicates that the change in Gag distribution evident in panels A and C reflects co-localization of Gag with HA-LDI-1. Expression of HA-LDI-1 interfered with release of RSV Gag-GFP in VLP assays (Figure 3, panels A and B, lanes 1–3). Inhibition was dependent on the amount of DNA encoding HA-LDI-1 that was transfected (twofold at an LDI : gag ratio of 2 and 2.5-fold at an LDI : gag ratio of 3). Electron microscopy studies of cells transfected with HA-LDI-1 (not shown) revealed VLPs in large inclusion bodies. Possibly, formation of these bodies interfered with antibody detection of the protein, as the expression level of HA-LDI-1 in the cell lysate did not appear as dose-dependent as the effect on VLP release. The level of HA-LDI-1 inhibition was similar to that obtained using FL LDI-1 protein containing an inactivating mutation in the catalytic domain (58). In contrast, HA-LDI-1 did not significantly interfere with HIV-1 Gag release (Figure 3, panel A, lanes 4–6; panel B, $n = 10$). Moreover, no co-localization with HA-LDI-1 was detected (panels C–E). The different spatial relationship

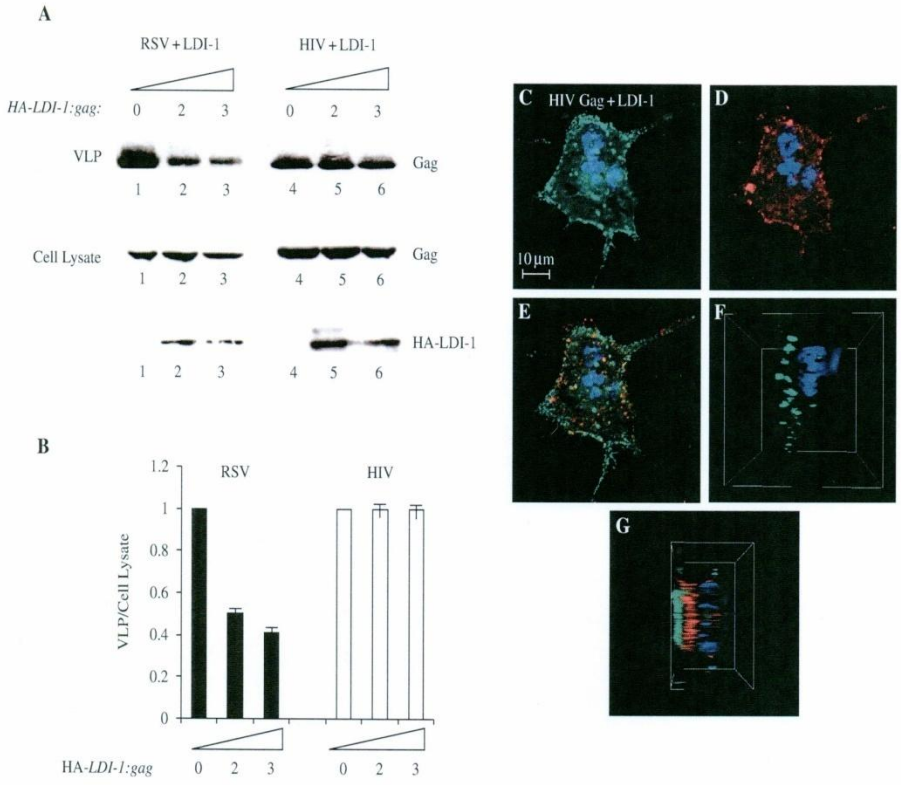

Figure 3: Effect of L-domain-interacting protein (LDI)-1 expression on HIV-1-virus-like particle (VLP) release. Panel A: Western analysis. COS-1 cells were transfected with DNA encoding Rous sarcoma virus (RSV) Gag-green fluorescent protein (GFP) (lanes 1–3) or HIV-1 Gag-green fluorescent protein (GFP) (lanes 4–6) alone (lanes 1 and 4) or with HA-LDI-1 (lanes 2, 3, 5 and 6) at *HA-LDI-1* to *gag* ratios of 2:1 (lanes 2 and 5) or 3:1 (lanes 3 and 6). The Gag and LDI-1 proteins were detected using anti-GFP or anti-HA antibodies, respectively. Top panel: Gag-GFP in VLPs; center and lower panels: Gag-GFP (center) and HA-LDI-1 (lower) in cell lysates. Panel B: Semi-quantitative analysis of VLP release. The panel shows the ratio of the Gag signal in VLP isolated from the media to the Gag signal in cell lysates (VLP/cell lysate). Panels C–E: COS-1 cells were transfected with DNA encoding RSV Gag-GFP (green, panel C) and HA-LDI-1 (red, panel D). Panel E shows the merged images. Panels F and G: Three-dimensional renderings of stacked *z* sections through a cell expressing Gag and LDI-1. Left, HIV-1 Gag alone; right, LDI-1 co-expressed with HIV-1 Gag.

between HIV-1 Gag-GFP and HA-LDI-1 as compared with RSV Gag-GFP and HA-LDI-1 was particularly evident in a three-dimensional composite of confocal images (panels F and G). The green fluorescence of HIV-1 GFP was detected as a defined layer in the absence (panel F) or presence (panel G) of HA-LDI-1. The red fluorescence attributable to HA-LDI-1 also was clearly defined and no co-localization was detected. Thus, HA-LDI-1 co-localized with RSV Gag and inhibited its release but did not associate with nor inhibit HIV-1 Gag release.

HA-LDI-1 associates with Tsg101 and competes with endogenous Nedd4 for interaction with Tsg101

The results above suggest that the RSV and HIV Gag-trafficking pathways are separate or, alternatively, that Nedd4 functions upstream of Tsg101 in the same pathway. To distinguish these possibilities, we next tested for Tsg101–LDI interaction. As shown in Figure 4A, the HA-LDI-1 expressed in transfected COS-1 cells (lane 2) was immunoprecipitated by antibody against Tsg101 (lane 4), as indicated by Western analysis using an antibody against the HA tag on the LDI-1 protein. Extracts prepared from cells that were not transfected with DNA encoding HA-LDI-1 (lanes 1, 3 and 5) contained no cross-reactive material and, in a control experiment using preimmune rabbit serum, no non-specific immunoprecipitation (Ip) was detected (lane 6), indicating that recognition of HA-LDI-1 was specific. Reprobing the blot with an anti-Tsg101 monoclonal antibody indicated that Tsg101 was present in the immune-precipitates (panel D). The results indicate that Tsg101 interacted with HA-LDI-1 specifically. As Tsg101 recognized both the endogenous Nedd4 protein in COS-1 cells and HA-LDI-1, we determined whether HA-LDI-1 could compete with the endogenous Nedd4 protein for interaction with Tsg101. To test this, we determined whether HA-LDI-1 interfered with Tsg101 binding to endogenous Nedd4 in cells expressing HIV-1 Gag, as measured by immune precipitation. Cells expressing Gag were used to provide a negative control in the cell lysate, as our previous studies indicated that LDI-1 does not bind the PTAP motif in HIV-1 Gag (26) and that HA-LDI-1 did not co-localize with HIV-1 Gag (Figure 3C). As shown in Figure 4, lanes 1 and 2, expression of HA-tagged LDI-1 (panel A) did not inhibit accumulation of endogenous Nedd4 (panel B, lanes 1 and 2), HIV-1 Gag (panel C, lanes 1 and 2) or endogenous Tsg101 (panel D, lanes 1 and 2). Although there appeared to be increased accumulation of Gag in the presence of HA-LDI-1 (panel C, lane 2), this was not reproducibly detected ($n = 8$). The polyclonal antibody against Tsg101 co-immunoprecipitated both Nedd4 (panel B, lane 3) and HIV-1 Gag (panel C, lane 3), as well as Tsg101 itself (panel D, lane 3). However, the presence of HA-LDI-1 in the extract (panel A, lane 4) reduced co-Ip of Nedd4 with Tsg101 approximately two-fold to fourfold (panel B, compare lanes 3 and 4; $n = 3$). In contrast, expression of HA-LDI-1 did not detectably diminish the interaction of Tsg101 with HIV-1 Gag (panel C, lanes 3 and 4). As expected, Tsg101 was immunoprecipitated by the anti-Tsg101 antibody (panel D, lane 3), and LDI-1 expression did not prevent Tsg101 Ip (panel D, lane 4). Immunoprecipitation reactions using the preimmune control serum confirmed that co-immunoprecipitation of HA-LDI-1, Nedd4 and HIV-1 Gag required Tsg101 (panels A–D, lanes 5 and 6). The results indicate that the HA-tagged LDI-1 fragment can compete with endogenous Nedd4 for Tsg101 binding while not detectably affecting the interaction of Tsg101 with HIV-1 Gag. We do not know whether Tsg101 bound to HIV-1 Gag and Tsg101 linked to Nedd4 represent the same or different complexes.

The biochemical interaction of Tsg101 with HA-LDI-1 detected by co-Ip was confirmed using confocal microscopy. As noted above, HA-tagged LDI-1, expressed alone, was detected throughout the cytoplasm (Figure 5A). Full-length myc-tagged Tsg101, in contrast, localized in the perinuclear region (panel B). However, following co-expression of the two proteins (panel C),

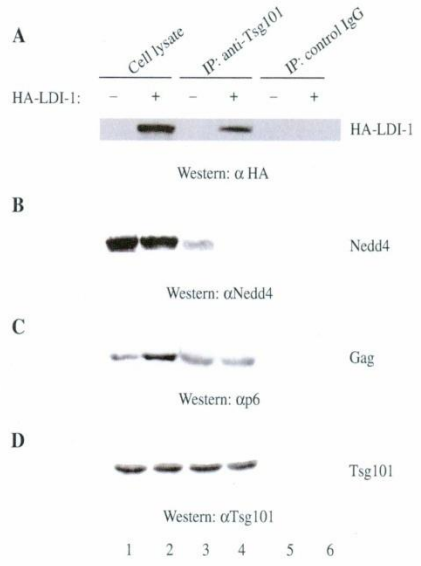

Figure 4: Panels A–D, Effect of L-domain-interacting protein (LDI)-1 expression on Tsg101–Nedd4 interaction. Extracts prepared from cells transfected with DNA encoding HIV-1 Gag (lane 1) or Gag and LDI-1 (lane 2) were incubated with buffer alone (lanes 3 and 5) or buffer containing antibody against Tsg101 (lane 4) or control IgG (lane 6). After washings, the samples were examined for immunoprecipitated proteins by SDS–PAGE and Western analysis. The panels show immunoblots of the same polyacrylamide gel that was successively probed for LDI-1, Nedd4, Gag and Tsg101. Panel A: HA-LDI-1 visualized by using antibody against the HA-tag on the protein. Panel B: Nedd4 detected by using the anti-Nedd4 antibody. Panel C: Gag detected by using antibody against the p6 domain. Panel D: Tsg101 detected by using the mouse monoclonal antibody against Tsg101.

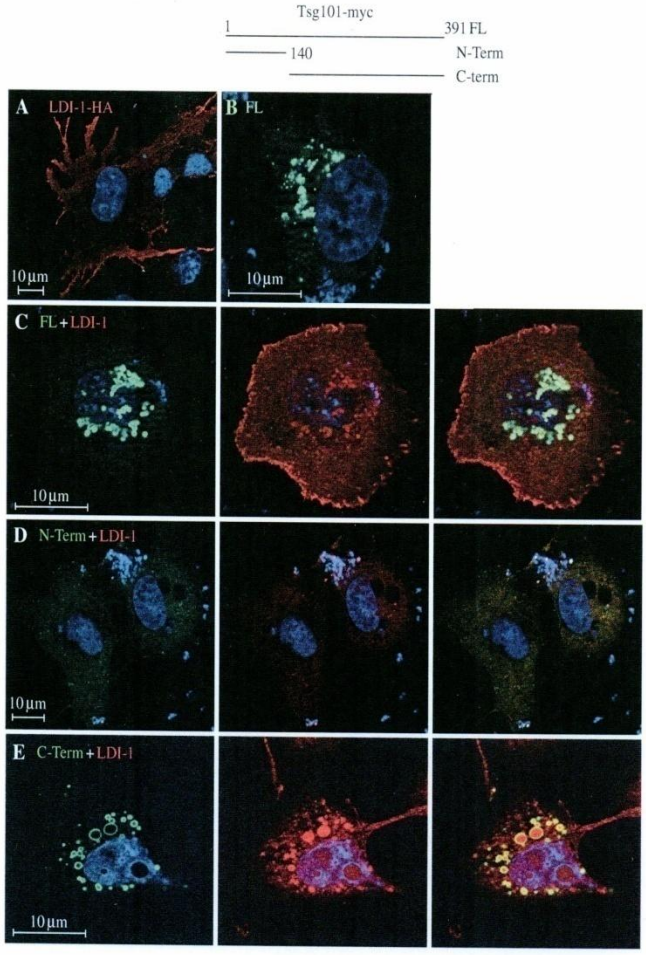

Figure 5: Comparison of cells co-expressing L-domain-interacting protein (LDI)-1 and Tsg101. Top center, schematic drawing of Tsg101-related proteins used in this study. COS-1 cells plated on slides for examination by confocal microscopy were transfected with (i) Panel A: DNA encoding HA-LDI-1 alone; (ii) Panel B: DNA encoding Tsg101 FL alone; (iii) Panel C: LDI-1 (red) and Tsg101-FL (green); (iv) Panel D: LDI-1 and Tsg101N-term; or (v) Panel E: LDI-1 and Tsg101 C-term. The HA-LDI-1 to tsg ratio was 1:1.

some of the LDI-1 (red) appeared to localize to the perinuclear region that contained Tsg101 (green). Merged images revealed proximal red and green but not yellow fluorescence, suggesting that the proteins were in the same region but not directly associated. Both the perinuclear vesicular localization of Tsg101 FL and the proximity to HA-LDI-1 were abrogated by deletion of Tsg101 C-terminal residues 140–391 (panel D). Also, both HA-LDI-1 and Tsg101 fragments exhibited weak, diffuse fluorescence, similar to the pattern observed when they were expressed alone (panel A and data not shown). This suggested that the association of Tsg101 FL with HA-LDI-1 required determinants in the C-terminal region of Tsg101. Consistent with this notion, a significant fraction of HA-LDI-1 co-localized with a C-terminal fragment containing residues 140–391 in the perinuclear region (panel E). In contrast to the FL Tsg101 protein, LDI-1 and C-terminal fragment were directly associated, as indicated by the yellow fluorescence in the merged images. The results support the finding that Tsg101 and HA-LDI-1 associate and indicate that determinants in the C-terminal region of Tsg101 mediate the interaction.

Tsg101 and RSV Gag co-localize

Because HA-LDI-1 interacted with Tsg101 and competed with endogenous Nedd4 for the protein, we determined whether RSV Gag and Tsg101 co-localized intracellularly (Figure 6). In the absence of Tsg101-myc expression, RSV Gag-GFP exhibited dispersed, punctate fluorescence as expected (panel A, open arrow). The same field shows cells that co-expressed Gag-GFP and Tsg101-myc (solid arrows). Under these conditions, both Gag (green) and Tsg-myc (red) accumulated in the perinuclear region and co-localized, as indicated by the yellow fluorescence. This

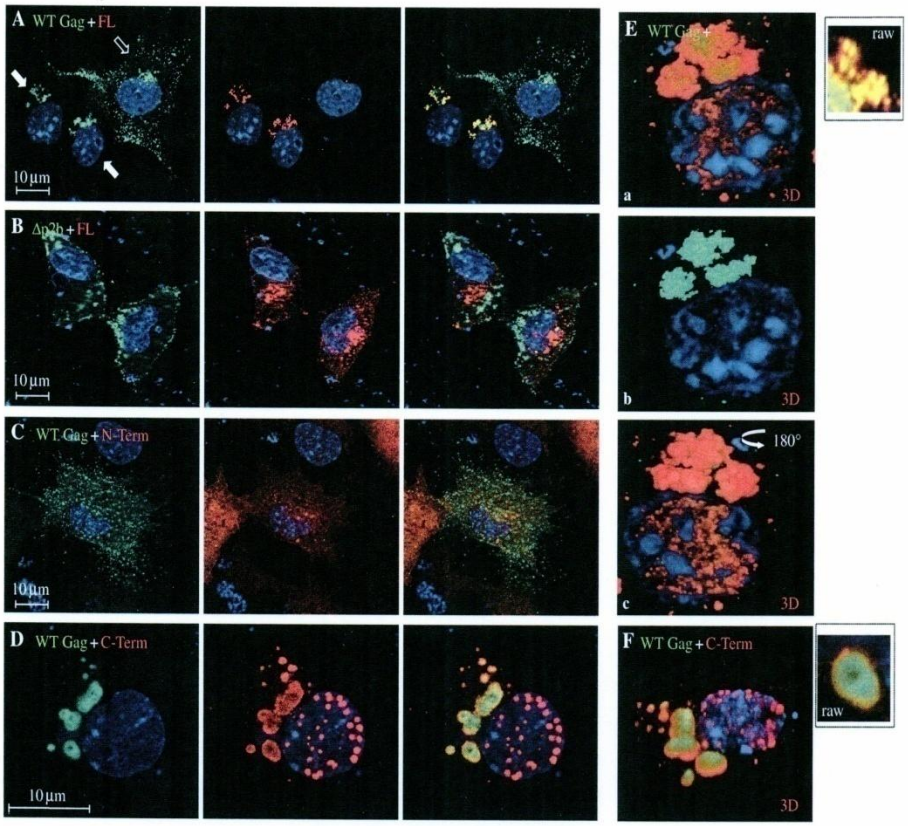

Figure 6: Comparison of cells co-expressing Rous sarcoma virus (RSV) Gag and Tsg101. COS-1 cells were transfected with (i) Panel A: DNA encoding RSV wild-type (WT) Gag-green fluorescent protein (GFP) and Tsg101-FL (red); (ii) Panel B: Δp2b Gag-GFP and Tsg101-FL; (iii) Panel C: WT Gag and Tsg101N-term; or (iv) Panel D: WT Gag and Tsg101 C-term. Panel E (a, b, three-dimensional spatial images of a cell in panel A expressing Gag and Tsg101-FL; a) merged Tsg-FL/Gag images; b) Gag; and c) Tsg101-FL. Panel F: three-dimensional spatial image of cell in panel D. The *tsg* to *gag* ratio was 3:1. The open arrow in panel A indicates a cell in the field expressing Gag alone. Closed arrows indicated cells expressing Gag and Tsg101-FL. The image in panel D is enlarged ×2.5 relative to the magnification of the image in panel A. The insets in panels E and F show images of the Tsg101 Gag clusters in panels A and D on the same scale.

co-localization required the p2b region of Gag that binds Nedd4 (26), as co-localization was abrogated by deletion of this region from the protein (panel B). Under these conditions, the subcellular distribution of Tsg101-FL was similar to that detected when Tsg101 was expressed alone (cf. Figure 5B). As was the case for HA-LDI-1, co-localization was not detected when Gag was co-expressed with the N-terminal fragment of Tsg101 (panel C). However, the C-terminal region that recognizes Tsg101's ESCRT-1-binding partners (41,64) retained the ability to localize in proximity to Gag (panel D). Proximity was indicated by the closeness of the red and green fluorescent signals rather than the yellow fluorescence produced with Tsg101-FL. Most of the structures in which Gag accumulated in the presence of the C-terminal fragment were also larger (approximately 200–750 nm) than those formed by Tsg101-FL (<100 nm, panel A). Differences in the co-localization of Gag and Tsg101-FL versus Gag and the Tsg101 C-terminal fragment were evident in three-dimensional spatial images (panels E and F, respectively; insets show the Gag-Tsg101 clusters in panels A and D on the same scale). As noted above, co-localization is visualized as significant intermingling of the red and green fluorescent signals rather than the yellow color detected in the two-dimensional image. Co-localization was apparent in the three-dimensional spatial image of the merged Gag and Tsg101-FL (panel Ea). Removal of the red signal from merged images (panel Eb) and rotation of the merged image by 180 ° (panel Ec) suggested that Gag was 'sandwiched' in the small structures formed by Tsg101-FL. In

contrast, in the larger structures formed by Tsg101 C-term, Gag was completely exposed (panel F). Taken together, the results indicate that RSV Gag co-localizes with Tsg101 and that co-localization is dependent on retention of the Nedd4-binding site in Gag. The results also suggest that determinants in the N-terminal region of Tsg101 influence the nature of the Tsg101-(Nedd4)–Gag interaction.

Effect of the C-terminal Tsg101 fragment on RSV Gag release

To determine whether the Tsg101–Gag interaction mediated by Nedd4 affected VLP release, we co-expressed RSV Gag with Tsg101-FL or fragments of the protein. The cells were metabolically labeled with ^{35}S-Met and Cys as described above (cf. Figure 1), viral proteins were immunoprecipitated from the cell lysate, VLPs were isolated from the media, and the samples were analyzed by SDS–PAGE and autoradiography. Figure 7 shows the amount of WT Gag detected in the media (upper panels) or in the cell lysates (lower panels). No significant inhibition was observed with the FL protein or the N-terminal Tsg101 fragment (Figure 7, panels A and B; $n = 8$). Similar results were obtained with the C-terminal fragment (panel C). In a control experiment, the effect of the C-terminal fragment on Mo-MLV Gag release was determined (panel D). Our results confirmed previous observations that the C-terminal fragment of Tsg101 inhibits Mo-MLV Gag release (65) (compare lane 6 with lanes 2–4 in panel E). Panel E shows the efficiency of Gag release, expressed as the ratio of Gag in VLP to Gag in cell lysate (VLP/cell lysate). Although dose-dependent inhibition of Mo-MLV Gag release was observed (panel E, right; $n = 2$), RSV Gag release (left) was reproducibly more resistant ($n = 8$). To determine whether the released particles were assembled normally, the VLPs were recovered from the media fraction and subjected to sucrose density gradient centrifugation to equilibrium. The $Pr76^{Gag}$ protein in the samples banded at the density of VLPs (data not shown). Similar results were obtained with COS-1 cells; with DNA encoding a myc-tagged Tsg101 fragment (43) instead of a HA-tagged fragment (65); with RSV Gag expressed from *p*CMV-RSV*gag* that encodes Gag-GFP (66) or from p2036 (26); and when samples were probed by Western analysis (data not shown). The results indicate that despite the striking effects of Tsg101 on Gag localization, neither the FL nor the truncated Tsg101 protein interfered with VLP release. The fact that the Tsg101 C-terminal fragment detectably inhibited Mo-MLV Gag release suggests that the fragment interacts differently with the Gag-E3 ligase complexes formed by RSV and Mo-MLV.

Electron microscopy analysis of the 293/E cells incubated with Tsg101-FL (Figure 8, panel A) or the N-term fragment (panel B) revealed no VLPs, indicating that they were released and that they did not adhere to the cells. In contrast, examination of cultures incubated with the C-term fragment (panel C) typically revealed single or double particles adhered to the cell surface (enlarged in inset C1) or outside the cells (inset C2, taken from another cell). Examination of released VLPs in two independent experiments indicated that approximately 60% (35 of 58) of the particles were tethered doublets, indicating a defect in particle-particle detachment. Thus, although Tsg101 was not required for VLP release, it appears that proper Tsg101–Nedd4 interaction is necessary for efficient particle separation.

Discussion

A conserved protein network required for endocytic trafficking of cellular proteins has been identified in yeast and mammalian cells (31,33,37–39). The functioning of this network is controlled by Vps4 AAA ATPases and, based on their requirement for active Vps4, budding of HIV-1, EIAV, Mo-MLV, MPMV, HTLV-1, Ebola virus and RSV (10,12,17,47,59, this study) exploits this machinery. Previous studies showed that HIV-1 Gag binds Tsg101 and RSV Gag binds Nedd4 through their respective L domains (25–28). Here, we provide evidence that endogenous Tsg101 and Nedd4 proteins are stably associated in the cytoplasm, thereby providing a possible point where the functionally exchangeable Tsg101-binding and Nedd4-binding L domains might converge. L-domain-interacting protein-1, a Nedd4-related DN inhibitor of RSV Gag release, did not significantly inhibit HIV-1-VLP release (Figure 3). This finding is not surprising, as the HIV-1 L domain does not bind Nedd4-related proteins (26). Similarly, we found that a DN inhibitor of Tsg101 that affects HIV-1 Gag (43,65) and Mo-MLV Gag (65, this study) failed to block release of RSV Gag in our study. These observations indicate that Tsg101 and Nedd4 must function independently of each other in HIV-1 and RSV Gag trafficking. However, while intact Tsg101 was not required for efficient RSV Gag release in our studies, Nedd4 interaction with the FL Tsg101 protein was necessary for efficient particle–particle fission. This conclusion would appear to conflict with the results of a recent study where the C-terminal Tsg101 fragment was found to inhibit RSV Gag release (67). However, we suspect that the stronger inhibition observed in that study reflects differences in compartmentalization of the adventitiously expressed Tsg101 proteins. This notion is supported by the fact that Tsg101-Nedd4 co-localization was L-domain-dependent in our study (cf. Figure 6) but not in the aforementioned report. Thus, the RSV- and HIV Gag-trafficking pathways are linked through Tsg101–Nedd4 interaction even if both cellular proteins are not strictly required for the release *per se*.

Figure 9A shows four aspects of HIV and RSV trafficking. (i) DN Vps4 regulates recycling of Vps proteins between cytosol and endocytic vesicles. Sensitivity to DN Vps4 indicates a requirement for functional endocytic trafficking

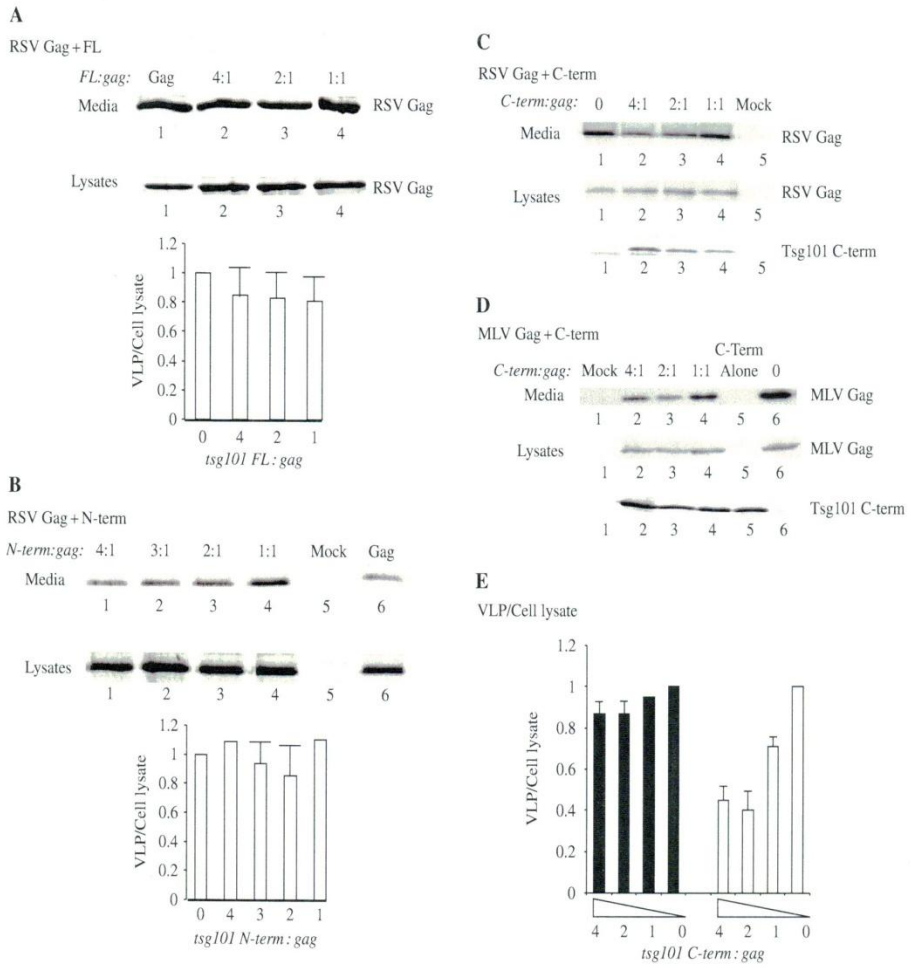

Figure 7: Effect of the Tsg101 C-terminal fragment on Rous sarcoma virus (RSV) and Mo-MLV Gag release. Panels A–C: Effect of Tsg101 full-length and Tsg101 fragment expression on RSV Gag release. Gag was expressed in 293/E cells alone or with the indicated Tsg101 protein at the indicated ratio of *tsg* : *gag* DNA. The cells were metabolically labeled with ^{35}S-Met and Cys at 48 h after transfection, and media and cell lysate fractions were analyzed. The radiolabeled proteins in cell lysates were immunoprecipitated with polyclonal antibody against RSV antibody. An aliquot of the lysate in panel C was examined for Tsg101 by using antibody against the hemagglutinin (HA) tag on the protein in Western analysis. Panel D: Parallel study of the effect of Tsg101 C-term expression on Mo-MLV Gag release. Cells were harvested at 48 h post transfection and examined by Western analysis using antibody against the Mo-MLV CA protein. The blot was re-probed with antibody against HA to detect the Tsg101 protein. Proteins in cell lysates and virus-like particles (VLPs) isolated from media fractions were separated by SDS–PAGE, and autoradiograms were prepared. Panels A, B and E: semi-quantitative analysis of VLP release (VLP/cell lysate). The panels show the ratio of the Gag signal in VLP isolated from the media to the Gag signal in cell lysates.

machinery; both HIV and RSV Gag exhibit Vps4 DN sensitivity. (ii) HIV Gag accesses the machinery through interaction between its L-domain (PTAP) and the PT/SAP-binding pocket in the N-terminal UEV domain of Tsg101. Association with Tsg101 may allow HIV Gag to enter the early endosome and the MVB-sorting compartment, recruit ESCRT complexes and budding machinery and be transported with these to sites of release on the plasma membrane. (iii) Tsg101 interacts with Nedd4, but the Nedd4 component is not critical for HIV Gag release, perhaps because its contribution is redundant with other E3 ligases in the cell. Rous sarcoma virus and Mo-MLV

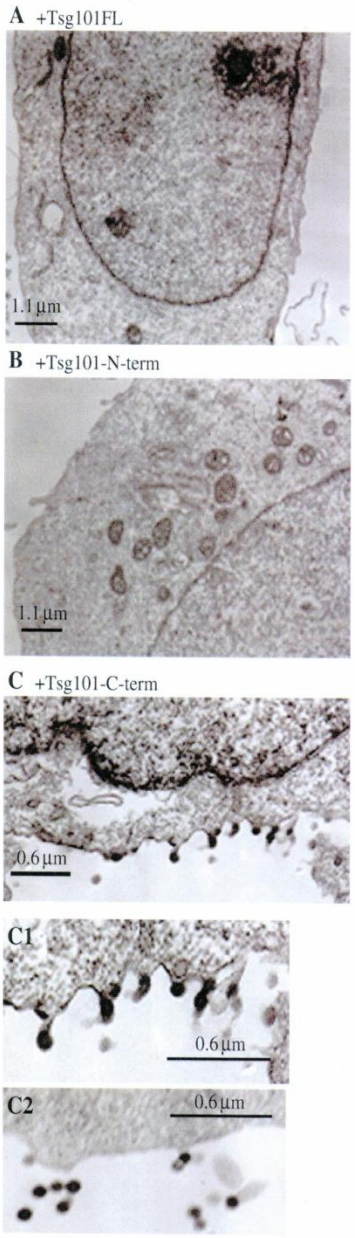

Figure 8: Electron microscopy (EM) of cells co-transfected with Rous sarcoma virus (RSV) *gag* and *tsg101* full-length, *tsg101* N-Term or *tsg101* C-term. Cells were prepared for thin section EM as described in *Materials and Methods*. Panel C1: enlargement of a region with doublet particles tethered to the cell; C2: released doublet particles in the extracellular region.

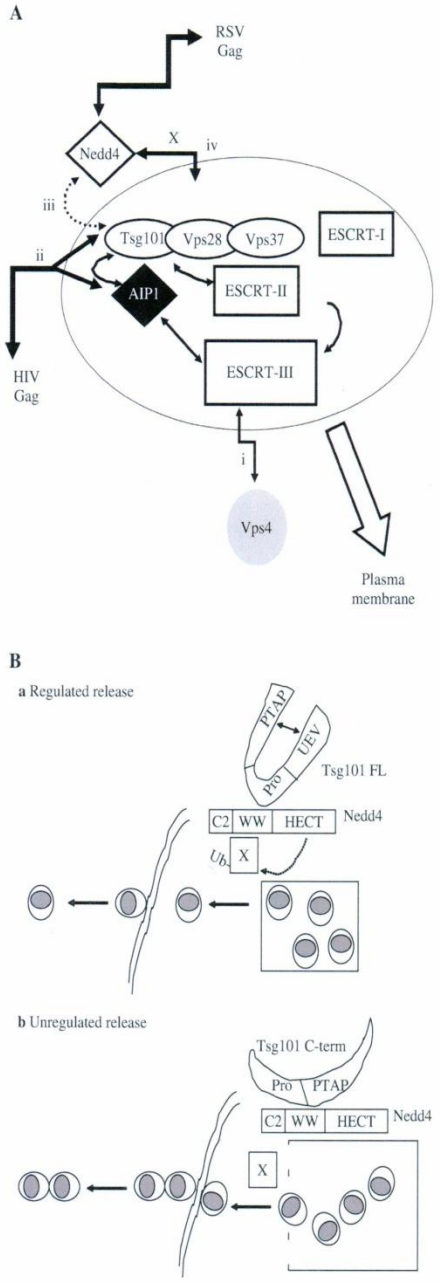

Figure 9: A) Relationship between Rous sarcoma virus (RSV) and HIV-1 Gag-trafficking pathways. B): a) Regulated RSV Gag release mediated by Tsg101–Nedd4 interaction and b) unregulated release resulting from Nedd4 interaction with the Tsg101 C-terminal fragment.

Gag have both been shown to interact with more than one E3 ligase (26,68). Similarly, Tsg101 is not critical for RSV Gag release. By analogy with Mo-MLV, where siRNA-mediated depletion of Tsg101 did not inhibit Gag release (27), RSV release is not expected to require Tsg101: like Mo-MLV, it contains a PY-type L domain. Interestingly, in our study, the C-terminal fragment of Tsg101 had different effects on Mo-MLV and RSV Gag release. It has been reported that the PY motif of Mo-MLV Gag (DPPPYR) binds the E3 ligases WWP1 and WWP2 (68) and not Nedd4 (which binds the PPPPYL motif of RSV Gag) (26). This finding suggests that there are different E3 ligases for different PY motifs. The different manifestations of Tsg101 C-terminal-mediated inhibition might be explained if the fragment interacts with WWP1/WWP2 and Nedd4 differently and if other ligases can provide the release function for RSV Gag. (iv) In contrast to HIV, RSV Gag accesses the machinery through interaction with HECT domain E3 ligases. We speculate that a second factor, designated as X in Figure 9A, provides the link between RSV Gag, Nedd4 and ESCRT protein network.

Although adventitious expression of the Tsg101 C-terminal fragment did not inhibit RSV Gag release in our studies, it nevertheless interfered with a step in the release process, i.e. budding of single particles. Because the Tsg101–Nedd4 interaction was altered by truncation of the N-terminal region, as revealed in both raw images and high-resolution three-dimensional images of the complex (Figure 6), we speculated that, in contrast to Tsg101-FL, the C-terminal Tsg101 fragment interfered with a Nedd4 function that regulates the timing of budding and fission events at the release site to ensure that bud fission occurs before new budding is initiated (Figure 9B). This may be the case for particles detected at the cell surface (Figure 8C) as well as for particles in the intracellular structures visualized using confocal microscopy (Figure 6D), where Gag appeared to be surface-exposed (Figure 6F). Possibly, this putative Nedd4 function involves the X factor proposed to link RSV Gag to the ESCRT machinery (cf. Figure 9A). Closely clustered extracellular RSV particles have been detected following treatment with proteasome inhibitors, which were suggested to limit the pool of free Ub (66). If an ubiquitination event is indeed required for particle-particle fission, our finding that the number of tethered particles increased significantly following co-expression of Gag with the Tsg101 C-term fragment suggests that interaction with the fragment inhibited Nedd4-dependent ubiquitination. Possibly, deletion of the UEV domain in Tsg101 exposed downstream Pro-rich sequences that are normally sequestered, and these, in turn, bound WW domains in Nedd4. These new interactions may have interfered with Nedd4 modification of factor X and, thereby, X-mediated regulation of particle release.

To date, Tsg101 has been shown to interact with the E3 enzymes Mdm2, p300 and Tsg101-associated ligase (69–72). Interestingly, however, although Tsg101 and Nedd4 are both involved in Ub-mediated functions in endocytic trafficking, the two proteins have not previously been linked. Nedd4-mediated monoubiquitinylation is a recognition signal for endocytic trafficking (60). As Tsg101 recognizes monoubiquitinylated cargo and regulates cargo sorting into MVBs (33,40), our findings potentially link these two cellular machineries. Similarly, Nedd4-mediated ubiquitination is a regulator of exocytosis in certain cell types (73). Perhaps our findings indicate that Tsg101 and Nedd4 participate in coordination of sorting and exocytosis events.

The functional exchangeability of the L domains combined with the ability of Tsg101 to interact with different E3 ligases may explain why retroviral trafficking mechanisms once appeared to be flexible and different. However, as all of the domains now appear to be under Vps4 control, there is ultimately no alternative release route for Gag that has entered the endocytic machinery, even if different endocytic pathways are used. Mutations to resistance against agents that target the viruses' use of the machinery should thus be difficult to generate. However, HIV-1 exhibits variable degrees of L-domain-dependence under certain conditions (74,75). Also, as shown here and elsewhere (67), RSV Gag exhibits variable degrees of sensitivity to the Tsg101 C-terminal fragment. It will, thus, be crucial to identify factors that influence whether and how endocytic trafficking pathways are used in order to block alternative routes of virus release.

Materials and Methods

Constructs

HIV-1 and RSV Gag C-terminally tagged with GFP (Gag-GFP) were expressed from *p*CMV-HIV-1*gag* or *p*CMV-RSV*gag* (26,75). Constructs encoding RSV $Pr76^{Gag}$ or N-terminally HA-tagged LDI-1 (amino acids 1–570) in plasmid 2036 were described in Kikonyogo et al. (26). DNA encoding human *vps4A* or *vps4A*-E228Q was a gift of W Sundquist (University of Utah; 27) and was cloned with an HA-tag into the p2036 vector. DNA encoding Hrs-FLAG, Tsg101-myc or fragments thereof was described in Goff et al. (43). Constructs encoding HA-tagged N- or C-terminal fragments of the Tsg101 protein were gifts from E. Freed (60). A construct encoding MLV Gag was a gift from S. Goff (9).

Cell culture, transfection, preparation of cytoplasmic extracts and virus isolation

COS-1 cells were cultured in DMEM supplemented with fetal bovine serum and antibiotics to 60% confluency at 37 °C. Where indicated, the cells were transfected by using the FuGene 6 reagent (Roche, Indianapolis, IN, USA) according to the instructions of the manufacturer. At 48 h post transfection, the cells were harvested by scraping into cold PBS and collected by centrifugation. The pelleted cells were washed with cold PBS, allowed to swell in cold hypotonic buffer [10 mM Tris–HCl (pH 7.4) and 1 mM $MgCl_2$] containing protease inhibitors and disrupted using a Dounce homogenizer with a type B pestle. The total lysate (1 mL) was spun for 10 min at 1000 × *g* at 4 °C to remove unbroken cells, nuclei and mitochondria, producing a total cytoplasmic fraction. For Ip experiments, the cytoplasmic extract was cleared of large particulate material by centrifugation at 10 000 × *g*. To isolate the VLPs assembled by Gag, we filtered the cell culture media (0.45 μm), applied to a cushion of 20% sucrose in a centrifuge tube and then spun at 274000 xg for 90 min at 4 °C (Beckman SW41 rotor). The pelleted VLPs were suspended in 50 μL

of PBS by gentle shaking at 4 °C. Samples were analyzed using SDS–PAGE and Western analysis. Semi-quantitative determinations of VLP release (VLP/cell lysate ratios) were made using a phosphorimager. Where indicated, 293/E cells were also examined. The 293/E cell line is an adenovirus-transformed human embryonic kidney cell line, which is stably expressing the EBNA1 protein of EBV. Transfection and metabolic labeling of cells were performed as previously described (26). Forty-eight hours post transfection, cells were washed twice with PBS and metabolically labeled with ^{35}S-Met and Cys for 2.5 h. Cell lysate and media fractions were collected as described above, and RSV or Mo-MLV Gag was immunoprecipitated using specific polyclonal antibodies.

Ip assay

Protein A agarose beads (Pierce, Rockford, IL, USA) prewashed with immunoprecipitation (Ip) buffer [50 mM Tris–HCl (pH 7.5), 300 mM NaCl, 0.1% Triton-X-100 (TX-100)] containing protease inhibitors (1 mM, Roche), were incubated with the appropriate antibody, added to cytosolic extracts and rotated at 4 °C overnight. Immunoprecipitates were washed in Ip buffer, boiled in SDS sample buffer with 5% mercaptoethanol, resolved by SDS–PAGE and analyzed using Western blotting with the antibodies indicated in the text. Immunoprecipitated proteins were resolved using SDS–PAGE and analyzed using a phosphorimager.

Confocal microscopy

COS-1 cells were cultured in DMEM supplemented with fetal bovine serum and antibiotics to 60% confluency at 37 °C. Where indicated, the cells were transfected using the FuGene 6 reagent according to the instructions of the manufacturer. At 24 h post transfection, the cells were washed once in PBS and fixed in 4% formaldehyde (Fisher, Fairlawn, NJ, USA) in Ca^{2+}-free, Mg^{2+}-free PBS for 20 min. Samples were then washed three times for a total of 5 min with PBS, permeabilized with 0.1% TX-100 for 5 min and washed three times again with PBS. After blocking for 10 min in PBS containing 1% BSA, the cells were incubated with primary antibody for 1 h at 37 °C, rinsed with PBS and then incubated with TRITC-tagged secondary antibody for 30 min at 37 °C. The nuclear stain, Hoechst (Molecular Probes, Eugene, OR, USA), was added in the last 10 min. After rinsing, the cells were mounted using *p*-phenylenediamine and Immunomount. Confocal Images were captured with an inverted fluorescent/dic Zeiss Axiovert 200M microscope equipped with an AxioCam HRm camera (Zeiss, Thornwood, NY, USA) and mercury arc lamp light source using a ×63 Plan-Apochromat (NA 1.40) oil objective and operated using AXIOVISION version 4.1 (Zeiss) software. More than 40 cell images were examined from duplicate samples in each experiment. Approximately 20 optical sections along the *z*-axis were acquired in increments of 0.4 μ. Figures show the central image or, where indicated, a composite of sections through the *z* plane of the cell rendered as a three-dimensional image. The fluorescent data sets were deconvolved using the constrained iterative method (AXIOVISION version 4.1). The following excitation and emission wavelengths were used for imaging: Hoechst stain, $\lambda_{ex}360 \pm 20/\lambda_{em}460 \pm 25$; fluorescein isothiocyanate (for GFP), $\lambda_{ex}480 \pm 20/\lambda_{em}535 \pm 25$; Texas Red (for TRITC), $\lambda_{ex}560 \pm 25/\lambda_{em}645 \pm 35$.

EM

Sixty-millimeter dishes of 293/E cells transfected with p2036-Gag were transfected with DNA encoding the protein indicated in the text above. Total DNA transfected per dish was normalized by using the p2036 vector. Forty-eight hours post transfection, cells were washed with PBS at room temperature and were fixed in 2.5% glutaraldehyde in 0.1 M sodium phosphate buffer (pH 7.4) at 4 °C for 30 min. Cells were scraped from the tissue culture dish and pelleted at 1000 × *g* for 10 min at 4 °C. The cell pellet was fixed for an additional 2 h in 2.5% glutaraldehyde and postfixed for 1 h with osmium tetroxide. The cell pellet was dehydrated in a series of alcohol washes and embedded in Epon. Ultrathin sections were stained with uranyl acetate and lead citrate and examined using a Zeiss 900 electron microscope.

Protein detection

Proteins were separated by electrophoresis through SDS-polyacrylamide gels. Following electrophoresis, the gels were transferred to nitrocellulose and were analyzed using Western blotting with the antibodies specified in the text above. Tsg101 was detected by using mouse monoclonal antibody or polyclonal antibodies (Santa Cruz, Santa Cruz, CA, USA). Anti-Nedd4 polyclonal antibodies were kind gifts obtained from D Rotin (77). Anti-influenza HA epitope mouse monoclonal antibody was purchased from Covance, NJ, USA. Mouse monoclonal anti-CA antibody was purchased from NEN-DuPont (Newtown, CT, USA); monoclonal anti-FLAG antibody, anti-GFP and secondary antibodies were from Sigma (St. Louis, MO, USA). Anti-p6 rat monoclonal antibody was purchased from Advanced BioSciences (Dallas, TX, USA). Proteins were visualized by chemiluminescence using Lumi-Light reagents (Roche) or ECL (Amersham Biosciences, Piscataway, NJ, USA). The RSV polyclonal antibody used for Ip was prepared in rabbits immunized with detergent- and heat-denatured RSV.

Acknowledgments

We thank Dr E. Freed, Dr D. Rotin and Dr J. Wills for reagents. We are grateful to A. Goff and L.S. Ehrlich for helpful advice and discussions. This work was supported by National Institutes of Health grants GM 48294 (to C.C.) and CA 52047 (to J.L.). G.M. was partially supported by a W. Burghardt Turner Fellowship and by funding from NSF-Alliance for Graduate Education in the Professoriate (HRD 0450106).

References

1. Swanstrom R, Wills JW. Synthesis, assembly, and processing of viral proteins. In: Coffin JM, Hughes SH, Varmus, HE, editors. Retroviruses. New York: Cold Spring Harbor Laboratory Press; 1997, pp. 263–334.
2. Wills JW, Cameron CE, Wilson CB, Xiang Y, Bennett RP, Leis J. An assembly domain of the Rous Sarcoma Virus Gag protein required late in budding. J Virol 1994;68:6605–6618.
3. Xiang Y, Cameron CE, Wills JW, Leis J. Fine mapping and characterization of the Rous Sarcoma Virus Pr76gag late assembly domain. J Virol 1996;70:5695–5700.
4. Göttlinger HG, Dorfman T, Sodroski JG, Haseltine WA. Effect of mutations affecting the p6 Gag protein on human immunodeficiency virus particle release. Proc Natl Acad Sci USA 1991;88:3195–3199.
5. Huang M, Orenstein JM, Martin MA, Freed EO. p6 Gag is required for particle production from full-length human immunodeficiency virus type 1 molecular clones expressing protease. J Virol 1995;69: 6810–6818.
6. Demirov DG, Freed EO. Retrovirus budding. Virus Res 2004;106:87–102.
7. Puffer BA, Parent LJ, Wills JW, Montelaro RC. Equine infectious anemia virus utilizes a YXXL motif within the late assembly domain of the Gag p9 protein. J Virol 1997;71:6541–6546.
8. Yasuda J, Hunter EA. Proline-rich motif (PPPY) in the Gag polyprotein of Mason-Pfizer monkey virus plays a maturation-independent role in virion release. J Virol 1998;72:4095–4103.
9. Yuan B, Li X, Goff SP. Mutations altering the Moloney murine leukemia virus p12 Gag protein affect virion production and early events of the virus life cycle. EMBO J 1999;18:4700–4710.
10. Bouamr F, Melillo JA, Wang MQ, Nagashima K, de Los Santos M, Rein A, Goff SP. PPPYVEPTAP motif is the late domain of human T-cell leukemia virus type 1 Gag and mediates its functional interaction with cellular proteins Nedd4 and Tsg101. J Virol 2003;77:11882–11895.
11. Wang H, Machesky NJ, Mansky LM. Both the PPPY and PTAP motifs are involved in human T-cell leukemia virus type 1 particle release. J Virol 2004;78:1503–1512.

12. Gottwein E, Bodem J, Muller B, Schmechel A, Zentgraf H, Krausslich HG. The Mason-Pfizer monkey virus PPPY and PSAP motifs both contribute to virus release. J Virol 2003;77:9474–9485.
13. Harty RN, Paragas J, Sudol M, Palese PA. Proline-rich motif within the matrix protein of vesicular stomatitis virus and rabies virus interacts with WW domains of cellular proteins: implications for viral budding. J Virol 1999;73:2921–2929.
14. Harty RN, Brown ME, Wang G, Huibregtse J, Hayes FPA. PPxY motif within the VP40 protein of Ebola virus interacts physically and functionally with a ubiquitin ligase: implication for Filoviruses budding. Proc Natl Acad Sci USA 2000;97:13871–13876.
15. Ikeda M, Ikeda A, Longan LC, Longnecker R. The Epstein-Barr virus latent membrane protein 2A PY motif recruits WW domain-containing ubiquitin-protein ligases. Virology 2000;268:178–191.
16. Jayakar HR, Murti KG, Whitt MA. Mutations in the PPPY motif of vesicular stomatitis virus matrix protein reduces virus budding by inhibiting a late step in virion release. J Virol 2000;74:9818–9827.
17. Licata JM, Simpson-Holley M, Wright NT, Han Z, Paragus J, Harty RN. Overlapping motifs (PTAP and PPEY) within the Ebola virus VP40 protein function independently as late budding domains: involvement of host proteins Tsg101 and Vps4. J Virol 2003;77:1812–1819.
18. Mayer BJ, Eck MJ. SH3 Domains. Minding your P's and Q's. Curr Biol 1995;5:364–367.
19. Garnier L, Wills JW, Verderame MF, Sudol M. WW Domains and retrovirus budding. Nature 1998;381:744–745.
20. Katoh K, Shibata H, Susuki H, Nara A, Ishidoh K, Kominami E, Yoshimori T, Maki M. The ALG-2-interacting protein Alix associates with CHMP-4b, a human homologue of yeast Snf7 that is involved in multivesicular body sorting. J Biol Chem 2003;278:39104–39113.
21. Parent LJ, Bennett RP, Craven RC, Nelle TD, Krishna NK, Bowzard JB, Wilson CB, Puffer BA, Montelaro RC, Wills JW. Positionally independent and exchangeable late budding functions of the Rous sarcoma virus and human immunodeficiency virus Gag proteins. J Virol 1995;69:5455–5460.
22. Craven RC, Harty RN, Paragas J, Palese P, Wills JW. Late domain function identified in the vesicular stomatitis virus M protein by use of Rhabdovirus-Retrovirus chimeras. J Virol 1999;73:3359–3365.
23. Yuan B, Campbell S, Bacharach E, Rein A, Goff SP. Infectivity of Moloney murine leukemia virus defective in late assembly events is restored by late assembly domains of other retroviruses. J Virol 2000;74:7250–7260.
24. Li F, Chen C, Puffer BA, Montelaro RC. Functional replacement and positional dependence of homologous and heterologous L domains in equine infectious anemia virus replication. J Virol 2002;76:1569–1577.
25. VerPlank L, Bouamr F, LaGrassa TJ, Agresta B, Kikonyogo A, Leis J, Carter CA. Tsg101, a homologue of ubiquitin-conjugating (E2) enzymes, binds the L domain in HIV type 1 Pr55Gag. Proc Natl Acad Sci USA 2001;98:7724–7729.
26. Kikonyogo A, Bouamr F, Vana ML, Xiang Y, Aiyar A, Carter C, Leis J. Proteins related to the Nedd4 family of ubiquitin protein ligases interact with the L domain of Rous sarcoma virus and are required for Gag budding from cells. Proc Natl Acad Sci USA 2001;98:11199–11204.
27. Garrus JE, von Schwedler UK, Pornillos OW, Morham SG, Zavitz KH, Wang HE, Wettstein DA, Stray KM, Cote M, Rich RL, Myszka DG, Sundquist WI. Tsg101 and the vacuolar protein sorting pathways are essential for HIV-1 budding. Cell 2001;107:55–65.
28. Myers EL, Allen JF. Tsg101, an inactive homologue of ubiquitin ligase E2, interacts with human immunodeficiency virus type 2 Gag polyprotein and results in increased levels of ubiquitinated Gag. J Virol 2002;76:11226–11235.
29. Puffer BA, Watkins SC, Montelaro RC. Equine infectious anemia virus utilizes a YXXL motif within the late assembly domain of the Gag p9 protein. J Virol 1998;71:6541–6546.
30. Pornillos O, Garrus JE, Sundquist WI. Mechanisms of enveloped RNA virus budding. Trends Cell Biol 2002;12:569–579.
31. von Schwedler UK, Stuchell M, Muller B, Ward DM, Chung HY, Morita E, Wang HE, Davis T, He GP, Cimbora DN, Scott A, Krausslich HG, Kaplan J, Morham SG, Sundquist WI. The protein network of HIV budding. Cell 2003;114:701–713.
32. Babst M, Odorizzi G, Estepa EJ, Emr SD. Tumor susceptibility gene TSG101 and the yeast homologue, Vps23p, both function in late endosomal trafficking. Traffic 2000;1:242–258.
33. Katzmann DJ, Babst M, Emr SD. Ubiquitin-dependent sorting into the multivesicular body pathway requires the function of a conserved endosomal protein sorting complex, ESCRT-1. Cell 2001;106:145–155.
34. Strack B, Calistri A, Craig S, Popova E, Gottlinger HG. AIP-1/ALIX is a binding partner for HIV-1 p6 and EIAV p9 functioning in virus budding. Cell 2003;114:689–699.
35. Martin-Serrano J, Bieniasz PD. A bipartite late budding domain in human immunodeficiency virus type 1. J Virol 2003;77:12373–12377.
36. Martin-Serrano J, Yarovoy A, Perez-Caballero D, Bieniasz PD. Divergent retroviral late-budding domains recruit vacuolar protein sorting factors by using alternative adaptor proteins. Proc Natl Acad Sci USA 2003;100:12412–12419.
37. Katzmann DJ, Stefan CJ, Babst M, Emr SD. Vps27 recruits ESCRT machinery to endosomes during MVB sorting. J Cell Biol 2003;162:413–423.
38. Babst M, Katzmann DJ, Estepa-Sabal EJ, Meerloo T, Emr SD. ESCRT-III: an endosomal-associated heterooligomeric protein complex required for MVB sorting. Dev Cell 2002;3:271–282.
39. Babst M, Katzmann DJ, Snyder WB, Wendland B, Emr SD. Endosome-associated complex, ESCRT-II, recruits transport machinery for protein sorting at the multivesicular body. Dev Cell 2002;3:283–289.
40. Bache KG, Brech A, Mehlum A, Stenmark H. Hrs regulates multivesicular body formation via ESCRT recruitment to endosomes. J Cell Biol 2003;162:435–442.
41. Bishop N, Woodman P. Tsg101/mammalian Vps23 and mammalian Vps28 interact directly and are recruited to Vps4-induced endosomes. J Biol Chem 2001;276:11735–11742.
42. Pornillos O, Higginson DS, Stray KM, Fisher RD, Garrus JE, Payne M, He G-P, Wang HE, Morham SG, Sundquist WI. HIV Gag mimics the Tsg101 recruiting activity of the human Hrs protein. J Cell Biol 2003;162:425–434.
43. Goff A, Ehrlich LS, Cohen SN, Carter CA. Tsg101 control of human immunodeficiency virus type 1 Gag trafficking and release. J Virol 2003;77:9173–9182.
44. Scherer NM, Lehmann MJ, Jimenez-Soto LF, Ingmundson A, Horner SM, Cicchetti G, Allen PG, Pypaert M, Cunningham JM, Mothes W. Visualization of retroviral replication in living cells reveals budding into multivesicular bodies. Traffic 2003;4:785–801.
45. Pelchen-Matthews A, Kramer B, Marsh M. Infectious HIV-1 assembles in late endosomes in primary macrophages. J Cell Biol 2003;162:443–455.
46. Nydegger S, Foti M, Derdowski A, Spearman P, Thali M. HIV-1 egress is gated through late endosomal membranes. Traffic 2003;4:902–910.
47. Tanzi GO, Piefer AJ, Bates P. Equine infectious anemia virus utilizes host vesicular protein sorting machinery during particle release. J Virol 2003;77:8440–8447.
48. Morita E, Sundquist WI. Retrovirus budding. Annu Rev Cell Dev Biol 2004;20:395–425.
49. Lemmon SK, Traub LM. Sorting in the endosomal system in yeast and animal cells. Curr Opin Cell Biol 2000;12:457–466.
50. Komada M, Masaki R, Yamamoto A, Kitamura N. Hrs, a tyrosine kinase substrate with a conserved double zinc finger domain, is localized to the cytoplasmic surface of early endosomes. J Biol Chem 1997;272:20538–20544.

51. Raiborg C, Bache K, Gillooly D, Madhust I, Stang E, Stenmark H. Hrs sorts ubiquitinated proteins into clathrin-coated microdomains of early endosomes. Nat Cell Biol 2002;4:394–398.
52. Chin L-S, Raynor MC, Wei X, Chen HQ, Li L. Hrs interacts with sorting nexin 1 and regulates degradation of epidermal growth factor receptor. J Biol Chem 2001;276:7069–7078.
53. Bishop N, Horman A, Woodman P. Mammalian class E Vps proteins recognize ubiquitin and act in the removal of endosomal protein-ubiquitin conjugates. J Cell Biol 2002;157:91–101.
54. Lu Q, Hope LW, Brasch M, Reinhard C, Cohen SN. Tsg101 interaction with Hrs mediates endosomal trafficking and receptor downregulation. Proc Natl Acad Sci USA 2003;100:7626–7631.
55. Katz M, Shtiegman K, Tal-Or P, Yakir L, Mosesson Y, Harari D, Machluf Y, Asao H, Jovin T, Sugamura K, Yarden Y. Ligand-independent degradation of epidermal growth factor receptor involves receptor ubiquitylation and Hgs, an adaptor whose ubiquitin-interacting motif targets ubiquitylation by Nedd4. Traffic 2002;3:740–751.
56. Lloyd T, Atkinson R, Wu M, Zhou Y, Penetta G, Bellen H. Hrs regulates endosome membrane invagination and tyrosine kinase receptor signaling in Drosophila. Cell 2002;108:261–269.
57. Fujita H, Yamanaka M, Imamura K, Tanaka Y, Nara A, Yoshimori T, Yolota S, Himeno MA. Dominant negative form of the AAA ATPase SKD1/VPS4 impairs membrane trafficking out of endosomal/lysosomal compartments: class E Vps phenotype in mammalian cells. J Cell Sci 2003;116:401–414.
58. Vana ML, Tang Y, Chen A, Medina G, Carter C, Leis J. Role of Nedd4 and ubiquitination of Rous sarcoma virus Gag in budding of virus-like particles from cells. J Virol 2004;78:13943–13953.
59. Shehu-Xhilaga Ablan S, Demirov DG, Chen C, Montelaro RC, Freed EO. Late domain-dependent inhibition of equine infectious anemia virus budding. J Virol 2004;78:724–732.
60. Rotin D, Staub O, Haguenauer-Tsapis R. Ubiquitination and endocytosis of plasma membrane proteins: role of Nedd4/Rsp5p family of ubiquitin-protein ligases. J Membr Biol 2000;176:1–17.
61. Koonin EV, Abagyan RA. Tsg101 may be the prototype of a class of dominant negative ubiquitin regulators. Nat Genet 1997;16:330–331.
62. Ponting CP, Cai Y-D, Bork P. The breast cancer gene product Tsg101: a regulator of ubiquitination? J Mol Med 1997;75:467–469.
63. Pornillos O, Alam S, Rich RL, Myszka DG, Davis DR, Sundquist WI. Structural and functional interactions of the Tsg101 UEV domain. EMBO J 2002;21:2397–2406.
64. Eastman SW, Martin-Serrano J, Chung W, Zang T, Bieniasz PD. Identification of human Vps37C, a component of ESCRT-1 important for viral budding. J Biol Chem 2005;280:628–636.
65. Goila-Gaur R, Demirov DG, Orenstein JM, Ono A, Freed EO. Defects in human immunodeficiency virus budding and endosomal sorting induced by Tsg101 over-expression. J Virol 2003;77:9474–9485.
66. Patniak A, Chau V, Wills JW. Ubiquitin is part of the retrovirus budding machinery. Proc Natl Acad Sci USA 2000;97:13069–13074.
67. Johnson MC, Spidel JL, Ako-Adjei D, Wills JW, Vogt VM. The C-terminal half of Tsg101 blocks Rous sarcoma virus budding and sequesters Gag into unique nonendosomal structures. J Virol 2005;79:3775–3786.
68. Martin-Serrano J, Eastman SW, Chung W, Bieniasz PD. HECT Ubiquitin ligases and virus release. J Cell Biol 2005;168:89–101.
69. Li L, Liao J, Ruland J, Mak T, Cohen SN. A Tsg101/MDM2 regulatory loop modulates MDM2 degradation and MDM2/p53 feedback control. Proc Natl Acad Sci USA 2001;98:1616–1624.
70. Sun Z, Pan J, Hope W, Cohen S, Balk S. Tumor susceptibility gene 101 protein represses androgen receptor transactivation and interacts with p300. Cancer 1999;86:689–696.
71. Amit I, Yakir L, Katz M, Zwang Y, Marmor M, Citri A, Shtiegman K, Alroy I, Tuvia S, Reiss Y, Roubini E, Cohen M, Wides R, Bacharach E, Schubert U et al. Tal, a Tsg101-specific E3 ubiquitin ligase, regulates receptor endocytosis and retrovirus budding. Genes Dev 2004;18:1737–1752.
72. Grossman S, Deato M, Brignone C, Chan H, Kung A, Togami H, Nakatami Y, Livingston D. Polyubiquitination of p53 by a Ubiquitin Ligase activity of p300. Science 2003;300:342–344.
73. Hegde AN. Ubiquitin-proteasome-mediated local protein degradation and synaptic plasticity. Prog Neurobiol 2004;73:311–357.
74. Ono A, Freed EO. Cell-type dependent targeting of human immunodeficiency virus type 1 assembly to the plasma membrane and the multivesicular body. J Virol 2004;78:1552–1563.
75. Demirov DG, Orenstein JM, Freed EO. The late domain of human immunodeficiency virus type 1 p6 promotes virus release in a cell type-dependent manner. J Virol 2002;76:105–117.
76. Hermida-Matsumoto L, Resh MD. Localization of human immunodeficiency virus type 1 Gag and Env at the plasma membrane by confocal imaging. J Virol 2000;74:8670–8679.
77. Staub O, Yeger H, Plant PJ, Kim H, Ernst SA, Rotin D. Immunocolocalization of the ubiquitin-protein ligase Nedd4 in tissues expressing the epithelial Na+ channel (ENaC). Am J Physiol 1997;272:1871–1880.

CHAPTER 4: Alternative trafficking pathway of ASV Gag mediated by ESCRTs

Summary

In the previous chapter, I investigated the requirement for Tsg101 in ASV Gag trafficking and release using mammalian cell lines. In this chapter, I explore in more detail the requirement of ASV Gag for Tsg101 using avian cells, which are the natural hosts. I confirm that Tsg101 is not required for virus production in the natural host by demonstrating that siRNA targeted to mRNA encoding Tsg101 did not have a negative effect on VLP production in avian cells that were constitutively expressing ASV Gag, even though the endogenous pool of Tsg101 in these cells was depleted. I also show that Tsg101 can substitute for Nedd4, the natural cellular protein binding partner for ASV Gag, in promoting efficient budding by demonstrating that the release of a chimeric ASV Gag lacking the Nedd4 binding site was rescued by translational fusion to Tsg101. Surprisingly, however, Tsg101 directed ASV Gag to a different membrane region for VLP assembly and release since the particles containing Tsg101 lacked markers of endosomal-like membrane domains that were detected in particles assembled from the wild type ASV Gag protein. Based on this study, we conclude that Tsg101 can substitute for Nedd4 to allow ASV Gag release but these two cellular co-factors direct Gag release through functionally exchangeable but distinct pathways.

Specific Contribution: I designed and performed the experiments in Figures 1A, 4, 5A-H, and contributed to the writing of the manuscript. The attached publication, Medina *et al*, 2008 in the Virology Journal was provided by the copyright owner, Elsevier and permission has been granted for its use in this dissertation. License # 1970810613203

Virology 377 (2008) 30–38

Contents lists available at ScienceDirect

Virology

journal homepage: www.elsevier.com/locate/yviro

Tsg101 can replace Nedd4 function in ASV Gag release but not membrane targeting

Gisselle Medina [a,1], Andrew Pincetic [b,1], Lorna S. Ehrlich [a], Yongjun Zhang [b], Yi Tang [c], Jonathan Leis [b], Carol A. Carter [a,*]

[a] Department of Molecular Genetics and Microbiology, Stony Brook University, Stony Brook, N.Y. 11794-5222, USA
[b] Department of Microbiology and Immunology, Northwestern University Feinberg School of Medicine, Chicago, IL 60611, USA
[c] Children's Memorial Hospital, Chicago, IL 60611, USA

ARTICLE INFO

Article history:
Received 17 December 2007
Returned to author for revision
29 January 2008
Accepted 14 April 2008

Keywords:
Tsg101
Nedd4
ASV
HIV-1
Gag
L domain

ABSTRACT

The Late (L) domain of the avian sarcoma virus (ASV) Gag protein binds Nedd4 ubiquitin ligase E3 family members and is the determinant of efficient virus release in avian and mammalian cells. We previously demonstrated that Nedd4 and Tsg101 constitutively interact raising the possibility that Nedd4 links ASV Gag to the ESCRT machinery. We now demonstrate that covalently linking Tsg101 to ASV Gag lacking the Nedd4 binding site (Δp2b-Tsg101) ablates the requirement for Nedd4, but the rescue of budding occurs by use of a different budding mechanism than that used by wild type ASV Gag. The evidence that Tsg101 and Nedd4 direct release by different pathways is: (*i*) Release of the virus-like particles (VLPs) assembled from Gag in DF-1, an avian cell line, was resistant to dominant-negative interference by a Tsg101 mutant previously shown to inhibit release of both HIV and Mo-MLV. (*ii*) Release of VLPs from DF-1 cells was resistant to siRNA-mediated depletion of the endogenous pool of Tsg101 in these cells. (*iii*) VLPs assembled from wild-type ASV Gag exhibited highly efficient release from endosome-like membrane domains enriched in the tetraspanin protein CD63 or a fluorescent analogue of the phospholipid phosphatidylethanolamine. However, the VLPs assembled from the L domain mutant Δp2b or a chimeric Δp2b-Tsg101 Gag lacked these domain markers even though the chimeric Gag was released efficiently compared to the Δp2b mutant. These results suggest that Tsg101 and Nedd4 facilitate Gag release through functionally exchangeable but independent routes and that Tsg101 can replace Nedd4 function in facilitating budding but not directing through the same membranes.

Introduction

Expression of the retroviral structural precursor polyprotein, Gag, is sufficient for the production of non-infectious viral-like particles (VLPs; Gottlinger, 2001). Gag contains 3 distinct domains necessary for virus assembly and budding (Wills and Craven, 1991). The membrane-binding (M) domain mediates the association of Gag to the plasma membrane via a cluster of basic residues and, in some retroviruses, a myristic acid moiety co-translationally added to the N-terminus of the Gag precursor (Spearman et al., 1994; Zhou and Resh, 1996). The interaction (I) domain promotes Gag–Gag multimerization crucial for particle assembly (Burniston et al., 1999; Cimarelli et al., 2000; Sanderfur et al., 1998) and the late assembly (L) domain facilitates the pinching off of viral particles from the plasma membrane (Gottlinger et al., 1991; Xiang et al., 1996; *reviewed in* Bieniasz, 2006). L domains have been identified in all retroviruses studied to date, as well as in other families of enveloped viruses, such as the Rhabdoviruses, Paramyxoviruses, and Filoviruses (Bieniasz, 2006). Retroviral L domains are categorized into three classes, defined by their conserved amino acid core sequence: the Pro-Thr-X-Pro (usually PTAP) motif (Gottlinger et al., 1991); the Pro-Pro-X-Tyr (PY) motif (Wills et al., 1994); and the Tyr-X-X-Leu (YXXL) motif (Puffer et al., 1997). Acting as docking sites for cellular proteins, L domains recruit components of the endocytic trafficking pathway to execute the fission of viral from cellular membranes during the budding process (Garrus et al., 2001; Kikonyogo et al., 2001; Martin-Serrano et al., 2001, 2003; Strack et al., 2003; VerPlank et al., 2001; von Schwedler et al., 2003).

Through the PTAP motif, HIV-1 Gag binds directly to Tsg101 (Garrus et al., 2001; Martin-Serrano et al., 2001; VerPlank et al., 2001). Genetic screening utilizing the yeast two-hybrid assay identified ~20 proteins involved in vacuolar protein sorting that function in conjunction with Tsg101 [von Schwedler et al., 2003]. Disrupting the normal function of these vacuolar *p*rotein *s*orting (*vps*) proteins, termed "class E" Vps proteins, induces formation of abnormally enlarged endosomes (class E compartments) in which Vps proteins become trapped (Raymond et al., 1992) and VLP release is consequently blocked. The class E Vps proteins function in complexes called *e*ndosomal *s*orting *c*omplex required for *t*ransport (ESCRT)-0, -1, -2,

* Corresponding author. Life Sciences Bldg., Rm. 248, Stony Brook University, Stony Brook, N.Y. 11794-5222, USA. Fax: +1 631 632 9797.
E-mail address: ccarter@ms.cc.sunysb.edu (C.A. Carter).
[1] These authors contributed equally.

0042-6822/$ – see front matter © 2008 Elsevier Inc. All rights reserved.
doi:10.1016/j.virol.2008.04.024

and -3, which may normally be sequentially recruited from the cytosol to deliver cargo to the late endosome/multivesicular body (LE/MVB) compartment where it is sorted for delivery to its ultimate destination. In yeast, the destination is most often vacuoles (equivalent to lysosomes). The ESCRT complexes associated with the limiting membrane of late endosomes are released back into the cytosol through the action of the AAA ATPase Vps4 (Babst et al., 1998). Vps4 containing mutations that disrupt its ATPase activity are dominant negative inhibitors of VLP release (Garrus et al., 2001; Medina et al., 2005).

Tsg101 is a component of ESCRT-I that recognizes cargo proteins modified by ubiquitin, triggering the ESCRT machinery to induce MVB biogenesis (Bishop et al., 2002; Katzmann et al., 2001). PY motifs bind directly to members of the Nedd4 family of HECT ubiquitin (E3) ligases, which ubiquitinate cargo destined for delivery to degradative compartments. Nedd4 may therefore function upstream of Tsg101 and the other ESCRT proteins in the assembly and release pathway of ASV. Tsg101 and Nedd4 associate constitutively in the cytoplasm (Medina et al., 2005), however, Tsg101 also has been found to associate with several other E3 enzymes (Amit et al., 2004; Kim et al., 2007; Li et al., 2001). Here, we demonstrate that release of ASV Gag from avian cells is insensitive to dominant negative-interference or depletion of Tsg101, indicating that ASV Gag release may not require Tsg101 for budding. Also, although release of chimeric ASV Gag lacking the Nedd4 binding site was rescued by translational fusion to Tsg101, the particles containing Tsg101 lacked the markers of transit through endosome-like membrane domains that characterized wild-type ASV Gag release. Interestingly, the particles assembled from another ESCRT-1 component, Vps37C, behaved similarly while chimeric VLPs formed with an ESCRT-2 or an ESCRT-3 factor behaved like the wild-type. Together, these findings suggest that although the Tsg101- and Nedd4-directed pathways are functionally exchangeable in the release process, the cellular proteins facilitate release through independent mechanisms and different membrane domains.

Results

Co-expression of ASV Gag with a dominant negative interference fragment of Tsg101 (Tsg-DN) in avian cells did not reduce ASV release efficiency

Our previous findings showed that fragments of Tsg101 that inhibit release of HIV-1 and Mo-MLV Gag in a dominant-negative manner failed to appreciably inhibit ASV Gag release from 293E or COS-1 cells [Medina et al., 2005 *and data not shown*]. In this study, we examined ASV release from avian DF-1 cells (Himly et al., 1998; Schaefer-Klein et al., 1998). The same Tsg101 fragment used in the previous study (Tsg-DN; Medina et al., 2005) was transfected into the DF-1 cells. The fragment induced the formation of large, aberrant structures in the cytoplasm Fig. 1, panel A), as was previously observed in both avian and mammalian cells (Goila-Gaur et al., 2003; Johnson et al., 2005; Medina et al., 2005). The Tsg101 fragment was then co-transfected with GFP-tagged ASV Gag (containing a D37S mutation to inactive PR), and viral particles were harvested from the media fraction 48 h later. As shown in the Western blot in Fig. 1B and the semi-quantitative analysis of VLP release in Fig. 1C, virus release from DF-1 cells was resistant to dominant negative interference by the Tsg101 fragment. In a separate experiment, DF-1 cells constitutively expressing ASV (DF1/RCASPB(A) (Himly et al., 1998; Schaefer-Klein et al., 1998) were mock-transfected or transfected with DNA encoding Tsg-DN and examined by electron microscopy after thin sectioning (*panel D, left and right, respectively*). Fully assembled particles were observed outside of the mock-transfected and the Tsg-DN-transfected cells (*enlarged in insets D1 and D2, respectively*). The effect of expression of the Tsg-DN in DF-1/RCASPB(A) cells can be seen in the right panel in D, where aggregates of particles are detected inside of cells (*enlarged in inset D3*). These aggregates were not observed in the mock transfected cells (*left panel*). Taken together with the results in 293E and COS-1 cells (Medina et al., 2005), these observations suggest that ASV Gag assembly and release is resistant to any disruption of the endocytic machinery that expression of the Tsg101 fragment may cause in these cells.

Depletion of endogenous Tsg101 did not inhibit ASV Gag release

To further examine whether VLP release requires Tsg101 function, we determined the effect of siRNA-mediated depletion of the endogenous pool of Tsg101 in DF-1 cells on ASV Gag release. We used a siRNA sequence designed to specifically target avian Tsg101 expression. Gag proteins in lysates prepared from *gag*-transfected cells and VLP in media were harvested at 48 h post-transfection as described in Materials and methods and analyzed by SDS-PAGE and Western blotting. As shown in Fig. 2 (*panel A*), treatment with Tsg101-specific siRNA (20 or 50 nM) was sufficient to deplete cells of ~90% of the Tsg101 protein compared to the same amount of control, non-targeting siRNA (compare *lanes 1 and 2 to lanes 3 and 4, respectively*). Under these conditions, the steady-state level of actin and the amount of Gag detected in the lysate were not detectably reduced. The significant depletion of endogenous Tsg101 also failed to inhibit ASV Gag release. A semi-quantitative analysis (VLP/Cell lysate+VLP) *panel B*) indicated that the budding efficiency of ASV VLPs was not significantly different from control levels. These results indicate that WT ASV Gag release is not dependent on the steady-state level of Tsg101 in its natural host cell and suggest that budding may occur independently of Tsg101 and therefore, perhaps, the ESCRT-I complex.

Tsg101 replaced Nedd4 function in ASV Gag budding

Taken together, the observed resistance of ASV Gag budding to co-expression with Tsg-DN and to siRNA-mediated Tsg101 depletion indicates that ASV Gag is not strongly dependent on Tsg101 for release. To determine whether Tsg101 could substitute for Nedd4 in mediating the release function, the protein was translationally fused to the C-terminus of Gag-Δp2b, an L domain mutant that lacks the Nedd4 docking site, to form a chimeric Gag protein, Δp2b-Tsg101 (described in Materials and methods). As avian Tsg101 has not been isolated, human (293E), rather than avian, cells were used for these experiments so that the Tsg101 in the chimeric Gag protein, the Tsg101 being tested for its effect *in trans* (i.e., adventitiously expressed Tsg101), and the Tsg101 in the cytoplasm would all be identical sequences. As shown in Fig. 3, VLPs assembled from wild-type (WT) ASV Gag were released into the media with high efficiency (*panel A*) in the absence (*lane 1*) or presence (*lane 2*) of adventitious Tsg101 expression, consistent with previous findings (Medina et al., 2005). The L domain mutant Δp2b was released at <10% of WT efficiency (Kikonyogo et al., 2001; Medina et al., 2005) and this level was the same whether Tsg101 was expressed or not (*lanes 3 and 4*). Translational fusion of Tsg101 to the Gag-Δp2b mutant to form Gag Δp2b-Tsg101 resulted in production of significantly more VLPs (*lane 5*), indicating that the release function was rescued, however, the wild-type level was never achieved. An estimate of VLP release efficiency indicated that VLPs containing the chimeric ASV Gag protein budded at a level of ~50% compared to WT protein (*panel B*) ($n=4$). Consistent with previous findings (Martin-Serrano and Bieniasz, 2003), we observed that translational fusion of Tsg101 to an L domain mutant of HIV-1 Gag (P7L-Tsg101) resulted in efficient rescue (*panel B inset*). Although the level of rescue obtained for ASV Gag-Δp2b was lower than that obtained for HIV-1 Gag P7L under similar conditions, the results nevertheless indicate that Tsg101 can replace the Nedd4 function required for ASV Gag budding.

Tsg101 and Nedd4 direct VLP release from different membrane microdomains

Tsg101 and Nedd4 may direct release through functionally unlinked pathways. If so, a switch from the Nedd4-dependent mechanism to a Tsg101-dependent mechanism might be accompanied by changes in Gag trafficking. We therefore tested for changes in Gag delivery to the budding site using as membrane markers the endosomal lipid tracer, 1,2-dipalmitoyl-*sn*-glycero-3-phosphoethanolamine-*N*-[lissamine rhodamine B sulfonyl] (N-Rh-PE), a fluorescent

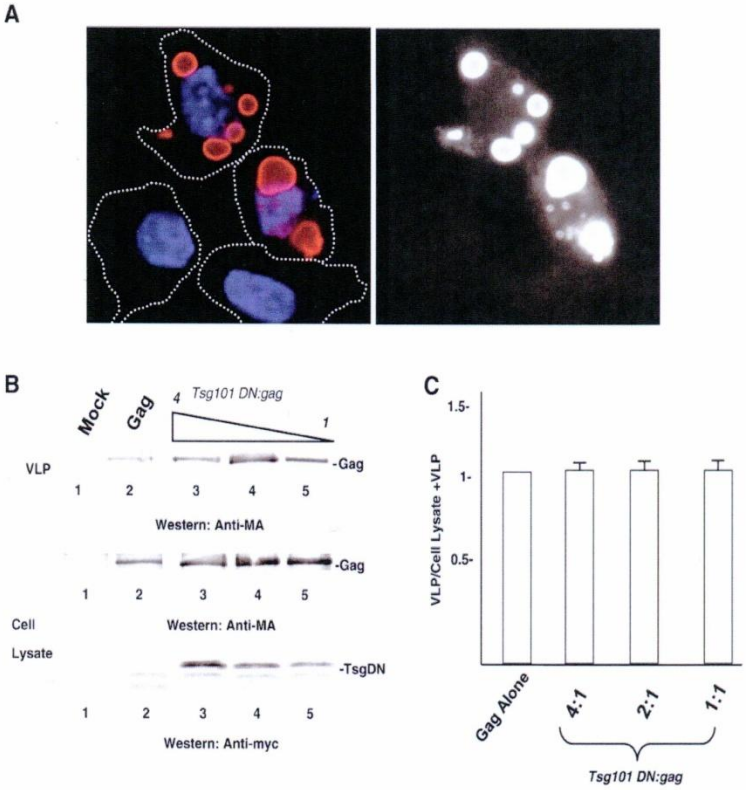

phosphatidyl ethanolamine analogue (Vidal et al., 1997; Willem et al., 1990) or the tetraspanin protein CD63, a marker of late endosome (LE) membranes found at steady-state mostly on LE/multivesicular body (LE/MVB) compartments but also on the plasma membrane (Nydegger et al., 2003, 2006). To do these experiments, 24 h post-transfection N-Rh-PE was added to the media for 1 h at 4 °C, the cells were then washed, and incubated an additional 24 h at 37 °C. In all cases, VLPs isolated from the media were purified through sucrose cushions, spun onto poly-lysine-coated coverslips, and examined by deconvolution confocal microscopy. As shown in Fig. 4A, only small amounts of the markers were detected in the VLPs formed when HIV-1 Gag was expressed alone. VLPs assembled from P7 L-GFP or P7L-Tsg101 also contained little N-Rh-PE (*panels B and C*) or CD63 (*not shown*).

To examine the VLPs assembled from ASV Gag, COS-1 cells were transfected with DNA encoding the WT Gag, the L domain mutant (Δp2b), or the chimeric Gag protein (Δp2b-Tsg101) and labeled with N-Rh-PE in the same manner as the cells described above expressing HIV-1 Gag. Fig. 5 shows images representative of the samples in at least three independent experiments. In contrast to HIV-1 Gag, most of the particles assembled from WT ASV Gag-GFP contained the lipid marker (82%, $n=300$), as indicated by the co-localization of the Gag-GFP and the rhodamine (red) fluorescence of N-Rh-PE in yellow particles (Fig. 5, *panel C*). The fluorescent signal was specific, as no signal was detected in mock-treated control samples derived from untransfected cells similarly treated with N-Rh-PE (*panel A*). In contrast to WT ASV particles, few VLPs assembled from the Δp2b-GFP mutant (*panel B*) contained the tracer (7%; $n=375$), indicating that these particles were not released from the same membrane region as WT VLPs and suggesting that Nedd4 binding is necessary for association with such membranes. Consistent with this supposition, WT but not Δp2b co-localized with N-Rh-PE-positive membranes in the cytoplasm (*not shown*). VLPs released from cells expressing the chimeric Δp2b-Tsg101 protein were detected by indirect immunofluorescence using antibody against the MA domain in Gag (*panel D*). Like the ASV Δp2b VLPs, few particles assembled from the chimeric Δp2b-Tsg101 Gag protein contained the N-Rh-PE tracer (1%, $n=650$). Similar results were obtained by fusing Vps37C (*panel E*). Interestingly, N-Rh-PE was detected in VLPs released from cells expressing Δp2b fused to Eap20 (*panel F;* 55%, $n=180$) or Chmp4B (*panel F, inset;* 40%, $n=20$). These results suggest that the WT and the chimeric VLPs containing Tsg101 or its binding partner Vps37C were released from different membrane regions. Apparently, Nedd4 was necessary for association with the membrane domains containing N-Rh-PE. Eap20 or Chmp4B could substitute for Nedd4 in this regard.

If Nedd4, but not Tsg101, indeed directs ASV VLP release from endosome-like membrane domains, CD63 might also be present in the particles. VLPs, isolated as described above, were therefore examined for CD63 by indirect immunofluorescence. As shown in *panel G*, VLPs assembled from WT ASV Gag contained the tetraspanin protein in amounts ranging from 10% ($n=150$) to 40% ($n=150$), supporting the conclusion that the particles budded through endosome-like membrane domains. In contrast, no CD63 was detected in VLPs assembled from Δp2b (*not shown*) or Δp2b-Tsg101 (*panel H*). The absence of both N-Rh-PE and CD63 from these particles supports the notion that Nedd4 directs Gag to endosome-like membrane domains while in its absence, either by deletion of the Nedd4 docking site or by substitution of Tsg101, Gag associates with a different membrane region.

Discussion

Unlike PTAP- and YPDL-type L domains, which bind Tsg101 (Vps23) and Alix (Vps31), respectively, and therefore directly link Gag to class E Vps proteins, the PY-type L domains, which bind the Nedd4 family of HECT ubiquitin ligases (Kikonyogo et al.; 2001; Vana et al., 2004), must access the MVB machinery in a different way. Previously, we established that Nedd4-like proteins bind to Tsg101 and that this interaction allows ASV Gag to co-localize with Tsg101 (Medina et al., 2005). This might provide ASV Gag with access to the Tsg101-directed pathway and to ESCRT factors that it requires for budding, such as Eap20 (Pincetic, Medina, Carter, and Leis, *submitted*).

We showed here that ASV Gag release from avian cells was not blocked following co-expression of Gag with Tsg-DN or by depletion of the endogenous pool of Tsg101. Similar interventions have been shown to inhibit release of HIV-1 Gag from primate cells (Garrus et al., 2001; Goila-Gaur et al., 2003; Medina et al., 2005 and *data not shown*). Tsg-DN has been shown to induce formation of aberrant endosomes that disrupt endocytic sorting (Goila-Gaur et al., 2003; Johnson et al., 2005). We detected similar aberrant structures in DF-1 cells. Nevertheless, we observed no inhibition of ASV Gag release. We demonstrated that Tsg101 can replace Nedd4 and rescue Δp2b release (Fig. 3). This observation suggests that the function of Nedd4 in ASV release can be replaced by Tsg101 and most likely explains the well-documented functional exchangeability of the HIV-1 and ASV L domains (Parent et al., 1995). However, our studies now provide evidence that the L domain contributes to membrane targeting as we found that different outcomes result from Nedd4-, Eap20-, or Chmp4B- *vs* Tsg101- or Vps37C-facilitated budding. It is interesting that neither Tsg101 nor Vps37C, which are linked in ESCRT-1, rescued the membrane targeting of WT ASV Gag. In contrast, this function was rescued by Eap20 and Chmp4B, which are linked through Chmp6 (Yorikawa et al., 2005).

Although the translational fusion of Tsg101 to Gag-Δp2b restored Gag release, it placed Tsg101 on every Gag molecule, raising the possibility that potential steric effects hindered an association between the chimeric Gag proteins and membranes containing N-Rh-PE or CD63. This possibility is unlikely because the chimeric Gag proteins were found to associate with N-Rh-PE- and CD63-positive membranes in the cytoplasm (*data not shown*). Moreover, we showed that the translational fusion of Eap20 or Chmp4B to Gag-Δp2b restored both release and WT targeting. Most likely, Tsg101 and Nedd4 do not direct ASV trafficking via the same route as we observed that depletion of Tsg101 was not effective in blocking release of the WT ASV Gag compared to the previously described effect (Garrus et al., 2001) of Tsg101 depletion on HIV Gag release. As already noted, Nedd4 function is apparently not required when Tsg101 is provided *in cis* (Pincetic, Medina, Carter, and Leis, *submitted*). These considerations lead us to conclude that Nedd4 family members direct release through a pathway that functionally parallels that directed by Tsg101. The fact that neither Δp2b-Tsg101 nor -Eap20 form a stable complex with Nedd4 (Pincetic, Medina, Carter, Leis) suggests that Nedd4 may not be needed to enter the pathways they target. Perhaps shared binding partners normally provide a conduit to Tsg101 and ESCRT-regulated trafficking pathways. It is

Fig. 1. Co-expression of ASV Gag and Tsg-DN in avian cells does not reduce ASV release efficiency. Panel A, confocal microscopy of DF-1 cells transfected with Tsg-DN. Left, field showing proximal untransfected cells and cells expressing TRITC-tagged Tsg-DN (red). Dashed lines show cell outline. Right, same field showing localization of Tsg-DN-induced structures within the cell. Panel B, DF-1 cells were mock-transfected (lane 1) or transfected with DNA encoding ASV gag (lanes 2–5) and the indicated ratio of Tsg-DN (lane 3, TsgDN: gag, 4 μg:1 μg; lane 4, 2 μg:1 μg; lane 5, 1 μg:1 μg). Media and cell lysate fractions were harvested at 48 h post-transfection. VLPs were isolated from the media as described in Materials and methods. Total cell lysates were immunoprecipitated overnight with anti-RSV polyclonal antibody. Gag protein in VLPs and lysates were detected by immunoblotting with anti-MA monoclonal antibody. TsgDN expression was determined by Western analysis of the cell lysate, using a monoclonal antibody against the myc tag on the Tsg101 fragment. Panel C, semi-quantitative analysis of VLP release (VLP/Cell lysate + VLP). The panels show the ratio of the Gag signal (determined using NIH image) in VLP isolated from the media to the sum of the Gag signals in cell lysate plus VLP ($n=2$). Panel D, electron microscopy of mock-transfected DF-1 cells constitutively expressing ASV [DF-1/RCASBP(A), left] or DF-1/RCASBP(A) cells transfected with DNA encoding TsgDN (right). Cells were prepared for thin section EM as described in Materials and methods. Arrows denote regions enlarged in the insets. Inset, D1, D2: Virus particles in extracellular space; D3, particles in intracellular vesicle.

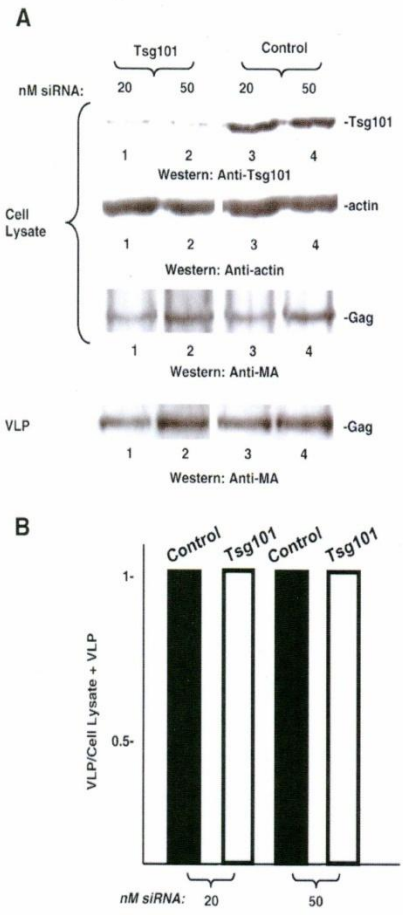

Fig. 2. Depletion of endogenous Tsg101 in DF-1 cells by siRNA-targeting. Panel A, DF-1 cells were transfected with Tsg101-specific siRNA (lanes 1 and 2) or control siRNA (lanes 3 and 4) for 48 h followed by transfection with DNA encoding ASV Gag-GFP for 24 h. Gag proteins in lysates and media were isolated as described in Materials and methods and analyzed by SDS-PAGE and Western blotting. The endogenous Tsg101 level in each sample was determined by Western analysis of the total lysate. Panel B, semi-quantitative analysis of ASV Gag release efficiency.

interesting to note that release of HIV with L domain mutations has been demonstrated to be rescued by over-expression of Nedd4-like variants (Chung et al., 2008; Usami et al., 2008). Over-expression of these variants in cells expressing HIV-1 Gag with Tsg101 and AIP-1 binding site mutations was found to rescue VLP release. Over-expression or depletion of the variants had no detectable effect on WT HIV-1, suggesting that rescue represents an alternative mechanism that the virus uses to release from cells. As noted above, Tsg101 is known to bind several E3 proteins in the cytoplasm, including avian Nedd4. As we found no requirement for Tsg101, it is unlikely that the interaction plays a critical role in the release function. Although the precise site of interaction between Tsg101 and Nedd4-like proteins has not been mapped, we showed previously that the interaction utilized the C-terminal region of Tsg101 and the N-terminal portion of the Nedd4 protein (Medina et al., 2005). This indicates that the interaction is not a canonical E2-E3 interaction, which would require the N-terminal ubiquitin-E2-like (UEV) domain in Tsg101 and the C-terminal catalytic (HECT) domain in Nedd4. In contrast, the rescue of the L domain defect of HIV by the variants cited above requires the ubiquitin–ligase activity of the enzyme (Chung et al., 2008; Usami et al., 2008). Even if Nedd4 recognizes Tsg101 as an E2 homologue, Nedd4-directed ASV Gag release need not be dependent on Tsg101 if Nedd4, like Tsg101, interacts with other ESCRT proteins.

The differences in use of membrane sites for budding by ASV and HIV-1 Gag may be related to the fact that the M domain membrane transport signals of ASV and HIV-1 Gag differ. The former is found in basic residues in the MA coding sequence and in the fourth alpha helix (Scheifele et al., 2003) while the latter is found in a bipartite motif comprised of basic residues and an N-terminal myristic acid moiety (Zhou et al., 1994). Moreover, Nedd4, which is recruited by the L domain located downstream of MA in the Gag precursor (Kikonyogo et al., 2001), contains a membrane-binding C2 domain (Dunn et al., 2004) that may direct ASV Gag to specific areas of the plasma membrane. This notion is supported by the observation that Gag, which binds the WW domain in Nedd4 (Kikonyogo et al., 2001), co-localized with the protein in different subcellular locations, depending on the presence or absence of the Nedd4 C2 domain (*data not shown*). We speculate that the combination of trafficking signals in both Nedd4 and ASV Gag transports these proteins to

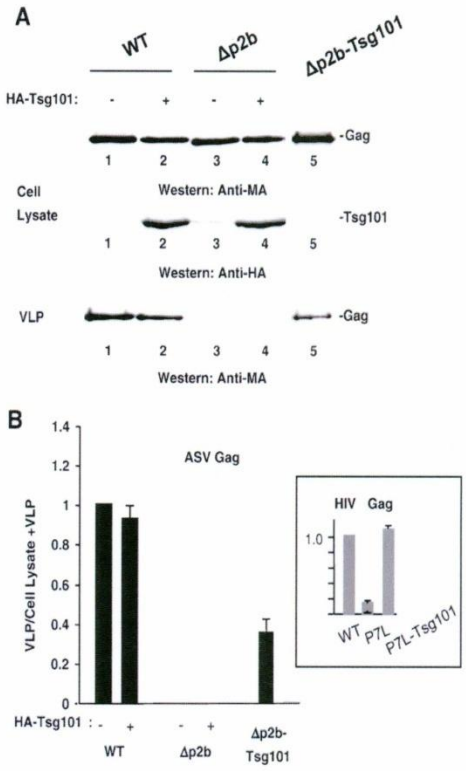

Fig. 3. Translational fusion of Tsg101 to the C-terminus of ASV Gag Δp2b rescues VLP release. Panel A, 293/E cells were transfected with DNA encoding WT ASV Gag (lanes 1 and 2) or L domain-deleted (Δp2b) ASV Gag (lanes 3 and 4) alone (lanes 1 and 3) or with DNA encoding HA-Tsg101 (lanes 2 and 4). Lane 5, cells were transfected with DNA encoding Gag-Δp2b-Tsg101. Cells were harvested 48 h later and examined by Western blotting. Panel A, top: cell lysate probed for Gag; middle: cell lysate probed for HA-Tsg101; bottom: VLP probed for Gag. Panel B, semi-quantitative analysis of ASV VLP release efficiency. Inset, rescue efficiency of P7 L-Tsg101.

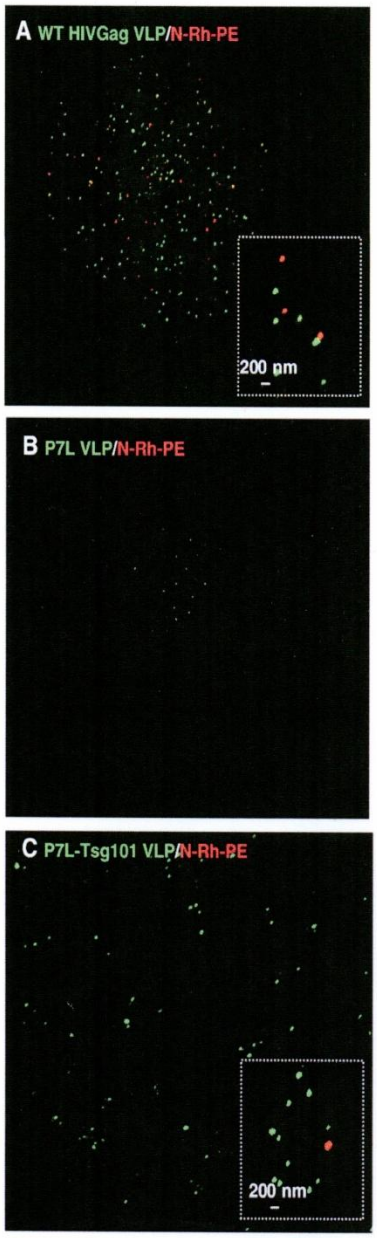

Fig. 4. Examination of WT and chimeric HIV-1 VLPs for N-Rh-PE. VLPs released from COS-1 cells transfected with DNA encoding WT HIV-1 Gag-GFP (panel A), P7L-Gag (panel B), or P7L-Tsg101 Gag (panel C) were isolated from the media as described in the text, spun onto poly-lysine-coated coverslips, and examined for the presence of N-Rh-PE. Panels A, C inset: higher magnification. The bar in panels A and C measures 200 nm.

different membrane sites for budding than the signals that direct HIV-1 Gag transport. It will be of interest to determine specifically how ESCRT factors *versus* Nedd4 family members facilitate trafficking and release of ASV Gag.

Materials and methods

Constructs and reagents

The following plasmids were previously described: *p*CMV-HIV-1*gag* or *p*CMV-ASV*gag* encoding HIV-1 and ASV Gag C-terminally tagged with green fluorescent protein (Gag-GFP; Medina et al., 2005); DNA encoding HA-Tsg101 (Lu et al., 2003); and DNA encoding myc-tagged fragments of Tsg101 (Li et al., 2001). DNA encoding ASV Gag Δp2b-Tsg101 was constructed as follows: p2036 (Kikonyogo et al., 2001) was doubly digested with KpnI and XbaI to remove the *gfp* coding region. Using PCR-based methods, a 5′ KpnI site was introduced upstream of the start codon of *ASV Gag-Δp2b*. Additionally, a 3′ HpaI site was introduced downstream of the *ASV Gag-Δp2b* coding sequence. Similarly, a 5′ HpaI and a 3′XbaI site were introduced upstream and downstream, respectively, of the full-length coding sequence of *tsg101*. Both PCR products were then ligated to the KpnI and XbaI doubly digested p2036 vector DNA to produce p2036 *ASVgag-Δp2b-tsg101*, in which Tsg101 is translationally fused in the correct reading frame to the C-terminus of ASV Gag-Δp2b. An identical strategy was followed to construct the HIV*gag P7L-tsg101* fusion construct and the ASV*gag-Δp2b-vps37C*, *-Δp2b-eap20*, and *-chmp4B* constructs. The following probes were purchased as indicated: Antibodies recognizing: actin, CD63, Tsg101, myc (Santa Cruz Biotechnology, Santa Cruz, CA, USA); GFP (Clontech Laboratories, Mountain View, CA, USA); influenza virus HA (Covance, Berkeley, Calif.); TRITC-tagged secondary antibody (Molecular Probes); and 1,2-dipalmitoyl-*sn*-glycero-3-phosphoethanolamine-*N*-[lissamine rhodamine B sulfonyl] (N-Rh-PE; Molecular Probes). Anti-AMV MA (p19) monoclonal antibody, which recognizes ASV MA, was developed by David Boettiger and was obtained from the Developmental Studies Hybridoma Bank under the auspices of the NICHD and maintained by the University of Iowa, Department of Biological Sciences. (Iowa City, IA, USA).

Cell culture, transfection, preparation of cytoplasmic extracts, and virus isolation

COS-1, 293/E, DF-1, or DF-1/RCAS/BP(A) cells were cultured in DMEM supplemented with fetal bovine serum (5%, 10%, 10%, and 10%, *respectively*) and antibiotics to 60% confluency at 37 °C. The relatively high ratio of cytoplasm to nucleus and ability to spread on tissue culture plates and coverslips make COS-1 cells advantageous for use in imaging studies. Expression of plasmids in the p2036 background was higher in 293/E cells (described in Kikonyogo et al., 2001) because 293/E cells stably express the EBNA1 protein of EBV and the p2036 constructs contain the EBV FR plasmid maintenance element that EBNA 1 binds. Therefore 293/E cells were used when proteins expressed from p2036 were to be detected by Western analysis. Unless otherwise indicated, the cells were transfected by using the FuGene 6 reagent (Roche, Indianapolis, IN, USA) according to the instructions of the manufacturer. At 48 h post-transfection, the cells were washed with phosphate-buffered saline (PBS) and lysed with RIPA buffer (1% Igepal CA-630, 0.5% sodium deoxychlolate, and 0.1% SDS in 1× PBS) containing protease inhibitor cocktail tablets (Roche) for 15 min at 4 °C. The lysate was then passaged through a 21-gauge needle and incubated on ice for 60 min. Cellular debris was pelleted at 10,000 ×g for 10 min at 4 °C (lysate fraction). ASV Gag was identified by Western blotting using specific anti-MA (ASV) monoclonal antibody. To isolate VLPs, the cell culture media was filtered (0.25 μm), applied to a cushion of 20% sucrose in a centrifuge tube and then spun at 30,000 rpm for 80 min at 4 °C (Beckman SW41 rotor). The pelleted particles were suspended by gentle shaking at 4 °C in 50 μl of PBS or RIPA buffer containing protease inhibitor cocktail. Samples were analyzed by SDS-PAGE and Western analysis. Equivalent amounts of cell lysates and of media fractions were used for all samples. Semi-quantitative determinations of VLP release (VLP/cell lysate+VLP ratio) were made using a phosphorimager and NIH Image.

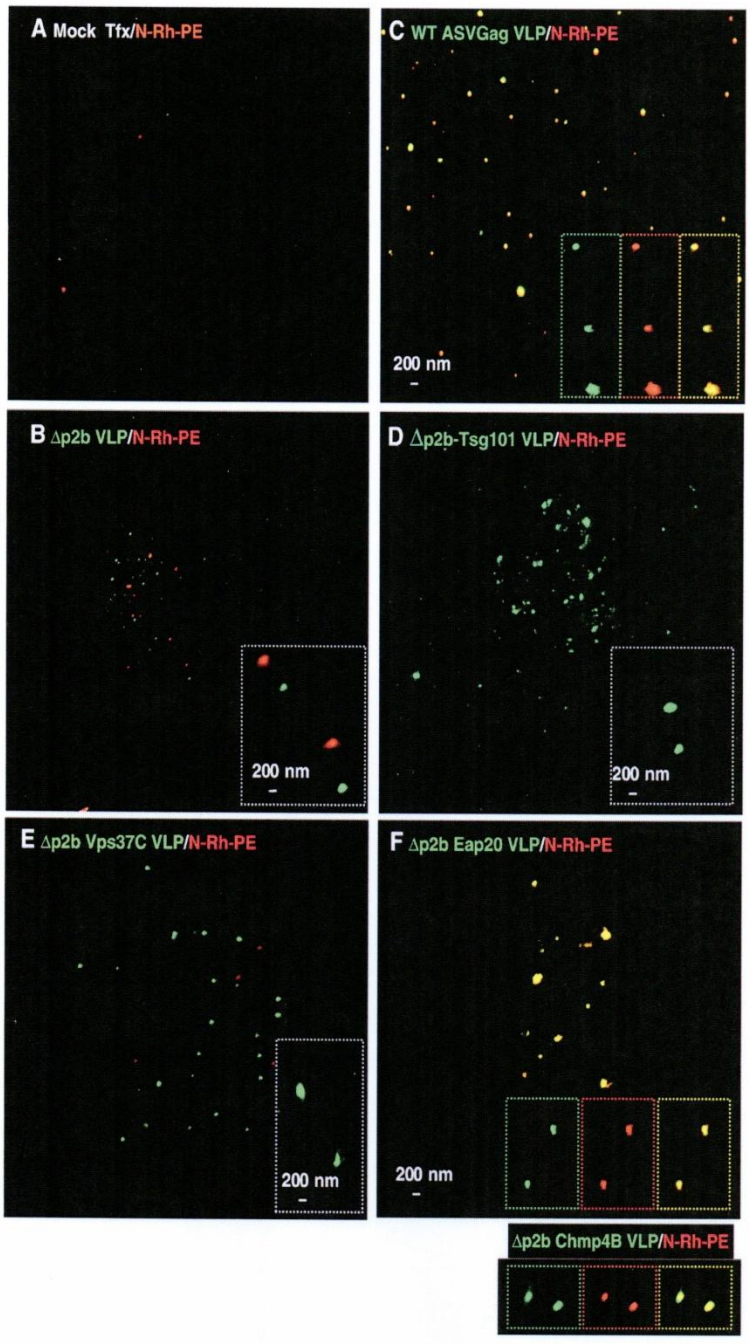

Fig. 5. Examination of WT and chimeric ASV VLPs for N-Rh-PE and CD63. VLPs from mock-transfected COS-1 cells (panel A) or cells transfected with DNA encoding WT ASV Gag-GFP (panels C and G), Gag Δp2b (panel B), Gag Δp2b-Tsg101 (panels D and H), GagΔp2b-Vps37C (panel E) or GagΔp2b-Eap20 (panel F) were isolated from the media as described in the text, spun onto poly-lysine-coated coverslips, and examined for the presence of N-Rh-PE directly or for CD63 by indirect immunofluorescence. The scale bar in the panel or inset measures 200 nm. Insets, panels C, F, and G show co-localizing Gag-GFP (left), N-Rh-PE (middle, panels C and F) or CD63 (middle, panel G), and merged images (right) for VLPs. The inset below panel F shows the same for GagΔp2b-Chmp4B VLPs. Insets, panels B, D, E, and H show the fluorescent signals in VLPs where GFP and N-Rh-PE or CD63 did not co-localize. In panels C and F, the magnification is the same in the panel and inset.

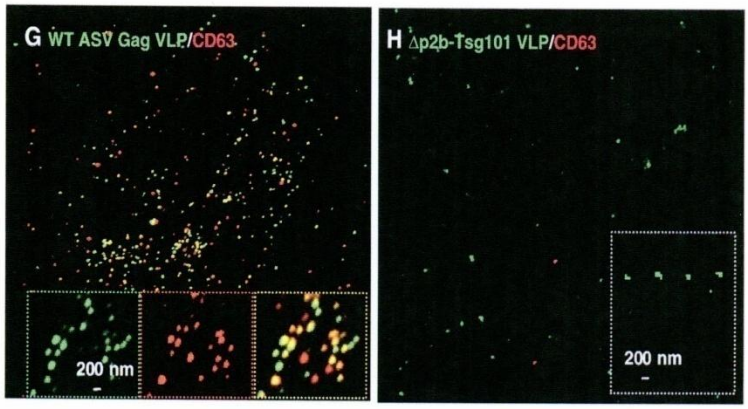

Fig. 5 (*continued*).

RNA interference

We obtained 21 nt RNA duplexes with symmetric 3′-UU overhangs corresponding to coding nucleotides 326–344 of avian Tsg101 (GUACUGUCCCGGUGAAAUA; Dharmacon, Lafayette, CO, USA). 20 or 50 nM of Tsg101 siRNA or a non-targeting control siRNA were transfected into DF-1 cells in six-well plates using Lipofectamine RNAiMax (Invitrogen, Carlsbad, CA, USA). 48 h post-siRNA transfection, DF-1 cells were transfected with p2036 encoding WT ASV Gag using FuGene 6. 24 h later, VLPs were pelleted through a 20% sucrose cushion at 100,000 ×*g* for 1 h. ASV Gag expression and VLP release were analyzed by Western blotting with anti-AMV p19 monoclonal antibody. The endogenous level of avian Tsg101 was analyzed by Western blotting with anti-Tsg101 antibody raised against full-length Tsg101 of mouse origin, which cross-reacts with mammalian and avian Tsg101.

Fluorescence microscopy

Fluorescent microscopy images were captured with an inverted fluorescent/dic Zeiss Axiovert 200 M microscope equipped with an AxioCam HRm camera (Zeiss, Thornwood, NY, USA) and mercury arc lamp light source using a 63× Plan-Apochromat (NA 1.40) oil objective and operated by AxioVision Version 4.5 (Zeiss) software.

Electron Microscopy

Sixty-millimeter dishes of DF1/RCASBP(A) cells were washed with PBS at room temperature and fixed in 2.5% glutaraldehyde in 0.1 M sodium phosphate buffer (pH 7.4) at 4 °C for 30 min. Cells were scraped from the tissue culture dish and pelleted at 1000 ×*g* for 10 min at 4 °C. The cell pellet was fixed for an additional 2 h in 2.5% glutaraldehyde and post-fixed for 1 h with osmium tetroxide. The cell pellet was dehydrated in a series of alcohol washes and embedded in Epon. Ultrathin sections were stained with uranyl acetate and lead citrate and examined using a Zeiss 900 electron microscope.

Protein detection

Proteins were separated by electrophoresis through 12.5% SDS-polyacrylamide gels. Following electrophoresis, the gels were transferred to nitrocellulose and analyzed by Western blotting with the antibodies specified in the text. Proteins were visualized by chemiluminescence using Lumi-Light reagents (Roche, Indianapolis, IN, USA).

Acknowledgments

This work was supported by National Institutes of Health grants AI068463 (to CC) and AI054143 (to JL). GM was supported in part by a W. Burghardt Turner Pre-doctoral Fellowship, the NSF-HRD funded SUNY AGEP Program at Stony Brook University, Grant #35583 and by NIH Pre-Doctoral Training grant 5T32 CA-09176. AP is supported by the NIH pre-doctoral Training Grant T32 AI060523.

References

Amit, I., Yakir, L., Katz, M., Zwang, Y., Marmor, M.D., Citri, A., Shtiegman, K., Alroy, I., Tuvia, S., Reiss, Y., Roubini, E., Cohen, M., Wides, R., Bacharach, E., Schubert, U., Yarden, Y., 2004. Tal, a Tsg101-specific E3 ubiquitin ligase, regulates receptor endocytosis and retrovirus budding. Genes Dev. 18, 1737–1752.

Babst, M.B., Wendland, B., Estepa, E.J., Emr, S.D., 1998. The Vps4p AAA ATPase regulates membrane association of a Vps protein complex required for normal endosome function. EMBO J. 17, 2982–2993.

Bieniasz, P., 2006. Late budding domains and host proteins in enveloped virus release. Virology 344, 55–63.

Bishop, N., Horman, A., Woodman, P., 2002. Mammalian class E vps proteins recognize ubiquitin and act in the removal of endosomal protein ubiquitin conjugates. J. Cell Biol. 157, 91–101.

Burniston, M., Cimarelli, A., Colgan, J., Curtis, S.P., Luban, J., 1999. Human immunodeficiency virus type 1 Gag polyprotein multimerization requires the nucleocapsid domain and RNA and is promoted by the capsid-dimer interface and the basic region of matrix protein. J. Virol. 73, 8527–8540.

Chung, H.Y., Morita, E., von Schwedler, U., Müller, B., Kräusslich, H.G., Sundquist, W.I., 2008. NEDD4L Overexpression Rescues Release and Infectivity of HIV-1 Constructs Lacking PTAP and YPXL Late Domains. J. Virol. 82, 4884–4897.

Cimarelli, A., Sandlin, S., Hoglund, S., Luban, J., 2000. Basic residues in human immunodeficiency virus type 1 nucleocapsid promote virion assembly via interaction with RNA. J. Virol. 74, 3046–3057.

Dunn, R., Klos, D.A., Adler, A.S., Hicke, L., 2004. The C2 domain of the Rsp5 ubiquitin ligase binds membrane phosphoinositides and directs ubiquitination of endosomal cargo. J. Cell Biol. 165, 135–144.

Garrus, J., von Schwedler, U.K., Pornillos, O.W., Morham, S.G., Zavitz, K.H., Wang, H.E., Wettstein, D.A., Stray, K.M., Cote, M., Rich, R.L., Myszka, D.G., Sunquist, W.I., 2001. Tsg101 and the vacuolar protein sorting pathways are essential for HIV budding. Cell 107, 55–65.

Goila-Gaur, R., Demirov, D.G., Orenstein, J.M., Ono, A., Freed, E.O., 2003. Defects in human immunodeficiency virus budding and endosomal sorting induced by Tsg101 overexpression. J. Virol. 77, 6507–6519.

Gottlinger, H., 2001. The HIV 1 assembly machine. AIDS 15, 13–20.

Gottlinger, H., Dorfman, T., Sodroski, J.G., Haseltine, W.A., 1991. Effect of mutations affecting the p6 Gag protein on human immunodeficiency virus particle release. Proc. Natl. Acad. Sci. U. S. A. 88, 3195–3199.

Himly, M., Foster, D.N., Bottoli, I., Iacovoni, S., Vogt, P.K., 1998. The DF-1 chicken fibroblast cell line: Transformation-induced by diverse oncogenes and cell death resulting from infection by avian leucosis viruses. Virology 248, 295–304.

Johnson, M.C., Spidel, J.L., Ako-Adjei, D., Wills, J.W., Vogt, V.M., 2005. The C-terminal half of Tsg101 blocks Rous sarcoma virus budding and sequesters Gag into unique nonendosomal structures. J. Virol. 79, 377–386.

Katzmann, D., Babst, M., Emr, S.D., 2001. Ubiquitin dependent sorting into the multivesicular body pathway requires the function of a conserved endosomal protein sorting complex ESCRT-1. Cell 106, 145–155.

Kikonyogo, A., Bouamr, F., Vana, M.L., Xiang, Y., Aiyar, A., Carter, C., Leis, J., 2001. Proteins related to the Nedd4 family of ubiquitin protein ligases interact with the L domain of Rous sarcoma virus and are required for Gag budding from cells. Proc. Natl. Acad. Sci. U. S. A. 98, 11199–11204.

Kim, B.Y., Olzmann, J.A., Barsh, G.S., Chin, L.S., Li, L., 2007. Spongiform neurogeneration-associated E3 ligase Mahogunin ubiquitylates Tsg101 and regulates endosomal trafficking. Mol. Biol. Cell 18, 1129–1142.

Li, L., Liao, J., Ruland, J., Mak, T., Cohen, S.N., 2001. A Tsg101/MDM2 regulatory loop modulates MDM2 degradation and MDM2/p53 feedback control. Proc. Natl. Acad. Sci. U. S. A. 98, 1616–1624.

Lu, Q., Hope, W., Brasch, M., Reinhrad, C., Cohen, S.N., 2003. Tsg101 interaction with Hrs mediates endosomal trafficking and receptor down-regulations. Proc. Natl. Acad. Sci. U. S. A. 100, 7626–7631.

Martin-Serrano, J., Bieniasz, P.D., 2003. A bipartite late-budding domain in HIV-1 type 1. J. Virol. 77, 12373–12377.

Martin-Serrano, J., Zang, T., Bieniasz, P.D., 2001. HIV 1 and Ebola encode small peptide motifs that recruit Tsg101 to sites of particle assembly to facilitate egress. Nat. Med. 7, 1313–1319.

Martin-Serrano, J., Yarovoy, A., Perez Caballero, D., Bieniasz, P.D., 2003. Divergent retroviral late budding domains recruit vacuolar protein sorting factors by using alternative adaptor proteins. Proc. Natl. Acad. Sci. U. S. A. 100, 12412–12419.

Medina, G., Zhang, Y., Tang, Y., Gottwein, E., Vana, M.L., Bouamr, F., Leis, J., Carter, C.A., 2005. The functionally exchangeable L domains in RSV and HIV-1 Gag direct particle release through pathways linked by Tsg101. Traffic 6, 880–894.

Nydegger, S., Foti, M., Derdowski, A., Spearman, P., Thali, M., 2003. HIV-1 egress is gated through late endosomal membranes. Traffic 4, 902–910.

Nydegger, S., Khurana, S., Krementsov, D.N., Foti, M., Thali, M., 2006. Mapping of tetraspanin-enriched microdomains that can function as gateways for HIV-1. J. Cell Biol. 173, 795–807.

Parent, L., Bennett, R.P., Craven, R.C., Nelle, T.D., Krishna, N.K., Bowzard, J.B., Wilson, C.B., Puffer, B.A., Montelaro, R.C., Wills, J.W., 1995. Positionally independent and exchangeable late budding functions of the Rous sarcoma virus and human immunodeficiency virus Gag proteins. J. Virol. 69, 5455–5460.

Puffer, B., Parent, L.J., Wills, J.W., Montelaro, R.C., 1997. Equine infectious anemia virus utilizes a YXXL motif within the late assembly domain of the Gag p9 protein. J. Virol. 71, 6541–6546.

Raymond, C.K., Howarld-Stevenson, I., Vater, C.A., Stevens, T.H., 1992. Morphological classification of the yeast vacuolar protein sorting mutants: evidence for a prevacuolar compartment in class E vps mutants. Mol. Biol. Cell 3, 1389–1402.

Sanderfur, S., Varthakavi, V., Spearman, P., 1998. The I domain is required for efficient plasma membrane binding of human immunodeficiency virus type 1 Pr55Gag. J. Virol. 72, 2723–2732.

Schaefer-Klein, J., Givol, I., Barsov, E.V., Whitcomb, J.M., Van-Brocklin, M., Foster, D.N., Fedspiel, M.J., Hughes, S.H., 1998. The EV-0-derived cell line DF-1 supports the efficient replication of avian leucosis-sarcoma viruses and vectors. Virology 248, 305–311.

Scheifele, L.Z., Rhoads, J.D., Parent, L.J., 2003. Specificity of plasma membrane targeting by the Rous sarcoma virus gag protein. J. Virol. 77, 470–480.

Spearman, P., Wang, J., Vander Heyden, N., Ratner, L., 1994. Identification of human immunodeficiency virus type 1 Gag protein domain essential to membrane binding and particle assembly. J. Virol. 68, 3232–3242.

Strack, B., Calistri, A., Craig, S., Popova, E., Gottlinger, H.G., 2003. AIP-1/ALIX is a binding partner for HIV-1 p6 and EIAV p9 functioning in virus budding. Cell 114, 689–699.

Usami, Y., Popov, S., Popova, E., Göttlinger, H.G., 2008. Efficient and specific rescue of human immunodeficiency virus type 1 budding defects by a Nedd4-like ubiquitin ligase. J. Virol. 82, 4898–4907.

Vana, M.L., Chen, A., Medina, G., Carter, C., Leis, J., 2004. Role of Nedd4 and ubiquitination of Rous sarcoma virus Gag in budding of virus-like particles from cells. J. Virol. 78, 13943–13953.

VerPlank, L., Bouamr, F., LaGrassa, T.J., Agresta, B., Kikonyogo, A., Leis, J., Carter, C.A., 2001. Tsg101, a homologue of ubiquitin conjugating (E2) enzymes, binds the L domain in HIV type 1 Pr55 (Gag). Proc. Natl. Acad. Sci. U. S. A. 98, 7724–7729.

Vidal, M., Mangeat, P., Hoekstra, D., 1997. Aggregation reroutes molecules from a recycling to a vesicle mediated secretion pathways during reticulocyte maturation. J. Cell Sci. 110, 1867–1877.

von Schwedler, U., Stuchell, M., Muller, B., Ward, D.M., Chung, H.Y., Morita, E., Wang, H.E., Davis, T., He, G.P., Cimbora, D.N., Scott, A., Krausslich, H.G., Kaplan, J., Morham, S.G., Sundquist, W.I., 2003. The protein network of HIV budding. Cell 114, 701–713.

Willem, J., Beest, M., Scherphof, G., Hoekstra, D., 1990. A non-exchangeable fluorescent phospholipid analog as a membrane traffic marker of the endocytic pathway. Eur. J. Cell Biol. 53, 173–184.

Wills, J., Craven, R.C., 1991. Form, function and use of retroviral Gag proteins. AIDS 5, 639–654.

Wills, J., Cameron, C.E., Wilson, C.B., Xiang, Y., Bennett, R.P., Leis, J., 1994. An assembly domain of the Rous sarcoma virus Gag protein required late in budding. J. Virol. 68, 6605–6618.

Xiang, Y., Cameron, C., Wills, J., Leis, J., 1996. Fine mapping and characterization of the Rous sarcoma virus Pr76gag late assembly domain. J. Virol. 70, 5695–5700.

Yorikawa, C., Shibata, H., Waguri, S., Hatta, K., Horii, M., Katoh, K., Kobayashi, T., Uchiyama, Y., Maki, M., 2005. Human CHMP6, a myristoylated ESCRT-III protein, interacts directly with an ESCRT-II component EAP20 and regulates endosomal cargo sorting. Biochem. J. 387, 17–26.

Zhou, W., Resh, M.D., 1996. Differential membrane binding of the human immunodeficiency virus type 1 matrix protein. J. Virol. 70, 8540–8548.

Zhou, W., Parent, L.J., Wills, J.W., Resh, M.D., 1994. Identification of a membrane-binding domain within the amino terminal region of human immunodeficiency virus type 1 Gag protein which interacts with acidic phospholipids. J. Virol. 68, 2556–2569.

CHAPTER 5: The non-ESCRT protein Spry2 and its role in Gag release

SUMMARY

In this chapter, I examine a non-ESCRT protein and its involvement in the release of retroviral Gag, with emphasis on HIV-1 Gag. As previously described, the recruitment of cellular proteins by retroviral L domains is required for efficient release from the plasma membrane. The well-documented endocytic cellular machinery composed of ESCRT proteins is hijacked by retroviral Gags to the plasma membrane to facilitate viral egress from the cell, however the mechanism is not well understood. In this study, I examined the role in Gag release of the cellular protein Sprouty2 (Spry2), which was identified in a proteomic analysis of membrane fractions containing ectopically expressed Gag. The Spry2 protein is known to function in the negative regulation of signaling events that are activated by growth receptor tyrosine kinases (RTKs). I observed that depletion of endogenous levels of Spry2 had a negative effect on VLP production as did overexpression of a C-terminal fragment of Spry2 protein. Interestingly, a mutant of Spry2 that had no detectable effect on WT Gag release promoted the release of a Gag mutant lacking a functional Tsg101 binding site. I conclude that in addition to modulating Tsg101-facilitated receptor downregulation, Spry2 also may play an important regulatory role in Tsg101-mediated HIV Gag release.

Specific Contribution: I designed and performed all of the experiments in this chapter and wrote the first draft of the manuscript.

ABSTRACT

It is now well established that growth factor receptors on the cell surface and retroviruses both utilize ESCRT machinery to promote trafficking associated with delivery of receptors to degradative compartments in the cell interior and viral budding from the plasma membrane, respectively. It has been proposed that Gag is targeted to release sites on the plasma membrane by the phospholipid PI(4,5)P_2. Sprouty2 (Spry2), a cellular protein that binds PI(4,5)P_2 and directs the down-regulation of cell surface receptors that is mediated by the ESCRT machinery, was identified in a proteomic analysis of membranes isolated from cells expressing Gag. Here, we show that depletion of the endogenous pool of Spry2 in COS-1 cells inhibits release of the virus-like particles (VLPs) assembled by Gag. Interestingly, although the C-terminal domain of Spry2 (Spry2- Δ175) contains determinants that direct the protein to its phosphatidylinositol 4,5-biphosphate [(PI(4,5)P_2]-binding sites on the plasma membrane, co-expression of Gag with the Spry2 C-terminal domain caused both proteins to be sequestered inside the cell and interfered with VLP release. Deletion of the Tsg101 binding site in Gag restored the ability of both Gag and SpryΔ175 to be delivered to the cell periphery but, as expected, not VLP release, suggesting that both Tsg101 and a determinant in the Spry2 N-terminus were required for efficient Gag egress. Consistent with this possibility, co-expression of the Gag mutant with a Spry2 mutant lacking the only conserved sequences in the N-terminal domain increased the efficiency of VLP release 5-fold. In contrast, co-expression of Gag with WT Spry2 had no detectable effect or an inhibitory effect. Examination of the cells by confocal microscopy revealed that WT Spry2 co-localized with PI(4,5)P_2 in complexes that were resistant to cold Triton X-100 extraction. In

contrast, the Spry2 mutant failed to co-localize with PI(4,5)P_2 following cold Triton extraction but, unlike the WT Spry2 protein, co-localized with caveolin-1. We conclude that in addition to modulating the trafficking of cellular proteins using ESCRT machinery for delivery to interior compartments, Spry2 also regulates Gag membrane targeting and release efficiency, perhaps by modulating PI(4,5)P2 accessibility at the plasma membrane.

INTRODUCTION

Assembly and release of retroviral particles, including HIV-1, is driven by the expression of Gag precursor proteins (35). Gag proteins are sufficient for the formation of virus like particles (VLP) in the absence of other viral components. VLP release is a complex process that requires the interplay between the L domains and different cellular proteins. In the case of HIV-1, as described in the introduction in Chapter One, VLP release is mediated by the interaction between its PTAP L domain and components of the ESCRT machinery (134). An intriguing feature of the ESCRT-mediated budding of HIV-1 is that recruitment of the endocytic machinery does not lead to degradation. In support of this notion, several studies have reported that HIV-1 Gag can concentrate on late endosomes/MVBs and progeny virus can effectively exit the cell (27, 97, 121, 134). In contrast, cellular cargo (e.g., EGFR) that also utilizes the ESCRT machinery gets targeted to the lysosome for degradation. Certainly, cellular proteins that regulate ESCRT-mediated pathways should provide clues about the mechanism that allow retroviruses to exit from the plasma membrane.

A recent observation from Kim *et al* indicates that the cellular protein Sprouty2 (Spry2) affects the endocytic trafficking of EGFR by preventing its down-regulation. Specifically, it was shown that Spry2 interfered with the interaction between Hrs and Tsg101: two components of the endocytic machinery that participate in the recognition of cellular cargo and recruitment of ESCRT complexes. Furthermore, Spry2 can also affect the trafficking of EGFR by interacting with the E3 ubiquitin ligase Cbl. Upon EGF induction, Spry2 undergoes phosphorylation on its tyrosine 55 (Y55) residue. This phosphorylation site functions as binding site for the SH2 domain of Cbl (33, 115). As

this same SH2 domain is required for Cbl to interact with the activated form of EGFR, the binding of Spry2 recruits Cbl away from EGFR and prevents its ubiquitination and internalization, which leads to a sustained MAPK signaling. Given the resemblance of the events that block ESCRT-mediated EGFR trafficking and the ESCRT-mediated budding of retroviral Gags, we examined the possibility that Spry2 regulates ESCRT-mediated trafficking pathways that are required for the efficient release of HIV-1 Gag.

In the present study we analyzed Spry2 and its involvement in the release of HIV-1 Gag. siRNA depletion of the endogenous levels of Spry2 in several cell lines (Cos-1, 293E, and Mia-PaCa) revealed that steady-state levels of Spry2 are required for efficient release of HIV-1 Gag. Over-expression experiments utilizing the HA-tagged full length Spry2 indicated that Spry2 can inhibit Gag VLP release and this inhibitory effect of Spry2 on Gag release was mapped to the C-terminal domain. This domain contains a conserved cysteine-rich domain, through which the protein binds to the plasma membrane by interacting with the phospholipid $PI(4,5)P_2$. Surprisingly, since it contains the sequences required for Spry2 translocation, analysis by confocal microscopy revealed that the overexpression of the Spry2 C-terminal domain prevented its translocation to the plasma membrane. The Spry2 C-terminal fragment was found in intracellular vesicles where it colocalized with Gag. Together, these observations suggest that determinants in the N-terminal region of Spry2 are important for translocation of both Spry2 and Gag to the plasma membrane. The notion that the C-terminal translocation domain and in particular the ability to interact with $PI(4,5)P_2$ are important for Spry2 and Gag localization to the plasma membrane was confirmed by showing that a Spry2 variant bearing a single amino acid substitution that prevents $PI(4,5)P_2$ binding, R252D, caused

Spry2 to remain intracellular and inhibited Gag VLP release. Examination of a Spry2 variant lacking a highly conserved sequence in the N-terminal region that binds to Cbl relieved the inhibitory effect exerted by the WT Spry2 protein on VLP release and even promoted release of P7L, a Gag mutant with a disrupted Tsg101 binding site. Comparison of the membrane localization of WT Spry2 and ΔCbl-Spry suggested that they localized in different subcellular compartments defined by the ability to co-localize with caveolin-1 and the ability to maintain association with $PI(4,5)P_2$ following cold Triton X-100 extraction. We conclude that Spry2 participates in Gag release by facilitating Gag targeting to $PI(4,5)P_2$ and modulating the availability of the phospholipid in specific domains of the plasma membrane.

RESULTS

Steady state levels of Spry2 are required for efficient release of HIV-1 Gag. In order to understand the significance of Spry2 to Gag assembly, we determined the effect of siRNA-mediated depletion of the endogenous pool of Spry2 in Cos-1 cells on HIV-1 Gag accumulation and VLP production. We utilized a siRNA sequence or a DNA based shRNA expression plasmid to deplete the endogenous levels of Spry2 in cells that were transfected with HIV Gag-GFP. Non-targeting siRNA or sh-vector were used as controls. As seen in Figure 1 (*panel A*), treatment with Spry2-specific siRNA (20-80 *nM*) significantly reduced the levels HIV-1 Gag released (*lanes 4- 6*) in a dose- dependent manner when compared to the control (*lanes 1-3*). The intracellular level of Gag was not detectably affected by the siRNA treatment. The low levels of endogenous Spry2 present in Cos-1 cells prevented its examination by Western blot analysis. We therefore determined the extent of depletion by quantitative-PCR (Q-PCR). Briefly, forty-eight hours post-transfection, total RNA was harvested and reversed transcribed. The resulting cDNAs were subjected to Q-PCR analysis to assess the expression levels of the *spry2* gene when treated with siRNA (*panel B*). The siRNA targeted to Spry2 reduced Spry2 expression by more than 90% at the highest siRNA dose tested. In contrast, transfection of siRNA directed at a random sequence did not suppress the endogenous level of Spry2, indicating that the observed depletion was specific and not due to off-target effects. Semi-quantitative analysis (Gag signal in VLP/Cell Lysate + VLP; *panel C*) indicated that under conditions where Spry2 was knocked down to > 90%, the efficiency of VLP release was reduced by 60-90%. The results indicate that the steady-state levels of Spry2

Figure 1. Steady state levels of Spry2 are required for efficient release of HIV-1 Gag VLPs**. A.** Cos-1 cells were transfected with Spry2-specific siRNA (lanes 4-6) or control siRNA (lanes 1-3) for 24 hours followed by transfection with DNA encoding HIV-Gag-GFP for 48 hours. Gag proteins in lysates and media were isolated as described in Materials and Methods and analyzed by SDS-PAGE and Western Blotting. **B.** Depletion of Spry2 by Q-PCR. Cos-1 cells were treated with siRNA against Spry2 or against a non-specific target (siControl), and transfected with Gag-GFP. Forty eight hours post tranfection total RNA was harvested and cDNAs were generated. cDNA levels were quantified by Q-PCR analysis using primers specific to Spry2. The data was normalized to the house-keeping gene *h60S* levels. The results represent the average of three independent experiments. **C.** Semi-quantitative analysis of VLP release. The panel shows the ratio of the Gag signal in VLP isolated from the media to the VLP signal plus the Gag signal in the cell lysate. Values reflect the mean ± SD of three independent experiments. Error bar represent the standard error (SEM); differences between experiments were examined with the Student's t test ($*p < 0.05$)

A.

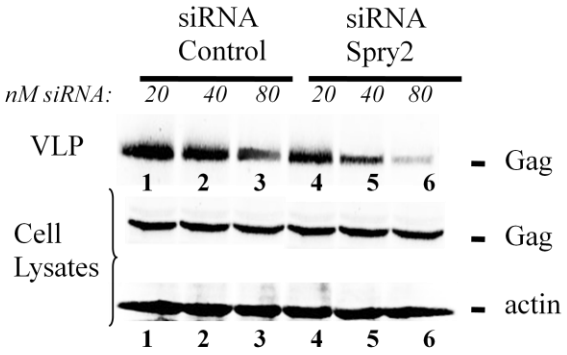
siRNA Control
siRNA Spry2
nM siRNA: 20 40 80 20 40 80
VLP
1 2 3 4 5 6
Gag
Cell Lysates
Gag
actin
1 2 3 4 5 6

B.

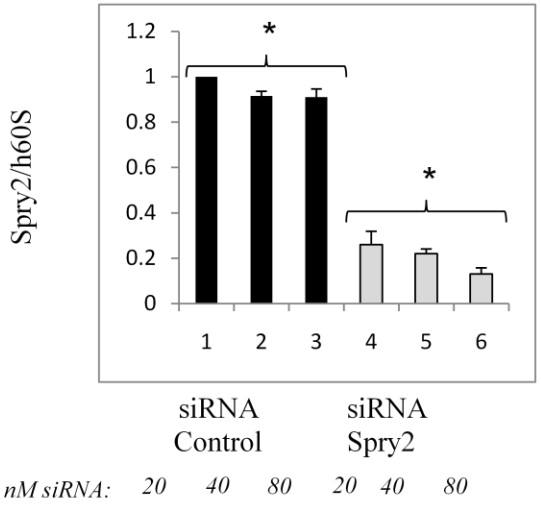
Spry2/h60S
1.2
1
0.8
0.6
0.4
0.2
0
*
*
1 2 3 4 5 6
siRNA Control
siRNA Spry2
nM siRNA: 20 40 80 20 40 80

C.

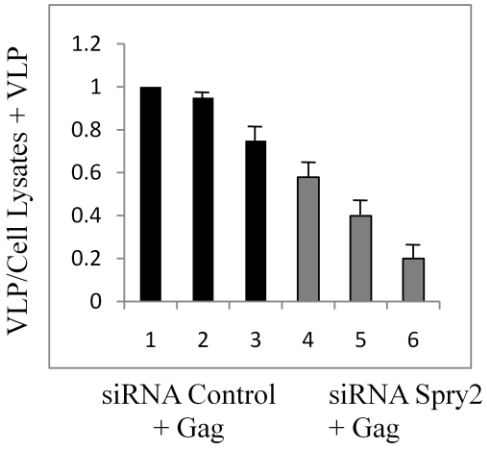
VLP/Cell Lysates + VLP
1.2
1
0.8
0.6
0.4
0.2
0
1 2 3 4 5 6
siRNA Control + Gag
siRNA Spry2 + Gag

are required for efficient VLP release. Similar results were obtained in experiments using shRNA (*data not shown*).

Overexpression of Spry2 full length and C-terminal fragment inhibits HIV-1 Gag release. Spry2 is known to be a general modulator of growth factor signaling and ESCRT-mediated trafficking. A number of interacting and associated proteins have been identified and contribute to Spry2's function (16, 29, 45, 55, 73, 117, 141). Many of these proteins interact with the C-terminal domain (61, 84). In particular, the C-terminal domain of Spry2 can interact with the lipid $PI(4,5)P_2$ at the plasma membrane during growth factor induction (73). To determine the function of Spry2 that is relevant for Gag release, we examined the effect of overexpressing full length Spry2 and Spry2 fragments (Figure 2A) on HIV-1 Gag release. Cos-1 cells were co-transfected with different concentrations of DNA encoding HA-tagged Spry2 in the presence of HIV-1 Gag-GFP and VLP production was examined. As shown in Figure 2 (*panel B*), the co-expression of HA-Spry2 and HIV-Gag-GFP resulted in a significant decrease in Gag VLP production at the higher doses tested (*lanes 2-5*). This was observed in five out of seven independent trials. Under circumstances where VLP release was not inhibitory, Spry2 expression was less than the one shown in this experiment. No effect on the intracellular levels of Gag was observed. Next, the regions of Spry2 responsible for the inhibitory effect in growth factor signaling were investigated, namely the fragments of the protein comprised of the Spry2 N–terminus (Spry2 1-175) or the C-terminal part (Spry2 Δ175). Cells that were co-expressing the HA-tagged Spry2 fragment containing the N-terminus in the presence of HIV-Gag-GFP (*panel C*) had no negative effect on the release of VLPs. In fact, an increase in VLP release was observed (*lanes 2-5*). This was observed

Figure 2. Over-expression of Gag of full length Spry2 or a C-terminal fragment inhibits HIV-1 Gag release. Western Analysis of VLPs and cell lysates for HIV-1 Gag-GFP, HA-Spry2 full length, HA-Spry2 N-term and C-term. **A.** Schematic drawing of Spry2 and fragments used in this study. **B-D.** Cos-1 cells were transfected with a fixed amount of DNA encoding HIV-Gag-GFP (*lane 1*) and increasing amounts of DNA encoding HA-Spry2 full length (***panel B***), Spry2 N-terminal fragment (aa 1-175, ***panel C***), or Spry2 C-terminal fragment (aa175-315, ***panel D***) *lane 2*, spry2:gag, 1µg:3µg; *lane 3*, 2µg: 3µg; *lane 4*, 3µg:3µg; *lane 5*, 4µg: 3µg). Media and cell lysate fractions were harvested at 48 hours post-transfection. **E.** Semi-quantitative analysis of VLP release (VLP/VLP + Cell Lysate). The panel shows the ratio of the Gag signal (determined using NIH image) in VLP isolated from the media to the Gag signal in the cell lysate. Values reflect the mean ± SD of seven (Spry2 WT) and four (N-term and C-term) independent experiments. Error bar represent the standard error (SEM); differences between experiments were examined with the Student's t test (*$p < 0.05$)

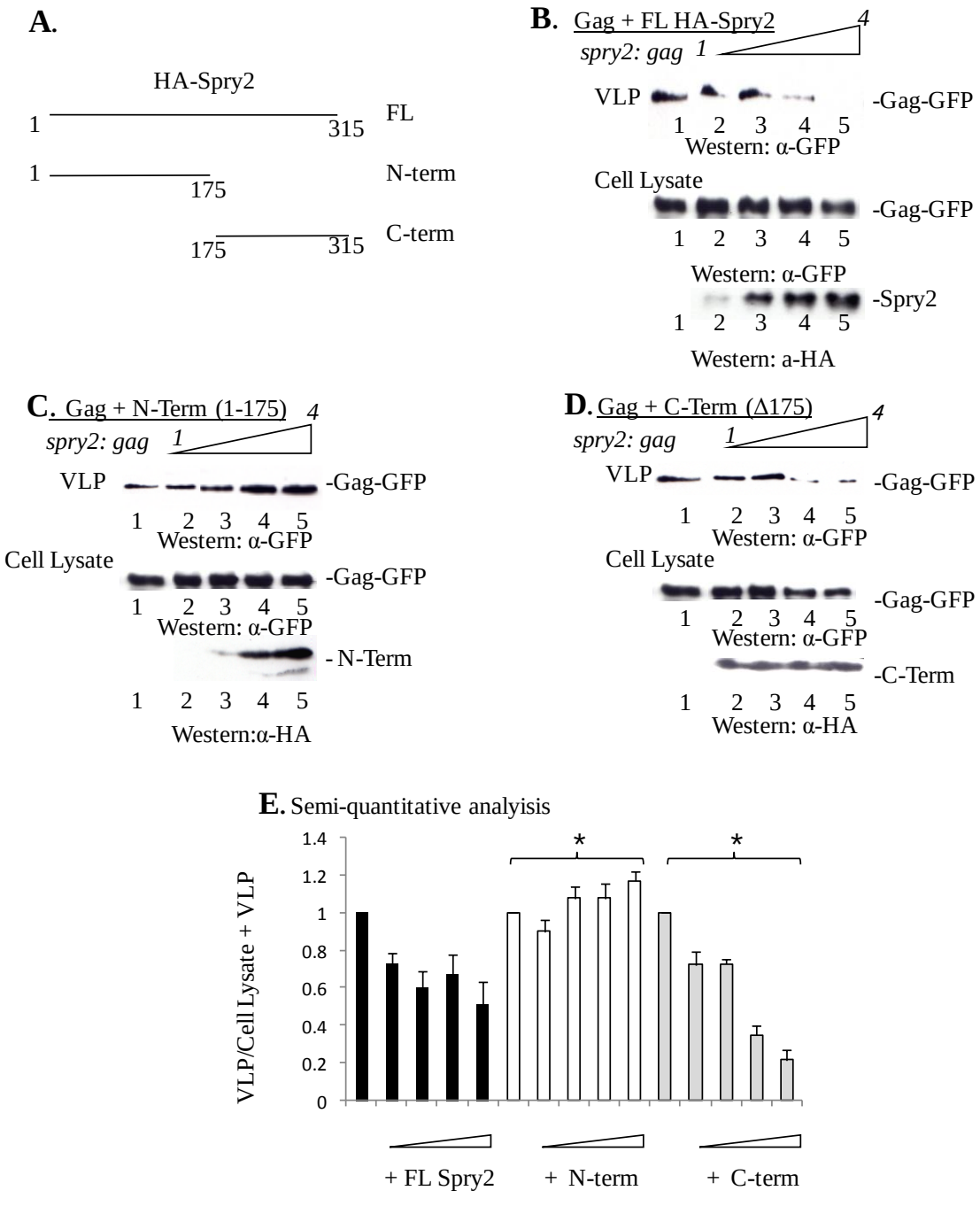
A.
HA-Spry2
1
315
FL
1
175
N-term
175
315
C-term
B. Gag + FL HA-Spry2
spry2: gag 1
4
VLP
-Gag-GFP
1 2 3 4 5
Western: α-GFP
Cell Lysate
-Gag-GFP
1 2 3 4 5
Western: α-GFP
-Spry2
1 2 3 4 5
Western: a-HA
C. Gag + N-Term (1-175)
spry2: gag 1
4
VLP
-Gag-GFP
1 2 3 4 5
Western: α-GFP
Cell Lysate
-Gag-GFP
1 2 3 4 5
Western: α-GFP
- N-Term
1 2 3 4 5
Western:α-HA
D. Gag + C-Term (Δ175)
spry2: gag 1
4
VLP
-Gag-GFP
1 2 3 4 5
Western: α-GFP
Cell Lysate
-Gag-GFP
1 2 3 4 5
Western: α-GFP
-C-Term
1 2 3 4 5
Western: α-HA
E. Semi-quantitative analyisis
VLP/Cell Lysate + VLP
1.4
1.2
1
0.8
0.6
0.4
0.2
0
*
*
+ FL Spry2
+ N-term
+ C-term

in four independent trials. In contrast, co-expression of the HA-Spry2 C-terminal fragment (*panel D*) had a significant negative impact on VLP production (*lanes 2-5*) without significantly impacting the intracellular levels of Gag. This observation was detected in four independent trials. A semi-quantitative analysis (*panel E*) of VLP release based on the comparison of Gag intensities in media and cell lysates indicated that the efficiency of Gag release was decreased by >80- 90% at the highest amount of HA-Spry2 WT or HA-Spry2 C-terminal fragment tested. The release efficiency of Gag was increased by an average of ~50% in the cases where an increase occurred. These results clearly indicate that the inhibitory budding effects associated with expression of Spry2 FL maps to the Spry2 C-terminal region. To determine the mechanism underlying the inhibition, deconvolution confocal microscopy was conducted. Cos-1 cells were transfected with HA-Spry2 WT alone, HIV-1 Gag-GFP alone or co-transfected with Gag and the full length Spry2 WT, the HA-Spry2 N-terminal fragment or the HA-Spry2 C-terminal fragment. Detection of the HA-tagged constructs was achieved by indirect immunofluorescent using an antibody against HA. As observed in Figure 3 (*panel A*), HA-Spry2 distribution was mainly cytosolic and perinuclear with a punctate appearance as was previously described (62). Cells expressing Gag-GFP (*panel B*) showed the typical punctate distribution throughout the cell and along the plasma membrane. In cells that were co-transfected with Gag-GFP and HA-Spry2 WT (*panel C*), a clear colocalization intracellularly as well as at the plasma membrane was observed (*panel C*). Furthermore, a more plasma membrane proximal localization of Spry2 was observed, suggesting that the expression of Gag-GFP disturbed the distribution of Spry2. It was also

Figure 3. HIV-1 Gag distribution is altered by co-expression with the Spry2 C-terminal fragment. Cos-1 cells were transfected with **A**) HA-Spry2 WT alone (red) or **B**) HIV-Gag-GFP alone (green). The HA-tagged construct were detected by indirect immunostaining using specific antibodies against the HA. Hoescht stain was used to detect the nucleus (stained blue). (*continued*)

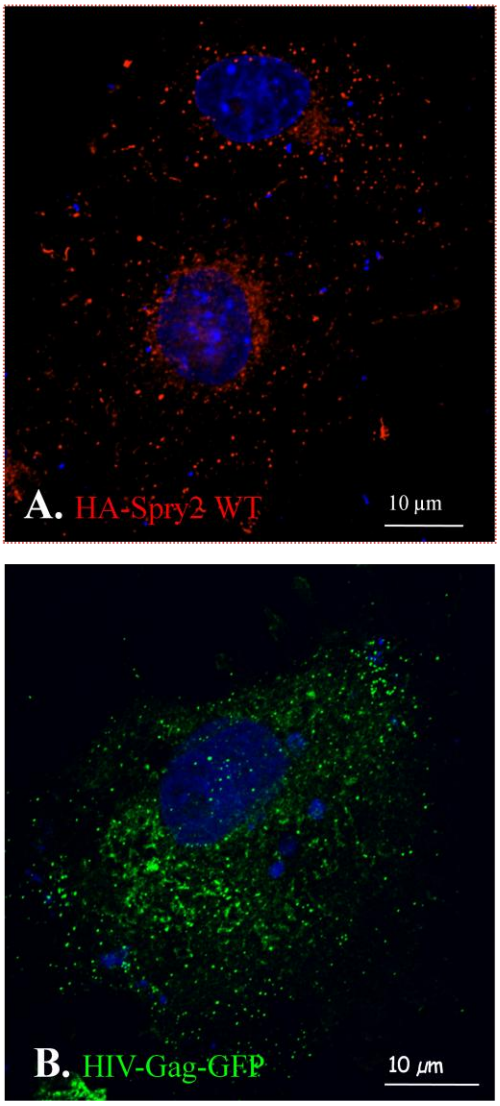
A. HA-Spry2 WT
10 µm
B. HIV-Gag-GFP
10 µm

Figure 3. (*continued*) Cos-1 cells were co-transfected with **C**) HIV-Gag-GFP (green) and HA-Spry2-FL (red), **D**) HA-Spry2 N-term or **E**) HA-Spry2 C-term. Colocalization is indicated by the yellow color in the merge images.

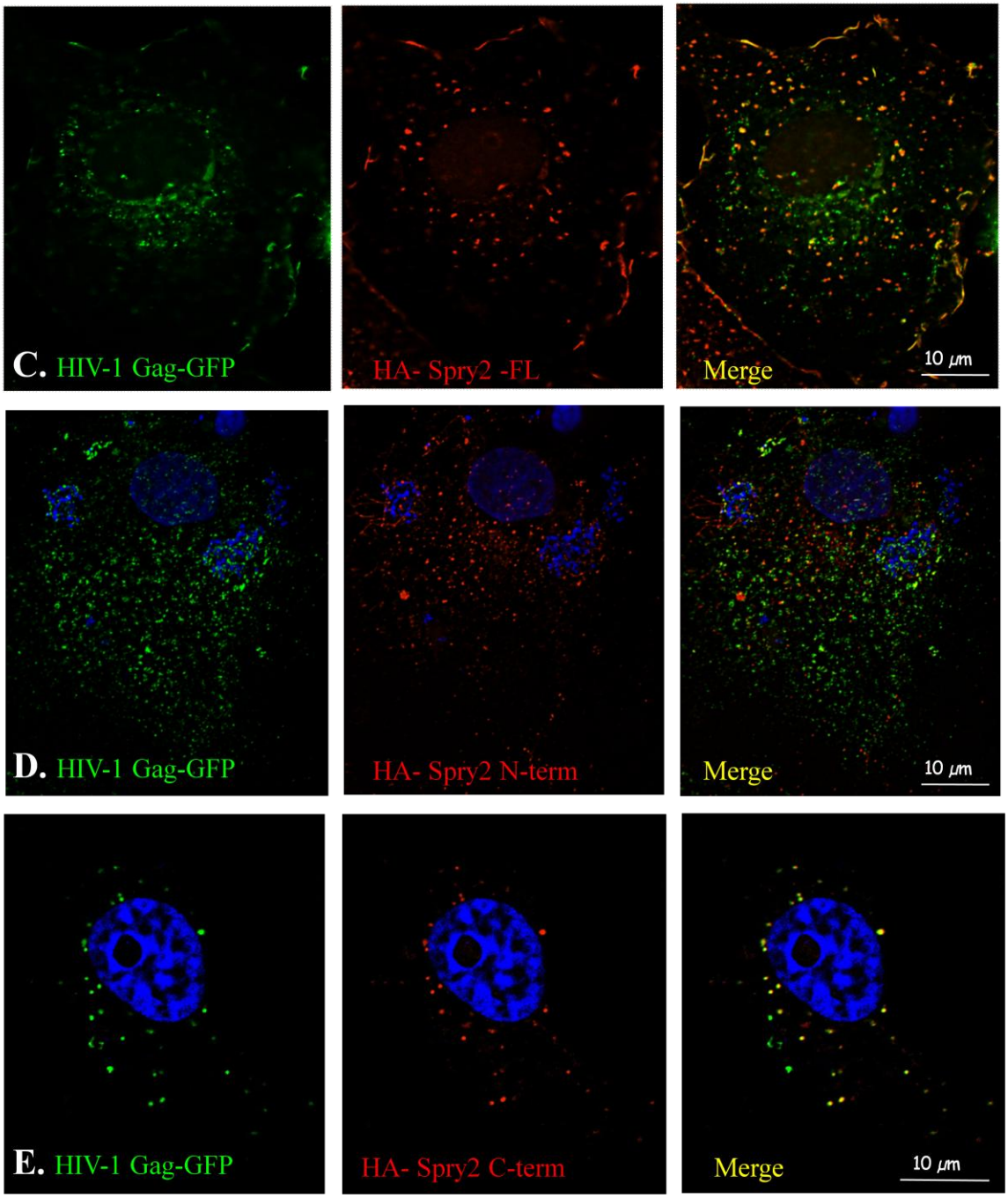
C. HIV-1 Gag-GFP
HA- Spry2 -FL
Merge
10 μm
D. HIV-1 Gag-GFP
HA- Spry2 N-term
Merge
10 μm
E. HIV-1 Gag-GFP
HA- Spry2 C-term
Merge
10 μm

observed that Gag's distribution was more intracellular. Cell expressing the Spry2 N-terminal fragment (*panel D*) showed a very peripheral punctate distribution but did not change the localization of Gag-GFP. In contrast, the Spry2 C-terminal domain had a dramatic effect on the localization of Gag (*panel E*). The Spry2 C-terminal fragment showed an exclusive cytoplasmic localization in the form of intracellular vesicles. In some cases, almost everyone of these vesicles co-localized with Gag-GFP, whose distribution also changed to exclusively cytoplasmic. In other cases, only a subset of the vesicles contained Gag. When looking at membrane proximal sites along the z-axis of the capture field, there was no evidence that Gag associated with the plasma membrane (*data not shown*). These findings suggest that while Spry2 full length could partially affect the localization of Gag, Gag appeared to be trapped with Spry2 in intracellular vesicles in the absence of the N-terminal region. Surprisingly, the translocation of Spry2 FL observed in cells expressing Gag (*panel C*) was not observed in cells expressing the C-terminal fragment even though the translocation domain which permits Spry2 to associate with the plasma membrane was intact. These findings suggest that determinants of the N-terminal part of Spry2 are required for proper translocation of both Spry2 and Gag to the plasma membrane.

Deletion of the PI(4,5)P_2 binding site in the C-terminal domain of Spry2 inhibits Gag VLP. It was clearly observed that the C-terminal domain was responsible for inhibiting Gag VLP release. This is surprising, as it the PI(4,5)P_2 –binding determinants in this region that permit Spry2 to translocate to the plasma membrane. The MA region in Gag also binds to PI(4,5)P2 and this binding is believed to be required for proper targeting of Gag to the plasma membrane and for efficient VLP release

Figure 4. Deletion of the PI(4,5)P_2 binding site in the C-terminal domain of Spry2 inhibits Gag VLP. A. Western blot analysis of VLP release. Cos-1 cells were transfected with DNA encoding HIV-Gag-GFP (*lane 1*) and increasing amounts of DNA DNA encoding HA-Spry2-FL (*lane 2 and 3*) or HA-Spry2 R252D (*lane 4 and 5*) at the indicated *gag* to *spry2* ratio. **B.** Semi-quantitative analysis of VLP release efficiency (VLP/VLP + Cell lysates).The panel shows the ratio of the Gag signal in VLP isolated from the media to the Gag signal in the cell lysate. **C., D.** Immunofluorescent images of Cos-1 cells transfected with HA-Spry2-FL (green, *panel C*) or HA-Spry2-R252D (*panel D*). HA-tagged constructs were detected by indirect immunofluorescence using a specific antibody against HA.

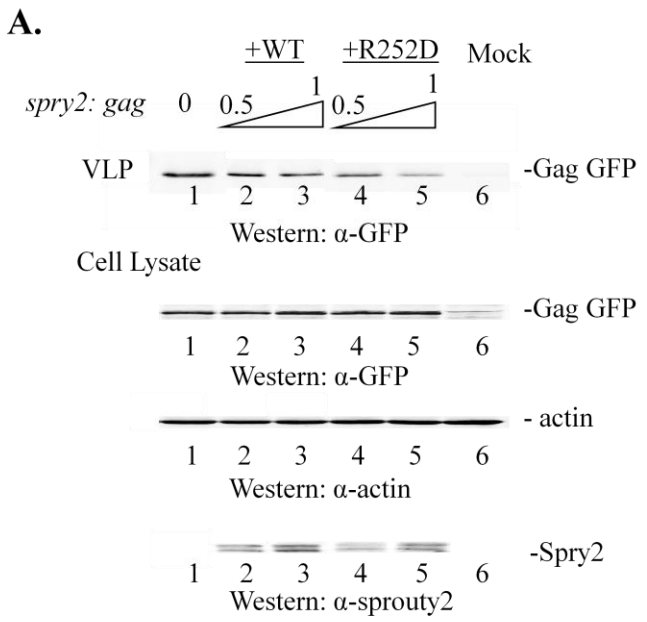
A.
+WT
+R252D
Mock
spry2: gag
0
0.5
1
0.5
1
VLP
-Gag GFP
1 2 3 4 5 6
Western: α-GFP
Cell Lysate
-Gag GFP
1 2 3 4 5 6
Western: α-GFP
- actin
1 2 3 4 5 6
Western: α-actin
-Spry2
1 2 3 4 5 6
Western: α-sprouty2

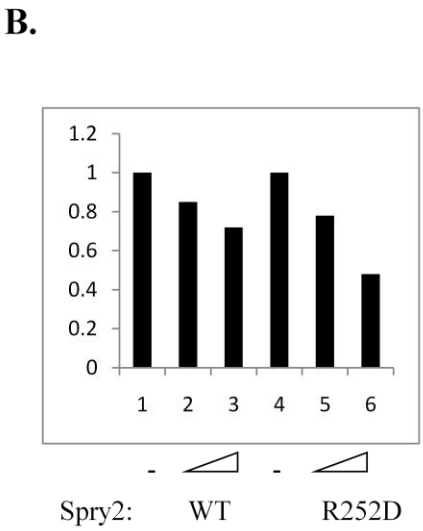
B.
1.2
1
0.8
0.6
0.4
0.2
0
1 2 3 4 5 6
- -
Spry2: WT R252D

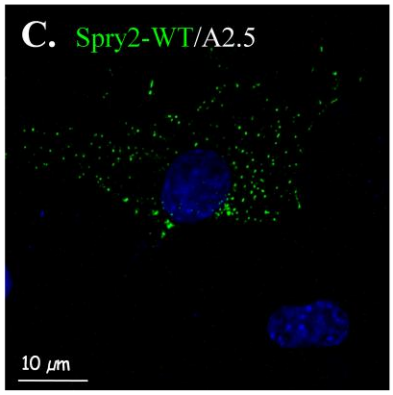
C. Spry2-WT/A2.5
10 μm

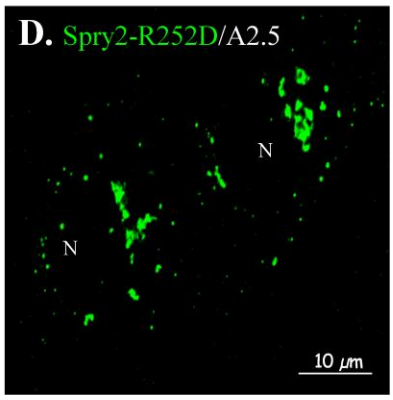
D. Spry2-R252D/A2.5
N
N
10 μm

(20, 101, 116). In order to examine the notion that Spry2 translocation to $PI(4,5)P_2$ on the plasma membrane is important for Spry2 and Gag localization, we utilized a Spry2 construct where the $PI(4,5)P_2$ binding site has been mutated (HA-Spry2-R252D). Cos-1 cells were mock transfected, and transfected with DNA encoding Gag-GFP, or co-transfected with DNA encoding Gag and either HA-Spry2-WT or HA-Spry2-R252D and virion production was examined by Western blotting. In general, co-expression of Gag with HA-Spry2-R252D either had the same effect as co-expression of Gag with WT Spry2, wherein both WT and mutated Spry2 inhibited VLP release (compare lanes 1 to 5 in Figure 4A) and by approximately the same degree (panel 4B) or neither inhibited VLP release significantly (*data not shown*). These results indicate that determinants in the N-terminal region of the Spry2 are important for Gag release and suggest that Spry2 interaction with $PI(4,5)P_2$ is not critical. To check that the mutation had affected Spry2 localization, confocal microscopy experiments were conducted using a line of Cos-7 cells that constitutively express Gag (Figure 4, *panel C and D*). As already presented, the localization of Spry2-WT showed a punctate cytoplasmic and plasma membrane distribution throughout the cell (*panel C*), however the mutation of the $PI(4,5)P_2$ binding site caused Spry2 to be concentrated into intracellular vesicles (*panel D*). These results confirm previous studies indicating that Spry2 $PI(4,5)P_2$ binding sites in the C-terminal translocation domain are important for proper localization of Spry2 to peripheral regions of the cell.

Deletion of conserved sequences in the N-terminal domain of Spry2 had no effect on WT Gag release but promotes release of Gag mutant lacking the Tsg101 binding site. As noted above, all mammalian Spry proteins contain a well conserved

Figure 5. Deletion of the highly conserved Spry2 Cbl binding site rescues release of a late domain Gag mutant. A. Western analysis of VLP release. Cos-1 cells were transfected with DNA encoding HIV-Gag-GFP alone (*lanes 1 and 2*) or P7L-Gag-GFP alone (*lanes 3 and 4*) or with HA-Spry2-ΔCbl (*lanes 5 to 7 and 8 to 10*) at *HA-Spry2* to *gag* ratios 0.5:1 (*lanes 5 and 8*); 1:1 (*lanes 6 and 9*); or 1:1.5 (*lanes 7 and 10*). The Gag and Spry2 proteins were detected using anti-GFP or anti-Spry2 antibodies, respectively. **B.** Semi-quantitative analysis of VLP release. The panel shows the ratio of Gag signal in VLP isolated from the media to the Gag signal in cell lysates and VLP (VLP/VLP +Cell lysates). Values reflect the mean ± SD of three independent experiments. Error bars represent the standard error (SEM).

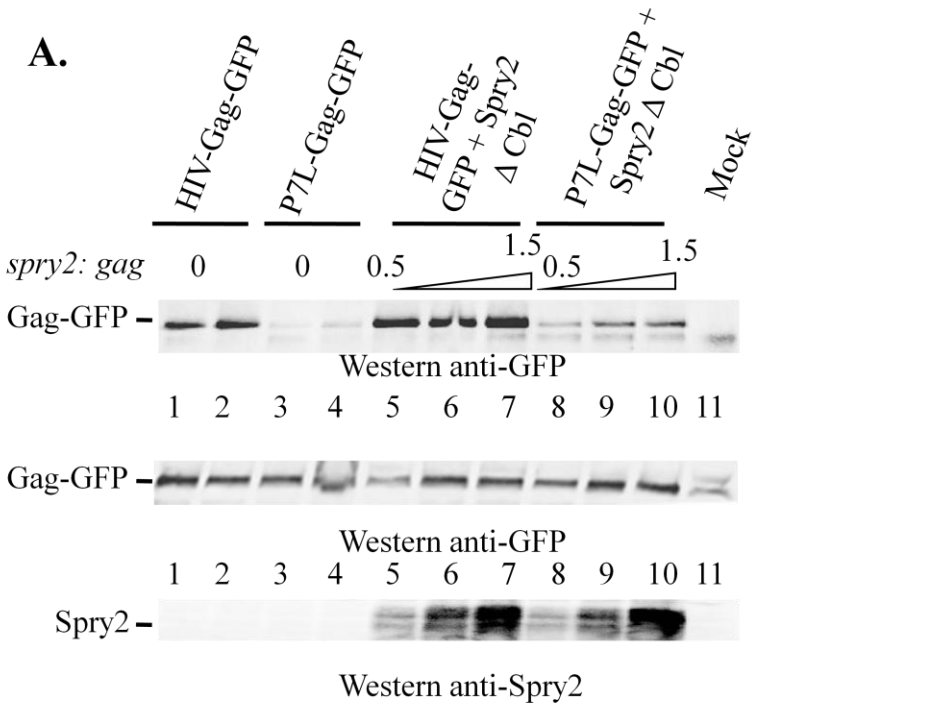
A.
HIV-Gag-GFP
P7L-Gag-GFP
HIV-Gag-GFP + Spry2 Δ Cbl
P7L-Gag-GFP + Spry2 Δ Cbl
Mock
spry2: gag
0
0
0.5
1.5
0.5
1.5
Gag-GFP
Western anti-GFP
1 2 3 4 5 6 7 8 9 10 11
Gag-GFP
Western anti-GFP
1 2 3 4 5 6 7 8 9 10 11
Spry2
Western anti-Spry2

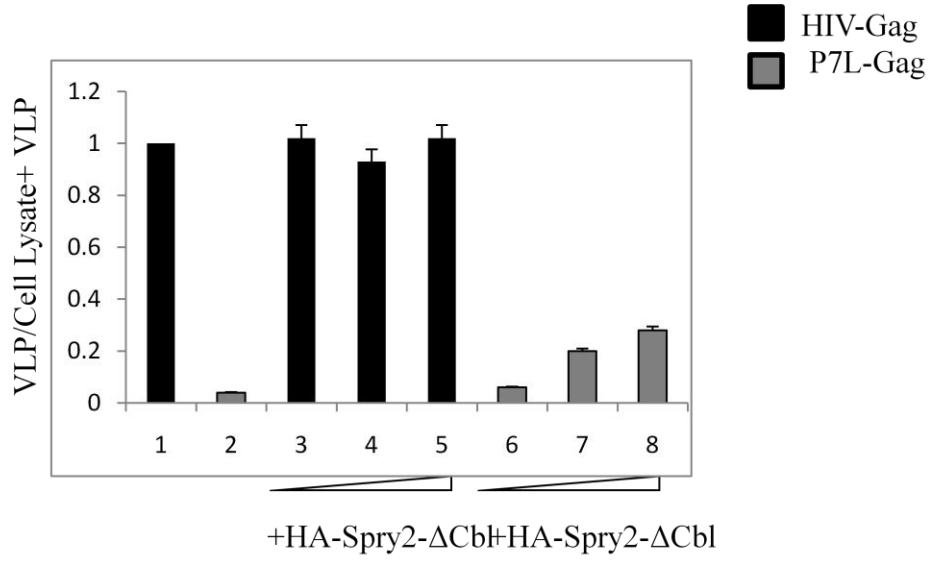
B.
HIV-Gag
P7L-Gag
VLP/Cell Lysate+ VLP
1.2
1
0.8
0.6
0.4
0.2
0
1 2 3 4 5 6 7 8
+HA-Spry2-ΔCbl+HA-Spry2-ΔCbl

region in their amino terminal end, that binds to the SH2 domain of the E3 ubiquitin ligase c-Cbl (141). In order to examine the importance of this site for VLP release, we utilized a construct encoding a variant of Spry2 containing a deletion that prevents its binding to c-Cbl (HA-Spry2ΔCbl). As seen in Figure 5, Cos-1 cells were mock transfected or transfected with DNA encoding HIV-1 Gag-GFP and different DNA concentrations of HA-Spry2 ΔCbl. Virus production was analyzed by Western blotting. As shown in Figure 5 (*panel A*) overexpression of the mutant form of Spry2 had little or no effect on the level of HIV-Gag VLP detected in the media (*lanes 5-7*) when compared to the control expressing Gag alone (*lanes 1 and 2*). However, a more dramatic effect on VLP release was observed in cells expressing a late domain Gag mutant (P7L-Gag). This mutant exhibits defective Tsg101 binding and is released very inefficiently (83). Compared to the control expressing P7L-Gag alone (*lanes 3 and 4*), cells that were co-transfected with P7L-Gag and HA-Spry2-ΔCbl showed an increase in the amount of VLP in the media and no change in the level of Gag intracellularly, indicating enhanced release efficiency (*lanes 8 to 10*). A semi-quantitative analysis (*panel B*) of VLP efficiency indicated that the expression of Spry2- ΔCbl in cells expressing P7L-Gag increased VLP production by approximately 7-fold at the highest DNA concentration tested. These results suggest that deletion of the Cbl binding site relieved the inhibition mediated through the C-terminal region of Spry2 that was often observed with the WT Spry2 protein. Furthermore, and most significantly, these observations suggest that deletion of the Cbl binding site in Spry2 can rescue VLP release in the absence of Tsg101 binding.

Figure 6. Intracellular relationship of Spry2 variants and Gag. Cos-1 cells were transfected with DNA encoding WT-Gag-GFP or P7L-GFP alone (***panel A***, left and right, respectively), P7L and the Spry2-C-Term fragment (***panel B***), WT and Spry2- ΔCbl (***panel C***), or P7L Gag and Spry2-ΔCbl (***panel D***) Merge images show the red (Spry2) and green (WT or P7L) signals. Hoescht stain reveals nucleus (blue).

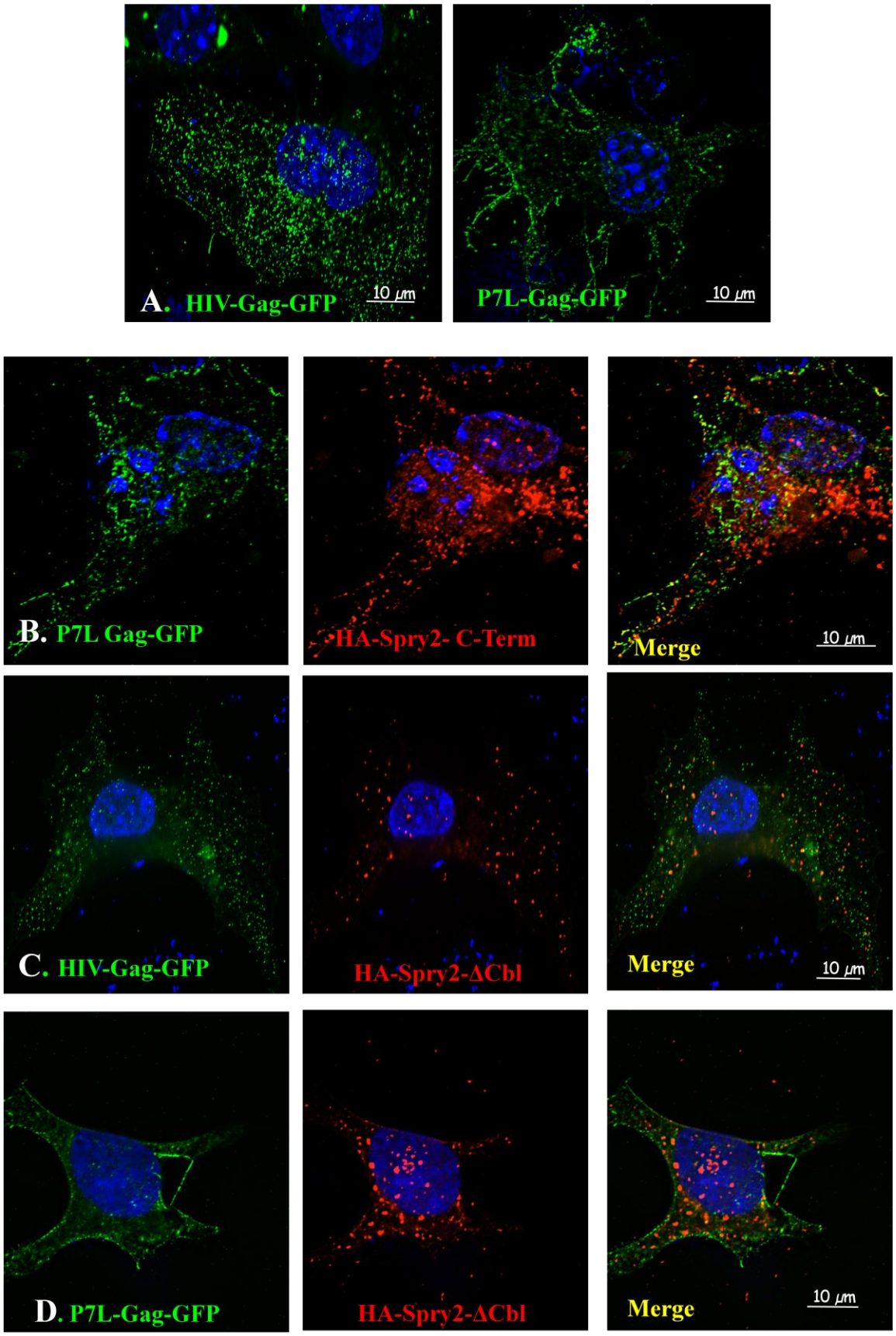
A. HIV-Gag-GFP
10 μm
P7L-Gag-GFP
10 μm
B. P7L Gag-GFP
HA-Spry2- C-Term
Merge
10 μm
C. HIV-Gag-GFP
HA-Spry2-ΔCbl
Merge
10 μm
D. P7L-Gag-GFP
HA-Spry2-ΔCbl
Merge
10 μm

Deletion of the Tsg101 binding site in Gag relieves Gag sensitivity to inhibition by the Spry2 C-terminal fragment. The observation that Spry2-ΔCbl had no effect on WT Gag release and rescued P7L-Gag release suggested that its relationship with Gag intracellularly is different from the relationship of Gag and the Spry2 C-terminal fragment. To examine this, we conducted confocal microscopy experiments to examine their localization. Cos-1 cells were transfected with DNA encoding HIV-Gag-GFP or P7L-Gag-GFP and HA-Spry2-ΔCbl or Spry2 C-Term. The Spry2 mutants were detected by indirect immunostaining using an antibody against the HA tag. As observed in Figure 6, cells transfected with either HIV-Gag-GFP (*panel A, left*) or P7L-Gag-GFP (*panel A, right*) exhibited an even punctate distribution throughout the cell. P7L-Gag-GFP exhibited a similar distribution when co-expressed with the Spry2-C-Term fragment (*panel B*). This contrasted significantly with the altered Gag distribution that was observed when WT Gag was co-expressed with Spry2-C-term, as described above (see Figure 3E above). Expression of HA-Spry2-ΔCbl did not disturb the localization pattern of WT Gag (*panel C*) or P7L-Gag (*panel D*). These results indicate that interference with Tsg101 binding altered the relationship between Gag and Spry2 such that Gag was no longer susceptible to the sequestration mediated by the Spry2-C-terminal fragment. Also, although examination by confocal microscopy did not provide an explanation, interference with the Spry2 N-terminal region must have altered the relationship of Spry2 with the Gag mutant, since co-expression with Spry2-ΔCbl rescued P7L release.

WT and ΔCbl-Spry2 exhibit different interactions with membrane components. One possible mechanism by which deletion of sequences in the N-terminal region of Spry2 might rescue Gag VLP release in the absence of Tsg101 binding is by

Figure 7. Intracellular relationship of Spry2 full length or Spry2 variant (Spry2-ΔCbl). and caveolin-1 (Cav-1) in the presence of Gag A. Confocal microspcopy of A2.5 cells (*panel A*) transfected with HA-Spry2 FL(green) and endogenous Caveolin-1 (Cav-1;red). Colocalization is observed in the merge imaged. The boxed region is magnified in the panel on the right. **B**. A2.5 cells expressing HA-Spry ΔCbl. Endogenous Cav-1 was detected by using specific antibodies against Cav-1

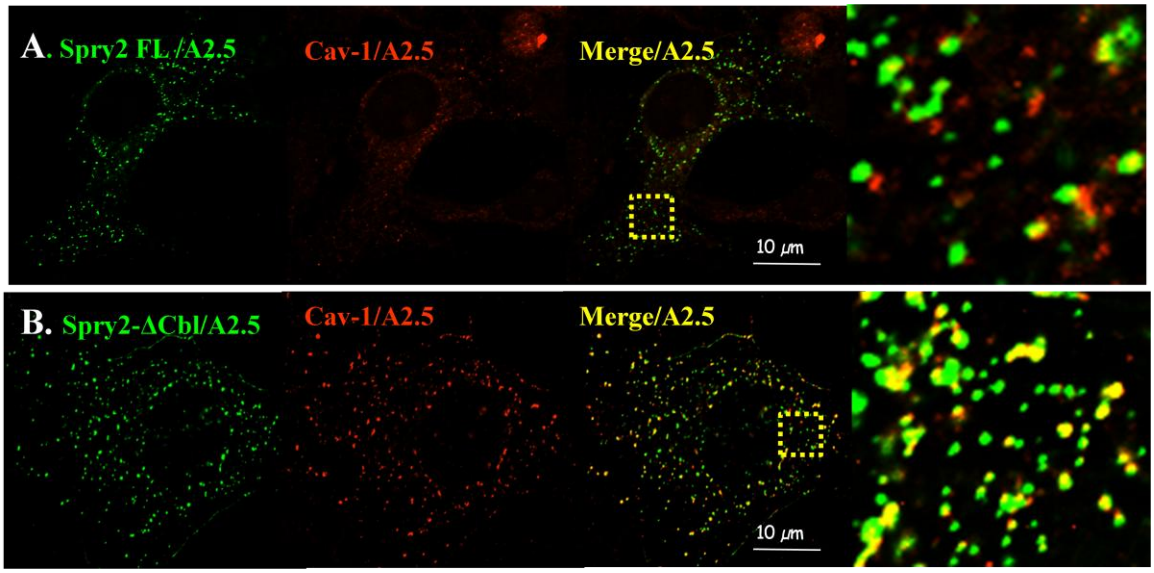
A. Spry2 FL /A2.5
Cav-1/A2.5
Merge/A2.5
10 μm
B. Spry2-ΔCbl/A2.5
Cav-1/A2.5
Merge/A2.5
10 μm

exposing determinants in the C-terminal region of the protein that might link P7L-Gag to ESCRT machinery or other factors that could facilitate VLP release. To examine this possibility, we tested for differences in the C-terminal regions of WT and ΔCbl-Spry2 by determining their ability to co-localize with a known C-terminal binding partner, caveolin-1 (binds aa175-315). As previously reported, Spry proteins can associate with caveolin-1 (cav-1) through its C-terminus (14, 55, 96); specifically it was shown that Spry2 can colocalize with cav-1 at vesicular structures and the plasma membrane (55). Cav-1 is the principal component of caveolae membranes, which are invaginations of lipid rafts that are rich in cholesterol, glycosphingolipids, and glycosyl-phosphatidylinositol (GPI)-linked molecules (112). We conducted experiments to examine the relationship of Spry2 with cav-1 in the presence of Gag. A2.5 cells were transfected in the presence of Spry2 full length or Spry2 ΔCbl. Twenty four hours post-transfection, cells were indirectly immunostained for detection of the HA-tagged constructs and endogenous cav-1 using specific antibodies. As observed in Figure 7, cells that were constitutively expressing HIV-Gag (A2.5) and transiently expressing Spry2 full length (*in green*; *panel A*), did not show an association with the cav-1 marker (*in red; panel A*). In contrast, A2.5 cells that were expressing Spry2-ΔCbl (*panel B*), showed a very close association with cav-1. Clear colocalization was observed in vesicular structures and at the plasma membrane. This was indicated by the yellow color *(merge*). These results suggest that in the presence of Gag, the accessibility of the C-terminal region and, specifically, the interactions of Spry2 WT and the Spry2 mutant with cav-1 compartments are different.

Figure 8. WT and ΔCbl differ in localization with detergent –resistant PI(4,5)P_2. Immunofluorescent of A2.5 cells that were mock transfected (*panel A and D*) or transfected with Spry2 FL (*green; panel B and E*) or Spry2 ΔCbl (*green; panel C and F*). The endogenous PI(4,5)P_2 was detected by using a specific antibody against PI(4,5)P_2 (red) by permeabilizing the cell with saponin (*panel A,B and C*) or Triton X-100 (*panel D, E and F*).

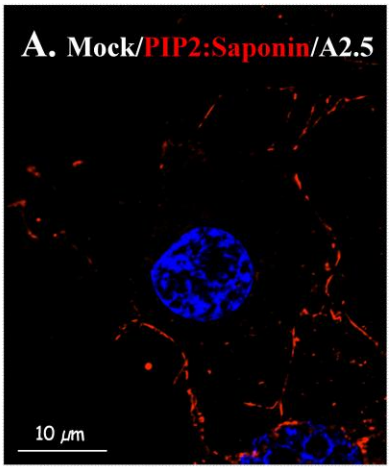
A. Mock/PIP2:Saponin/A2.5
10 μm

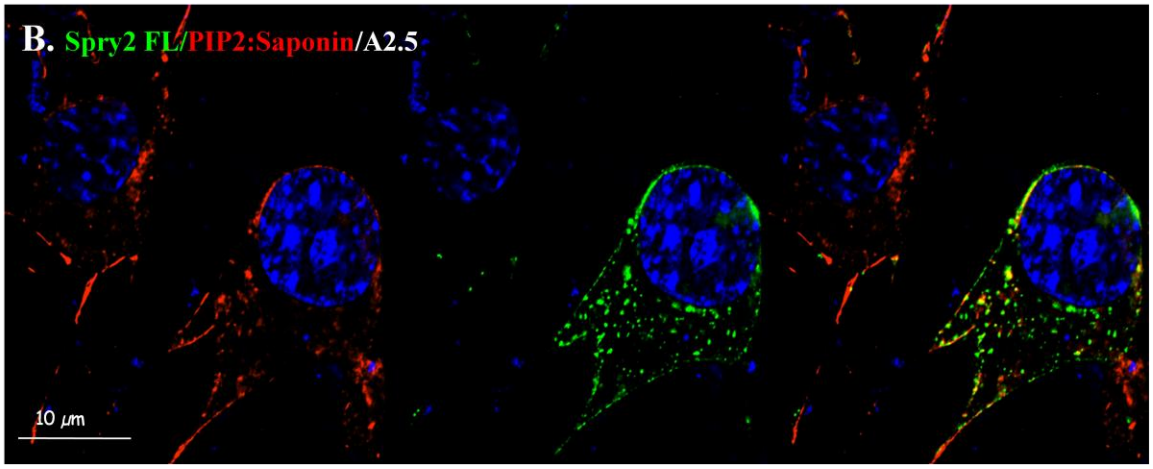
B. Spry2 FL/PIP2:Saponin/A2.5
10 μm

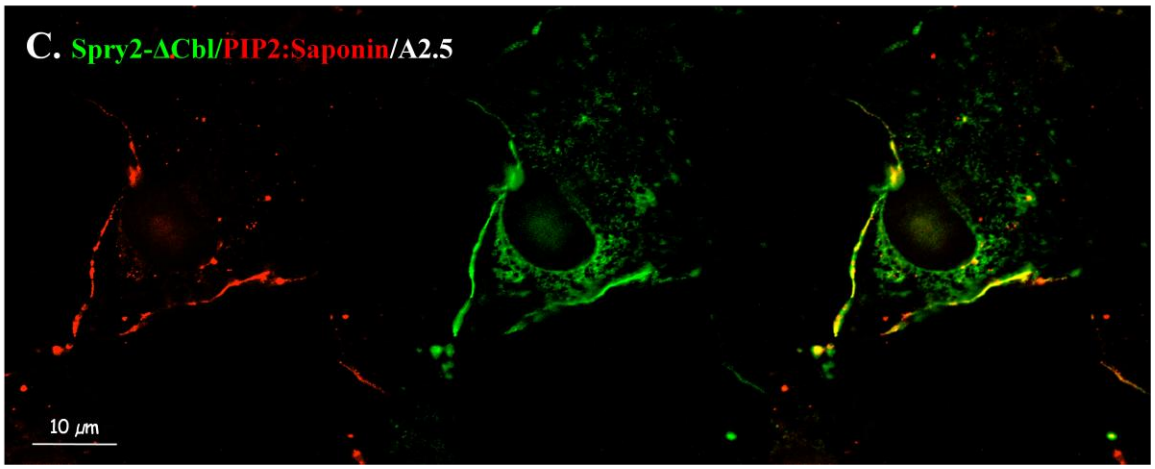
C. Spry2-ΔCbl/PIP2:Saponin/A2.5
10 μm

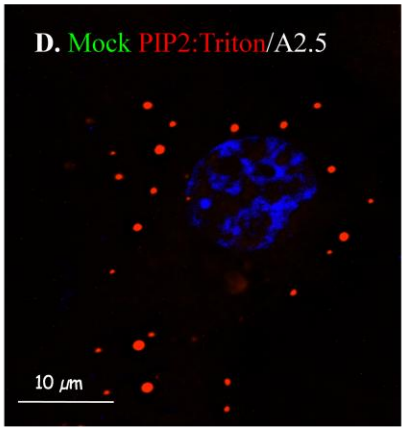
D. Mock PIP2:Triton/A2.5
10 μm

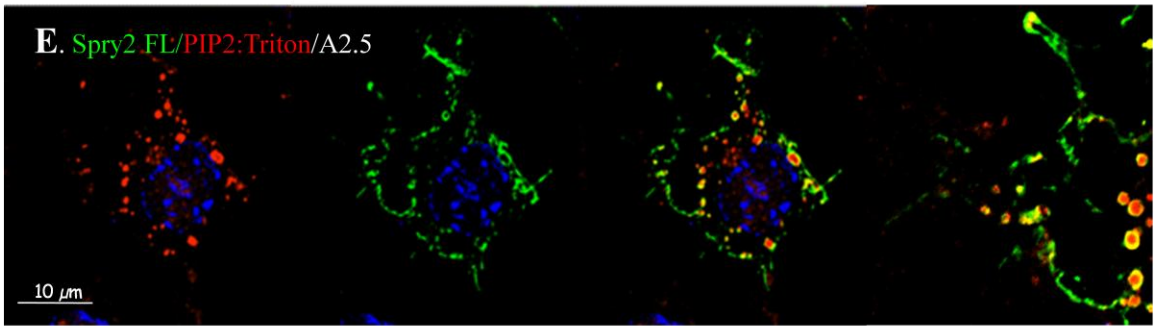
E. Spry2 FL/PIP2:Triton/A2.5
10 μm

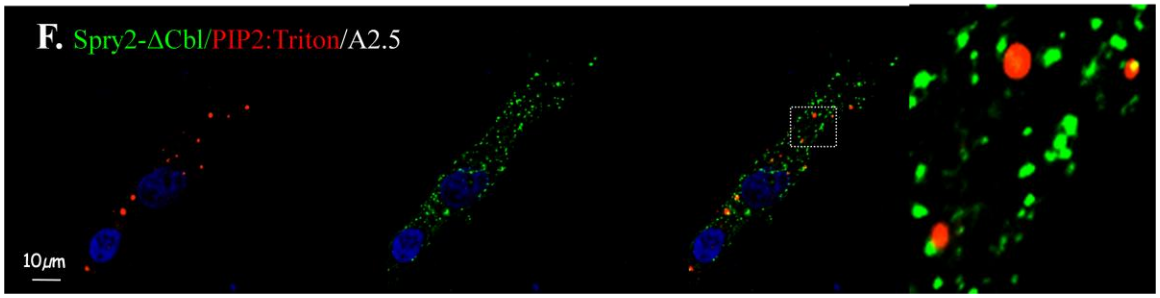
F. Spry2-ΔCbl/PIP2:Triton/A2.5
10μm

WT and ΔCbl-Spry2 interactions with PI(4,5)P_2 exhibit different sensitivity to Triton X-100 extraction. As discussed above, another factor that interacts with the C-terminal region of Spry2 is PI(4,5)P_2. To determine whether WT and ΔCbl-Spry2 interacted similarly or differently with this factor, we analyzed and compared the association between Spry2 FL and Spry2-ΔCbl with this phospholipid, using confocal microscopy. The detection of endogenous PI(4,5)P_2 was performed by utilizing two different permeabilization techniques: a) saponin; and b) Triton X-100 treatments. These two treatment detect PI(4,5)P2 associated at the plasma membrane and at distinct domains in the plasma membrane, respectively. As illustrated in Figure 8, localization of PI(4,5)P_2 in cells that were mock-transfected (*panel A)* was mainly at the plasma membrane. Similarly, in cells that were expressing Spry full length (*panel B*) or Spry-ΔCbl (*panel C*), PI(4,5)P_2 was distributed along the plasma membrane and both WT and mutated Spry2 co-localized with the phospholipid on the plasma membrane. This makes sense, since the PI(4,5)P_2 binding site in Spry2 was intact in both cases. However, cold Triton X-100 extraction allowed us to distinguish PI(4,5)P_2 populations that differed in ability to co-localize with Spry2. As observed in panel D, in mock-treated cells, PI(4,5)P_2 was mainly detected in Triton X-100-resistant vesicles that were scattered throughout the cytoplasm. In the presence of WT Spry2, PI(4,5)P_2 was detected in similar vesicular structures and also in peripheral regions at the plasma membrane. PI(4,5)P_2-Spry2 co-localization was detected in both locations (*panel E*). In contrast, in cells that were expressing Spry2-ΔCbl and extracted with cold Triton X-100, the PI(4,5)P_2 distribution was similar to that detected in the mock-treated cells and no co-localization between Spry2 and PI(4,5)P_2 was observed (*panel F*). These results indicated that Spry2 and

Spry2-ΔCbl differed in their ability to localize with Triton X-1000-resistant-PI(4,5)P_2 complexes and suggested that they associated with different regions of the plasma membrane. Thus, determinants in the N-terminal region of Spry2 might play a direct role in modulating the accessibility of PI(4,5)P_2 that is required for efficient Gag release or regulate C-terminal accessibility to Spry2-binding partners that control ESCRT machinery.

DISCUSSION

The results presented in this Chapter reveal important features of the ESCRT-mediated trafficking pathways required for the efficient release of HIV-1 Gag VLPs. In this study we describe the relationship of Gag with a regulator of ESCRT-mediated pathways that directs release through the plasma membrane. We explore the role of Spry2, a non-ESCRT protein that regulates ESCRT-mediated trafficking pathways and its relationship with Gag trafficking and release.

Here, we have used the siRNA and overexpression approach to elucidate Spry2's mode of action in the release of VLPs. We showed that endogenous levels of Spry2 are required for proper egress of HIV-1 VLPs. However, we observed that overexpression of Spry2 full length had a negative impact on the efficiency of VLPs and this inhibitory effect was mediated by Spry2 C-terminal domain. Immunofluorescent studies demonstrated that inhibition of VLP correlated with a concentration of Spry2 and Gag in intracellular locations. Specifically, we observed that deletion of the N-terminal domain of Spry2 blocked its translocation to the plasma membrane and also prevented the

localization of HIV Gag at the cell periphery, thereby inhibiting VLP release. These observations strongly indicated that N-terminal determinants of Spry2 participate in regulating Spry2 and Gag localization at the plasma membrane. Most likely, translocation of Spry2 to the plasma membrane regulates HIV-1 Gag plasma membrane localization. It is interesting to note in this regard that, although the translocation domain of Spry2 is located in the C-terminal domain (aa178-194; C-terminal domain = aa175-315), a region that permits Spry2 to bind microtubules is located in the N-terminal region (aa123-177; N-terminal domain = aa1-175).

As mentioned in the introduction, Spry2 can associated with PI(4,5)P_2 at the plasma membrane (73). Similarly, this phospholipid can directly interact with HIV-1 Gag, and is believe to target Gag to the plasma membrane and promotes VLP release (101, 116). Together, these findings suggest that PI(4,5)P_2 plays a critical role in directing Spry2 and Gag to the plasma membrane. In this study we observed that, although the interaction of Spry2 with PI(4,5)P_2 is regulated by its PI(4,5)P_2 binding site located in the C-terminal part, it is the Cbl binding site located in the N-terminal end that appears to be critical for facilitating Gag release. This was particularly evident in the absence of Tsg101 binding, suggesting that Spry2 might provide a link to ESCRT machinery that is cryptic or less apparent when Tsg101 is bound to Gag. Our studies also suggest that determinants in the N-terminal region of Spry2 influence the membrane region to which Spry2 is localized. Since Gag and Spry2-ΔCbl were found to be associated in immunoprecipitation experiments (not shown), it is likely that Spry2 influences the membrane region to which Gag is targeted.

In this study, we utilized the cellular marker, caveolin-1, to distinguish differences in localization of the WT Spry2 and a Spry2 mutant lacking N-terminal domain sequences. However, it is important to note that caveolin-1 participates in lipid transport, specifically of cholesterol and other lipids that make up lipid rafts (74), and can directly bind to Spry2 through the C-terminal domain (14). This fact, together with our observations, leads us to speculate that Spry2 might be modulating the trafficking of caveolar compartments that are rich in lipid rafts. As previously noted, lipid rafts are domains that have been implicated in HIV-1 assembly and release (94, 103). In addition, caveolin-1 has been shown to participate in the compartmentalization of signaling, specifically by modulating $PI(4,5)P_2$ hydrolysis in caveolar compartments (108). Therefore, future studies should address the importance of regulating the trafficking of caveolar compartments to the plasma membrane, specifically how Spry2 modulates the targeting of lipid rafts to the plasma membrane. This will provide an alternative mechanism to explain the Spry2 role in Gag release.

We observed that a Spry2 variant rescued release of a late domain Gag mutant in a dose-dependent manner. Although the data presented in this study cannot explain why this is the case, several possibilities can be discussed: *i)* Spry2 can bind to several proteins that permit Spry2 to act as a regulator of ESCRT-mediated pathways. One way of regulating this pathway is by the recruitment of endocytic complexes, including the CIN85/endophilins (42). This complex can provide a link to the endocytic machinery by interacting with ALIX. Recruitment of the ESCRT machinery that is required for efficient release can be sustained by the interaction between ALIX and ESCRT-III components in the absence of Tsg101; *ii*) Close examination of Spry2 C-terminal domain

revealed the sequence motif PTVP, which resembles a binding site for Tsg101. Furthermore, previous observations by confocal microscopy indicate that Tsg101 and Spry2 have can be found in close proximity (*data not shown*). If there is the formation of a Tsg101-Spry2 complex, then Spry2 can facilitate the targeting of Tsg101 to plasma membrane sites, where it is required for efficient Gag release. This provides an alternative method to direct Tsg101 and other ESCRT components to the membrane; and *iii*) Recent examination of a chimera protein (P7L-Gag-Eap20), where a component of the ESCRT-II complex (Eap20) was translationally fused to the C-terminal end of the late domain Gag mutant (P7L-Gag) indicated that Spry2 can co-localize with this protein intracellularly as well as at the plasma membrane (*data not shown*). This observation suggests that Spry2 can provide Gag with an alternative link to the ESCRT machinery independent of its interaction with Tsg101 or ESCRT-I components. Rescue experiments are currently being examined to provide support for this notion.

We believe that Spry2 functions as a regulator of ESCRT-mediated trafficking pathways by interacting with different components of the endocytic machinery and a modulator (in this study) of the availability of $PI(4,5)P_2$ in specific domains of the plasma membrane. HIV-1 Gag can take advantage of these two functions that are proposed in this study: Spry2 can prevent Gag from being downregulated once in the endocytic pathway and Spry2 can facilitate the availability of the phospholipid $PI(4,5)P_2$ in the membrane to target Gag to a specific $PI(4,5)P_2$-enriched membrane domain, allowing efficient VLP release.

MATERIAL AND METHODS

Cell culture and transfection.

Cos-1 cells were grown in Dulbecco's modified Eagle medium supplemented with 5% fetal bovine serum and 1% of penicillin and streptomycin. For transfection experiments, cells were seeded to obtain 60% confluency in a 100 mm tissue culture plate. For immunofluorescent experiments cells were seeded to obtain 40% confluency on a coverslips place in a 6 well tissue culture plate. Cells were grown at 37°C under 5% CO_2. Cells were transfected by using Fugene6 transfection reagent according to the instructions of the manufacturer.

Plasmids

pCMV-HIV-1 gag encoding HIV-1 Gag C-terminally tagged with green fluorescent protein (Gag-GFP) had been previously described (50). Briefly, plasmid p55M1234, a Rev-independent full length *gag* gene clones was used to amplify the Gag sequence by PCR to produce and EcoRI site at the 5'end and a BamHI at the 3' to allow the insertion into pEGFP-N1 in frame with the *gfp* gene. Site directed mutation of the Gag PTAP motif to generate the construct P7L-Gag-GFP encoding a Gag with a non-functional domain LTAP was constructed by using a site directed mutagenesis kit. The point mutation was sequenced to confirm the specific mutation. Plasmids encoding the human full length Spry2 N-terminally tagged with HA (pCGN-Spry2) and all fragments and point mutants were a generously provided by Dr. Dafna Bar-Sagi (New York University, NY, NY) and have been previously described (43). Briefly, the human Spry2 cDNA was subcloned in the HA tag-containing mammalian expression vector (pCGN), using standard PCR

reaction and molecular cloning techniques. The specific restriction sites utilized for the cloning were 5' XbaI and 3' BamHI.

RNA Interference

In this study, we used two methods to deplete the endogenous levels of Spry2. The DNA-based RNAi (Spry2shRNA) was a kind gift from Dr. Bar-Sagi and have been previously described (62). This plasmid DNA encodes a short hairpin RNA (shRNA) that targets the Spry2 gene. The specific targeting sequence is contained within the cysteine-rich domain of Spry2 (220-228aa). Briefly, the following oligonucleotides were annealed and subcloned to the BglII and Acc65I sited of pcDNA/SUPER: 5'GATCCCCGTGTGAAAGGTCTCTTCTATTCAAGAGATAGAAGAGACCTTTTCACACT TTTTGGAAG-3' and 5'GTACCTTCCAAAAAGTGGAAGGTCTCTTCTATCTCTTGAAT AGAAGAGACCTTTCACACGGG-3'. Small RNAs are synthesized from this DNA template under the control of an RNA polymerase III promoter in transfected cells. Pol III has the advantage of directing the synthesis of small, noncoding transcripts whose 3'ends are defined by termination within a stretch of 4-5 thymidines (9). The other method utilized was RNA –based RNAi and the synthetic siRNA directed against the human Spry2 and the siControl was purchased from Dharmacon (Lafayette, CO). The siRNA Spry2 was designed by the ON-TARGET plus siRNA database in Dharmacon's website.

Real-time PCR analysis

RNA was prepared from Cos-1 cells that were transfected with siRNA against the human Spry2 or siControl in the presence of HIV-1 Gag-GFP. Extraction of RNA was obtained

by using the Qiagen RNeasy kit and Qiashredder (Qiagen) according to the manufacturer's protocol. Aproximately 5ug of RNA was reverse transcribed using oligo-dT and Super Script III Reverse Transcriptase (Invitrogen, Carlsbad, CA). Quantitative PCR analysis was performed on a LightCycler (Roche) utilizing the cDNA templates and different primer pairs. The reaction consisted of FastStart DNA Master SYBR Green I (Roche), 2.5 mM $MgCl_2$, and 25µM of each primer. In brief, the PCR program consisted of 95°C for 10 minutes, proceeded by 45 amplification cycles of 95°C for 5 seconds, 55°C for 5 seconds, followed by 72°C for 10 seconds, and a final incubation at 82°C to avoid primer dimerization prior to quantification. For each gene, a standard curve based on successive cDNA dilutions was performed. To ensure a thorough calculation starting quantities of cDNAs of interest were compared to those of a house-keeping gene (*h60s*) in the same plate. After each qPCR, specificity of the amplification was controlled by a melting curve ranging from 55-95 °C. All primers were designed in regions flanking introns to exclude data alteration by possible DNA contamination. *Spry2* primers were designed by using Primer3 software (http://frodo.wi.mit.edu/cgi-bin/primer3/primer3_www.cgi) and generated by Operon Biotechnologies (Huntsville, AL). *Spry2* forward primer: 5'-CTAAGCCTGCTGGAGTGACC-3' with a Tm = 64.5°C; and *Spry2* reverse primer: 5'-GTGTTTCGGATGGCTCTGAT-3'with a Tm = 60.4°C. The p1 subunit of the human 60S ribosomal unit gene was utilized as a house-keeping gene in the QPCR reaction. The primers generated were as follows: *h60s* forward primer: 5'-ATCTACTCGGCCCTCATTCTGC-3' with a Tm = 58.7°C and *h60s* reverse primer: 5' GGTCCACCGGCCCCTACATT-3' with a Tm = 62.1°C.

Preparation of cytoplasmic extracts and virus isolation

At 48 hours post-transfection, the cells were harvested by scraping into cold Dulbecco's Phosphate-Buffered Saline (D-PBS) and collected by centrifugation at 3000 rpm for 10 min at 4°C. The pelleted cells were washed two times with cold D-PBS and allowed to swell with lysis buffer (1% Triton X-100; 160 mM NaCl, 20 mM Tris pH 8.0), containing protease inhibitors. The total lysate of approximately 1 ml was spun for 10 min. at 14,000 x g at 4°C to get rid of large particulate material. A similar procedure was utilized to prepare cytoplasmic extracts for the immunoprecipitation experiments. In order to isolate the virus-like particles produced (VLPs) produced by Gag, the cell culture media from each plate was filtered through a 0.45 µm filter and applied to a cushion of 20% sucrose in a centrifuge tube and spun at 37,000 rpm for 90 min at 4°C. The pelleted VLPs were resuspended in 50 ul of PBS and loading buffer at 4°C. Before loading in a 12.5% SDS-polyacrylamide gel, the samples were boiled at 100 °C for 5 min.

Protein detection

Proteins were separated by electrophoresis through 12.5% polyacrylamide gels. Following electrophoresis, the gels were transferred to nitrocellulose membranes and analyze by Western blotting. The membranes were blocked in 5% non-fat milk for 1 hour and then rinsed three times with PBS-T (1% Tween). Shortly after, the membranes were incubated with the primary antibody for 24 hours and rinsed. The corresponding secondary antibody was added at a 1:10,000 dilution in 5% non-fat milk dissolve in PBS-T and incubated for 1 hour at room temperature. Proteins were visualized by scanning the

membrane with Odyssey Infrared Imaging System and protein levels were quantified using the Odyssey software.

Antibodies

Sprouty2 was detected by using a polyclonal antibody (Sigma, St.Louis, MO) that recognizes the C-terminal region of Spry2 (Sigma, St.Louis, MO) or the N-terminal region of Spry2 (Upstate, NY) at 1:5000 dilution. HA tagged proteins were detected by using either monoclonal or polyclonal antibodies from Sigma; for Western blot analysis a 1:1000 dilution was used; for immunofluorescent experiments a 1:100 dilution was utilized. GFP tagged proteins were detected by using a monoclonal antibody from Clontech Laboratories at a 1:1000 dilution. Endogenous PI (4,5) P_2 was detected by using monoclonal antibodies from Abcam (Cambridge, MA) at a 1:100 dilution.

Fluorescence microscopy

Cos-1 cells were used for fluorescence imaging due to the relatively high ratio of cytoplasm to nucleus, which facilitates the analysis of cellular trafficking events. These cells were grown to 40% confluency on large square coverslips (22 x 22 mm) in six well plates in DMEM supplemented with fetal bovine serum and antibiotics (1% streptomycin and penicillin) and transfected as previously described. At 24 hours post-transfection, the cells were washed twice with PBS and fixed in 3.7% formaldehyde in PBS for 20 min at room temperature on a rocking platform and covered with aluminum foil. In samples that required detection of PI(4,5)P_2 at the plasma membrane, fixation and permeabilization was done simultaneously (3.7 % formaldehyde, 0.1% glutaraldehyde and 0.075 % mg/ml saponin) at room temperature for 20 min. as was previously described (44, 131). Samples were then washed three times with PBS, for 5 min. each wash and permeabilized with 0.1% Triton-X-100 for 4 min. and washed three times again with

PBS. After blocking for 10min in PBS containing 1% bovine serum albumin (BSA), the cells were incubated with primary antibody for 1 hour at 37°C, rinsed three times with PBS and then incubated with the secondary antibody conjugated with the fluorophore TRITC, Texas Red or FITC for 30 min at 37°C. The nuclear stain, Hoeschst (Molecular Probes, Eugene, OR) was added in the last 10 min. Samples were washed three times with PBS. After the final rinse, the cells were mounted using Vectashield hard set mounting medium (Vector Laboratories, Burlingame, CA). Confocal images were captured with an inverted fluorescent/dic Zeiss Axiovert 200M microscope equipped with an AxioCam HRm camera (Zeiss, Thornwood, NY) and mercury arc lamp light source using a 63x Plan-Apochromat (NA 1.40) oil objective and operated using Axiovision version 4.1-4.5 software. More than 40 cell images were examined from duplicate samples in each experiment. Approximately 20 optical sections along the z-axis were acquired (each z section measures 0.4μ). Most of the figures show the central image. The fluorescent data sets were deconvoluted using the constraint iterative method of the Axiovision software.

CHAPTER 6: Discussion

In this thesis I have addressed an important question concerning the ESCRT mediated pathways that are utilized by the functional exchangeable L domains of HIV-1 and RSV Gag, namely, how are the two entering the pathways that leads to efficient viral release. In addition, I have explored the possibility that a non-ESCRT cellular protein, Spry2, that modulates ESCRT-facilitated receptor downregulation, can facilitate Gag membrane targeting and release efficiency. The result observed in these studies has served to examine alternative pathways that are utilized by retroviral Gags (*summarized* i*n* Figure 1) that interconnect ESCRT and non-ESCRT cellular proteins for efficient release.

While the exiting pathway for the human retrovirus (HIV-1) exploits the endocytic-sorting cellular machinery by engaging Tsg101 and ALIX through PTAP and LYPX late (L) domains, the chicken retrovirus (RSV/ASV) uses PPXY L domains to recruit Nedd4 family ubiquitin ligases; however how this ubiquitin ligase connect PPXY L domains to the endocytic pathway is not clearly understood. The observations that Tsg101 and Nedd4 can stably associate in the cytoplasm suggested that both PTAP and PPXY domain converge at this point of the pathway, however, this idea was not consistent with our findings since dominant negative (DN) inhibitors of ASV-Gag did not inhibit HIV-1 VLP release. Similarly, DN inhibitors of HIV-Gag did not inhibit ASV-VLP. It became clear that although both retroviral Gags utilize the endocytic machinery; their interaction with Tsg101-Nedd4 complex was not the same. Recent studies have

Figure 1. The interconnected network of ESCRT and non-ESCRT cellular proteins required for efficient retroviral release. Schematic diagram showing the ESCRT and non-ESCRT proteins that are required for ASV and HIV-Gag release. Black lines indicate the pathways mediated by Nedd4 or Tsg101 that direct the release of functionally exchangeable PPPY or PTAP L domains; respectively. Green lines indicate the alternative pathways utilize by ASV Gag, mediated by either a) Tsg101; b) ESCRT-II; c) ESCRT-III. Pink and yellow blocks at the plasma membrane indicate different membrane domains defined by the phospholipids N-Rh-PE and $PI(4,5)P_2$; respectively. A non-ESCRT protein, Spry2 * regulates ESCRT mediated pathways and modulates $PI(4,5)P_2$ availability.

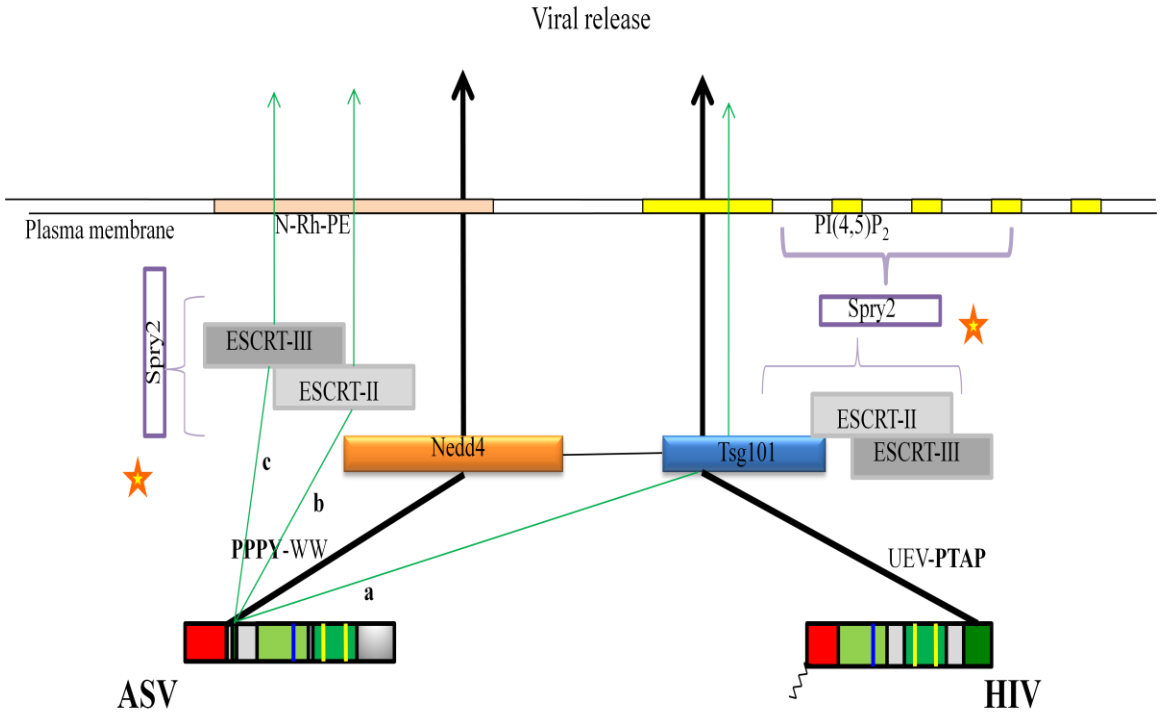
Viral release
Plasma membrane
N-Rh-PE
PI(4,5)P2
Spry2
ESCRT-III
ESCRT-II
Spry2
ESCRT-II
ESCRT-III
Nedd4
Tsg101
c
b
PPPY-WW
a
UEV-PTAP
ASV
HIV

shown that a native isoform of Nedd4-2 that lacks most of the C2 domain largely corrected HIV-1 release defects upon overexpression (130). This suggests that Nedd4 E3 ubiquitin ligases in addition to participate in the release of ASV-Gag, it also facilitates budding of HIV-1 Gag but the mechanisms are different. Most likely, Nedd4 is ubiquitinating components of the endocytic pathway. Indeed, it was shown that Nedd4 can ubiquitinate components of the ESCRT-1, specifically Tsg101 and Mvb12 (21) and this seems to be required for efficient VLP release. It is possible that in the case of HIV-1 Gag, Nedd4 is not directly interacting with Gag, and therefore, its function in release is different from the one observed in ASV-Gag whose direct interaction mediated by Nedd4 WW-PPXY association is critical for release. Specifically, Nedd4 has been shown to participate in the mono-ubiquitination of ASV Gag (132) which is required for release; however, the co-translational fusion of ubiquitin to ASV Gag did not prevented the inhibition of VLP release caused by a DN mutant of Nedd4. This indicated that Nedd4 has functions during Gag release in addition to the ubiquitination of Gag.

As observed in the results presented in Chapter 3, the DN mutant of Tsg101 did not prevent release of ASV-Gag, but blocked the separation of single particles. This observation suggested that Nedd4 and Tsg101 association play a crucial role in the formation of single VLPs. This suggestion is supported by the observation that Nedd4 and Tsg101 can bind to an adaptor protein called ALIX(82, 95, 125, 134), an essential protein in the MVB pathway (98) that participates in membrane deformation and/or vesicle formation, as it binds endophilins and the conical lysobisphosphatidic acid, which is abundant in endosomal vesicles (17, 85). Therefore, it is possible that the Nedd4-Tsg101 complex can bring ALIX to budding sites for regulation of fusion events at the

release site to ensure that bud fission occurs before new budding is initiated. Although this suggestion could potentially explain the defects observed in ASV Gag VLPs upon expression of the C-terminal region of Tsg101 (Chapter 3), it cannot explain why ASV Gag VLPs were not sensitive to the depletion of endogenous Tsg101 (Chapter 4). Perhaps, when ASV-Gag binds to Nedd4, the affinity for interacting with Tsg101 is suppressed. Future experiments should explore the affinity of Tsg101 with Nedd4 under certain conditions, specifically when either ASV or HIV-1 Gag is present.

In addition to Nedd4's possible role in recruiting adaptor proteins (e.g., ALIX), we demonstrate that Nedd4 can function in directing the release of ASV-Gag VLPs through specific membrane sites (Chapter 4). Most likely, directing Gag to the plasma membrane depends on the C2 domain in Nedd4, which allows interaction with lipids on the plasma membrane. The results observed in Chapter 4, indicated that ASV-Gag trafficking mediated by ESCRT-I components can re-direct Gag assembly and release to different sites on the plasma membrane. Specifically, we observed that translational fusion of Tsg101 to the C-term of a late domain Gag mutant (Δp2b) restored Gag VLP release. However, it did not restore the release through specific membrane sites that were defined by the lipid marker N-Rh-PE or CD63. This can be explained by the fact that C2 domains, such the one present in Nedd4, interacts with anionic lipids (e.g., phosphatidylethanolamine) on the plasma membrane (114) marking the site of release, while Tsg101 does not have an intrinsic membrane binding domain but can be directed to the plasma membrane by other mechanisms (138). Furthermore, we demonstrate that components of ESCRT-II and ESCRT-III (Eap20 and Chmp4B) translationally fused to the C-terminus of Δp2b-Gag restored the release of ASV-Gag VLPs through pathways

similar to ASV-Gag WT. This revealed a potential for ESCRT-II and ESCRT-III to function in the budding pathways of ASV-Gag. Indeed, the depletion of endogenous levels of Eap20 inhibited VLP release of ASV-Gag (Pincetic unpublished data). Examination of ESCRT-II components and its relation with ASV-Gag release are currently being tested.

The studies presented in Chapter 3 and 4, clearly suggest that even though the functional exchangeable L domains, PTAP and PPPY, enter the endocytic pathways through different mechanisms, they both rely on a functional ESCRT-mediated system to egress from the cell. The hijacked ESCRT machinery usually participates in the downregulation of cellular cargo (e.g., EGFR) through the lysosomal pathway. Therefore, Gag proteins must have a way of preventing degradation in the lysosome and reach the plasma membrane. In order to explore this notion, we investigated the role of Spry2, a protein known to regulate ESCRT-mediated trafficking pathways of the cellular receptor EGFR, in Gag VLP release.

The ability of Spry2 to regulate trafficking pathways mediated by ESCRT proteins was based on the following observations: i) Spry2 can prevent the downregulation of EGFR through the lysosome by blocking the mono-ubiquitination of the receptor (141); ii) Spry2 can prevent the interaction between Hrs and Tsg101 (62), two ESCRT components required for the recruitment of other ESCRT proteins at the endosomal membrane. Based on these findings and our results, we believed that Spry2 participates in Gag release by regulating their trafficking pathways and facilitates the availability of $PI(4,5)P_2$ in the membrane to target Gag to specific membrane domains, allowing efficient VLP release.

Regulation of Gag trafficking pathways seems to be important for determining the choice of viral assembly and release sites. As described in the literature, HIV-1 Gag VLP release is cell type dependent (102); in T cells Gag proteins assemble and exit the cell through the plasma membrane, while in macrophages Gag almost exclusively concentrates on late endosomes/MVBs and progeny virions bud into the lumen of MVBs. The choice of plasma membrane versus endosomal pathway provides the virus with a strategy to avoid the immune system. For example, intracellular assembly may promote viral persistence since intracellular virions in macrophages retain infectivity for an extended period of time and can efficiently transfer the infection to lymphocytes upon contact (120). Thus, understanding the molecular mechanisms that regulate the choice of viral assembly site is very critical for HIV-1 pathogenesis. Therefore, it is possible that HIV-1 can utilize Spry2 to regulate the ESCRT-mediated trafficking pathways and facilitate Gag targeting to the plasma membrane once the immune system weakens. Indeed, it has been reported that high levels of Spry2 are found in macrophages, specifically in placental Hofbauer cells (2) during pregnancy. Based on this studies and the one presented in this thesis, it is tempting to propose a novel involvement of Spry2 in the transmission of HIV-1 from mother to child.

In this thesis, I have explored the different routes that retroviral Gag proteins take in order to reach their cell surface localization and found that their intracellular paths direct their exiting through specific domains on the plasma membrane. Here, we have found alternative trafficking pathways that are utilized by two distinct retroviruses that can functionally exchange their L domains; however, this raises several more questions. Although it has been proposed that ESCRT-complexes are assemble in a sequential

manner when cellular cargo needs to be degraded, we observed that this might not be the case, since it appeared that not all retroviral Gags (HIV versus ASV) required all the components of the ESCRT machinery. In addition, it is not clear how the different Nedd4 E3 ligases are participating in directing Gag release of HIV-1 and ASV-Gag. The different requirements might rely on the intrinsic membrane binding domain that is present in HIV-1 Gag, which is absent on ASV-Gag. Further studies should address these differences. Understanding the different trafficking pathways taken by different retroviruses and identifying mechanisms that regulate these pathways should provide a new venue for identifying new anti-retroviral therapies against HIV.

REFERENCES

1. **Ames, J. B., Tanaka, T., Stryer, L., Ikura, M.** 1996. Portrait of a myristoyl switch protein. Curr. Opin. Struct. Biol. **41:**5776-5787.
2. **Anteby, E. Y., Natanson-Yaron, S., Greenfield, C., Goldman-Wohl, D., Haimov-Kochman, R., Holzer, H., Yagel, S.** 2005. Human Placental Hofbauer cells express Sprouty proteins: a possible modulating mechanism of villous branching. Placenta **26:**476-483.
3. **Babst, M., Katzmann, D.J., Estepa-Sabal, E.J., Meerlo, T., Emr, S.D.** 2002. ESCRT-III: an endososome-associated heterooligomeric protein complex required for MVB sorting. Dev. Cell **3:**271-282.
4. **Babst, M., Katzmann, D.J., Snyder, W.B., Wendland, B., Emr, S.D.** 2002. Endosome-associated complex-ESCRT-II, recruits transport machinery for protein sorting at the multivesicular body Dev. Cell **3:**283-289.
5. **Babst, M., Odorizzi, G., Estepa, E.J., Emr, S.D.** 2000. Tumor susceptibility gene TSG101 and the yeast homolog, Vps23p, both function in late endosomal trafficking. Traffic **1:**242-258.
6. **Babst, M., Sato, T.K., Banta, L. M., Emr, S.D.** 1997. Endosomal transport function in yeast requires a novel AAA-type ATPase, Vps4p. EMBO J **16:**1820-1831.
7. **Babst, M., Wendland, B., Estepa, E.J., Emr, S.D.** 1998. The Vps4p AAA ATPase regulates membrane association of a Vps protein complex required for normal endosome function. EMBO J **17:**2982-2993.

8. **Bieniasz, P. D.** 2006. Late budding and host proteins in enveloped virus release. Virology **344:**55-63.

9. **Bogenhagen, D. F., Shigeru, S., Brown, D.D.** 1980. A control region in the center of 5S RNA gene directs specific initiation of transcription: II. The 3'border of the region. Cell **19:**27-35.

10. **Bouamr, F., Melilo, J.A., Wang, M.Q., Nagashima, K., de Los Santos, M., Rein, A., Goff, S.P.** 2003. PPPYVEPTAP motif is the late domain of human T-cell leukemia virus type 1 Gag mediates its functional interaction with cellular proteins Nedd4 and Tsg101. J Virol **77:**11882-11895.

11. **Braaten, D., Ansari, H., Luban, J.** 1997. The hydrophobic pocket of cyclophilin is the binding site for the human immunodeficiency virus type 1 Gag polyprotein. J Virol **71:**2107-2113.

12. **Burniston, M. T., Cimarelli, A., Colgan, J., Curtis, S.P., Luban, J.** 1999. Human immunodeficiency virus type 1 Gag polyprotein multimerization requires the nucleocapsid domain and RNA and is promoted by the capsid-dimer interface and the basic region of matrix protein. J Virol **73:**8527-8540.

13. **Cabrita, M. A., Christofori, G.** 2003. Sprouty proteins: antagonists of endothelial cell signaling and more. Thromb Haemost **90:**586-590.

14. **Cabrita, M. A., Jaggi, F., Widjaja, S.P., Chistofori, G.** 2006. A functional interaction between sprouty proteins and caveolin-1. J Biol. Chem **281:**29201-29212.

15. **Carlton, J. G., Martin-Serrano, J.** 2007. Parallels between cytokinesis and retroviral budding: a role for the ESCRT machinery. Science **316:**1908.

16. **Chandramouli, S., Yu, C.Y., Yusoff, P., Lao, D.H., Leong, H.F., Mizuno, K., Guy, G.R.** 2008. Tesk interacts with Spry2 to abrogate its inhibition of ERK phosphorylation downstream of receptor tyrosine kinase signaling. J Biol. Chem **283:**1679-1691.

17. **Chatellard-Causse, C., Blot, C., Torch, C.S., Missotten, M., Sadoul, R.** 2002. Alix (ALG-2 interacting protein X), a protein involved in apoptosis, binds to endophilins and induces cytoplasmic vascuolization. J Biol. Chem **277:**29108-29115.

18. **Chen, C., Li, F., Montelaro, R.C.** 2001. Functional roles of equine infectious anemia virus Gag p9 in viral budding and infection. J Virol **75:**9762-9770.

19. **Christofori, G.** 2003. Split personalities: the agonistic antagonist Sprouty. Nat. Cell Biol. **5:**377-379.

20. **Chukkapalli, V., Hogue, I.B., Boyko, V., Hu, W.S., Ono, A.** 2008. Interaction between the human immunodeficiency virus type 1 Gag matrix domain and phosphatidylinositol-(4,5)-bisphosphate is essential for efficient gag membrane binding. J Virol **82:**2405-2417.

21. **Chung, H. Y., Morita, E., von Schwedler, U., Muller, B., Krausslich, H.G., Sunquist, W.I.** 2008. Nedd4L overexpression rescues the release and infectivity of human immunodeficiency virus type 1 constructs lacking PTAP and YPXL late domains. . J Virol **82:**4884-4897.

22. **Cimarelli, A., Sandin, S., Hoglund, S., Luban, J.** 2000. Basic residues in human immunodeficiency virus type 1 nucleocapsid promote virion assembly via interaction with RNA. J Virol **74:**3046-3057.

23. **Coffin, J. M., Hughes, S.H., Varmus, H.E.** 1997. Retroviruses. New York: Cold Spring Harbor Laboratory Press.

24. **Craven, R. C., Harty, R.N., Paragas, J., Palese, P., Will, J.W.** 1999. Late domain function identified in the vesicular stomatitis virus M proteins by use of rhabdovirus-retrovirus chimera. J Virol **73:**3359-3365.

25. **Dalton, A. K., Murray, P.S., Murray, D., Vogt, V.M.** 2005. Biochemical characterization of rous sarcoma virus MA protein interaction with membranes. J Virol **79:**6227-6238.

26. **Demirov, D. G., Ono, A., Orenstein, J.M., Freed, E.O.** 2002. Overexpression of the N-terminal domain of Tsg101 inhibits HIV-1 budding by blocking late domain function. Proc. Natl. Acad. Sci. U.S.A. **99:**955-960.

27. **Dong, X. H., Li. A., Derdowski, L., Ding, A., Brnett, X., Chen, T.R., Peters, T.S., Dermody, E., Woodruff, J., Wang, J., Spearman, P.** 2005. AP-3 directs the intracellular trafficking of HIV-1 Gag and plays a key role in particle assembly. Cell **120:**663-674.

28. **Ebbets-Reed, D., Scarlata, S., Carter, C.A.** 1996. The major homology region of the HIV-1 gag precursor influences membrane affinity. Biochemistry **35:**14268-14275.

29. **Edwin, F., Singh, R., Endersby, R., Baker, S.J., Patel, T.B.** 2006. The tumor suppressor PTEN is necessary for human Sprouty 2-mediated inhibition of cell proliferation. J Biol. Chem **281:**4816-4822.

30. **Ehrlich, L. S., Krausslich, H.G., Wimmer, E., Carter, C.A.** 1990. Expression of Escherichia coli and purification of human immunodeficiency virus type 1 capsid protein (p24). AIDS Res. Hum. Retroviruses **6:**1169-1175.

31. **Feng, G. H., Lih, C.J., Cohen, S.N.** 2000. Tsg101 protein steady-state level is regulated posttranslationally by an evolutionary conserved COOH-terminal sequence. Cancer Res. **60:**1736-1741.

32. **Feng, Y. X., Campbell, S., Harvin, D., Ehresmann, B., Ehresmann, C., Rein, A.** 1999. The human immunodeficiency virus type 1 Gag polyprotein has nucleic acid chaperone activity: possible role in dimerization of genomic RNA and placemement of tRNA on the primer binding site. J Virol **73:**4251-4256.

33. **Fong, C. W., Leong, H.F., Wong, E.S., Lim, J., Yusoff, P., Guy, G.R.** 2003. Tyrosine phosphorylation of Sprouty2 enhances its interaction with c-Cbl and is crucial for its function. J Biol. Chem **278:**33456-33464.

34. **Franke, E. K., Yuan, H.E., Luban, J.** 1994. Specific incorporation of cyclophilin A into HIV-1 virions. Nature **372:**359-362.

35. **Freed, E. O.** 1998. HIV-1 gag proteins: diverse functions in the virus life cycle. Virology **251:**1-15.

36. **Garrus, J. E., von Schwedler, U. K., Pornillos, O. W., Morham, S. G., Zavitz, K. H., Wang, H. E., Wettstein, D. A., Stray, K. M., Cote, M., Rich, R. L., Myskza, D. G., Sunquist, W. I.** 2001. Tsg101 and the vacuolar protein sorting pathways are essential for HIV-1 budding. Cell **107:**55-65.

37. **Gottlinger, H. G., Dorfman, T., Sodroski, J.G., Haseltine, W.A.** 1991. Effects of mutations affecting the p6 gag protein on human immunodeficiency virus particle release. . Proc. Natl. Acad. Sci. U.S.A. **88:**3195-3199.

38. **Grigorov B., D. D., Smagulova F., Pechoux C., Mougel M., Muriaux D., Darlix J.** 2007. Intracellular HIV-1 Gag localization is impaired by mutations in the nucleocapsid zinc fingers. *Retrovirology***:**4:54.

39. **Gruenberg, J., Maxfield, F.** 1995. Membrane transport in the endocytic pathway. Curr. Opin. Cell Biol. **7:**552-563.

40. **Guy, G. R., Wong, E.S., Yusoff, P., Chandramouli, S., Lo, T.L., Lim, J., Fong, C.W.** 2003. Sprouty: how does the branch manager work? J Cell Sci **116:**3061-3068.

41. **Hacohen, N., Kramer, S., Sutherland, D., Hiromi, Y., Krasnow, M.A.** 1998. sprouty encodes a novel antagonist of FGF signaling that patterns apical branching of the Drosophila airways. Cell **92:**253-263.

42. **Haglund, K., Schmidt, M.H., Wong, E.S., Guy, G.R., Dikic, I.** 2005. Sprouty2 acts at the Cbl/CIN85 interface to inhibit growth factor receptor downregulation. Embo Rep **6:**635-641.

43. **Hall, A. B., Jura, N., DaSilva, J., Jang, Y.J., Gong, D., Bar-Sagi, D.** 2003. hSpry2 is targeted to the ubiquitin-dependent proteasome pathway by c-Cbl. Curr. Biol **13:**308-314.

44. **Hammond, G. R., Dove, S.K., Nicol, A., Pinxteren, J.A., Zicha, D., Schiavo, G.** 2006. Elimination of plasma membrane phosphatidylinositol (4,5)-

bisphosphate is required for exocytosis from mast cells. J Cell Sci **119:**2084-2094.

45. **Hanafusa, H., Torii, S., Yasunaga, T., Matsumoto, K., Nishida, E.** 2004. Shp2, and SH2-containing protein-tyrosine phosphatase, positively regulates receptor tyrosine kinase signaling by dephosphorylating and inactivating the inhibitor Sprouty. J Biol. Chem **279:**22992-22995.

46. **Hanafusa, H., Torii, S., Yasunaga, T., Nishida E.** 2002. Sprouty1 and Sprouty2 provide a control mechanism for the Ras/MAPK signaling pathway. Nature **4:**850-858.

47. **Harty, R. N., Brown, M.E., Wang, G., Huibregtse, J., Hayes, F.P.** 2000. A PPxY motif within the VP40 protein of Ebola virus interacts physically and functionally with a ubiquitin ligase: implications for filovirus budding. Proc. Natl. Acad. Sci. U.S.A. **97:**13871-13876.

48. **Harty, R. N., Paragas, J., Sugol, M., Palese, P.** 1999. A proline-rich motif within the matrix protein of vesicular stomatitis virus and rabies virus interacts with WW domains of cellular proteins: implications for viral budding. J Virol **73:**2921-2929.

49. **Heidecker, G., Lloyd, P.A., Fox, K., Nagashima, K., Derse, D.** 2004. Late assembly motifs of human T-cell leukemia virus type 1 and their relative roles in particle release. J Virol **78:**6636-6648.

50. **Hermida-Matsumoto, L., Resh, M.D.** 2000. Localization of human immunodeficiency virus type 1 Gag and Env at the plasma membrane by confocal imaging. J Virol **74:**8670-8679.

51. **Hirano, S., Suzuki, N., Slagsvold, T., Kawasaki, M., Trambaiolo, D., Kato, R., Stenmark, H., Wakatsuki, S.** 2006. Structural basis of ubiquitin recognition by mammalian Eap45 GLUE domain. Nat. Struct. Mol. Biol **13:**1031-1032.

52. **Ho, D. D.** 1997. Dynamics of HIV-1 replication in vivo. J Clin Invest **99:**2565-2567.

53. **Huang, M., Orenstein, J. M., Martin, M.A., Freed, E.O.** 1995. p6 Gag is required for particle production from full-length human immunodeficiency virus type 1 molecular clones expressing protease. J. Virol. **69:**6810-6818.

54. **Hurley, J. H.** 2008. ESCRT complexes and the biogenesis of multivesicular bodies. Curr. Opin. Cell Biol. **20:**4-11.

55. **Impagnatiello, M. A., Weitzer, S., Gannon, G., Compagni, A., Cotten, M., Christofori, G.** 2001. Mammalian sprouty-1 and -2 are membrane-anchored phosphoprotein inhibitors of growth factor signaling in endothelial cells. J Cell Biol. **152:**1087-1098.

56. **Jacks, T., Power, M.D., Masiarz, F.R., Luciw, P.A., Barr, P.J., Vamus, H.E.** 1988. Characterization of ribosomal frameshifting in HIV-1 *gag-pol* expression. Nature **331:**280-283.

57. **Katz, M., Shtiegman, K., Tal-Or, P., Yakir, L., Mosesson, Y., Harari, D., Machluf, Y., Asao, H., Jovin, T., Sugamura, K.,Yarden, Y.** 2002. Ligand-independent degradation of epidermal growth factor receptor involves receptor ubiquitination and Hgs, an adaptor whose ubiquitin-interaction motif targets ubiquitination by Nedd4. Traffic **3:**740-751.

58. **Katzmann, D. J., Babst M., Emr, S.D.** 2001. Ubiquitin-dependent sorting into multivesicular body pathway requires the function of a conserved endosomal protein sorting complex, ESCRT-I. Cell **106:**145-155.

59. **Katzmann, D. J., Stefan, C.J., Babst, M., Emr, S.D.** 2003. Hrs regulates multivesicular body formation via ESCRT recruitment to endosomes. J Cell Biol. **162:**413-423.

60. **Kikonyogo, A., Bouamr, F., Vana, M. L., Xiang, Y., Aiyar, A., Carter, C.A., Leis, J.** 2001. Proteins related to the Nedd4 family of ubiquitin protein ligases interact with the L domain of Rous sarcoma virus and are required for Gag budding from cells. Proc. Natl. Acad. Sci. U.S.A. **98:**11199-11204.

61. **Kim, H. J., Bar-Sagi, D.** 2004. Modulation of signaling by Sprouty: a developing story. Nat. Rev. Mol. Cell. Biol **5:**441-450.

62. **Kim, H. J., Taylor, L.J., Bar-Sagi, D.** 2007. Spatial regulation of EGFR signaling by Sprouty2. Curr. Biol **17:**455-461.

63. **Koonin, E. V. a. A., R.A.** 1997. TSG101 may be the prototype of a class of dominant negative ubiquitin regulators. Nat. Genet. **16:**330-331.

64. **Kostelansky, M. S., Sun, J., Lee, S., Kim, J., Ghirlando, R., Hierro, A., Emr, S.D., Hurley, J.H.** 2006. Structural and functional organization of the ESCRT-I trafficking complex. Cell **125:**113-126.

65. **Langelier, C., von Schwedler, U.K., Fisher, R.D., De Domenico, I., White, P.L., Hill, C.P., Kaplan, J., Ward, D., Sunquist, W.I.** 2006. Human ESCRT-II complex and its role in human immunodeficiency virus type 1 release. J Virol **80:**9465-9480.

66. **Lazert, C., Chazal, N., Briant, L., Gerlier, D., Cortay, JC.** 2008. Refined study of the interaction between HIV-1 p6 late domain and ALIX. Retrovirology **5:**39.

67. **Le Blanc, I., Prevost, M.C., Dokhelar, M.C., Rosenberg, A.R.** 2002. The PPPY motif of human T-cell leukemia virus type 1 Gag protein is required early in the budding process. J Virol **76:**1569-1577.

68. **Lee, C. C., Putnam, A.J., Miranti, C.K., Gustafson, M., Wang L.M., Vande Woude, G.F., Gao, G.F.** 2004. Overexpression of sprouty2 inhibits HGF/SF-mediated cell growth, invasion, migration, and cytokinesis. Oncogene **23:**5193-5202.

69. **Li, F., Chen C., Puffer, B.A., Montelaro, R.C. .** 2002. Functional replacement and positional dependence of homologous and heterologous L domains in equine infectious anemia virus replication. J Virol **76:**1569-1577.

70. **Li, L., Cohen, S.N.** 1996. Tsg101: a novel tumor susceptibility gene isolated by controlled homozygous functional knockout of allelic loci in mammalian cells. Cell **85:**319-329.

71. **Li, L., Liao, J., Ruland, T., Mak, W., Cohen, S.N.** 2001. A TSG101/MDM2 regulatory loop modulates MDM2 degradation and MDM2/p53 feedback control. Proc. Natl. Acad. Sci. U.S.A. **98:**1619-1624.

72. **Lim, J., Wong, E.S., Ong, S.H., Yusoff, P., Low, B.C., Guy, G.R.** 2000. Sprouty proteins are targeted to membrane ruffles upon growth factor receptor tyrosine kinase activation. J Biol. Chem **275:**32837-32845.

73. **Lim, J., Yussoff, P., Wong, E.S., Chandramouli, S., Lao, D.H., Fong, C.W., Guy, G.R.** 2002. The cysteine-rich sprouty translocation domain targets mitogen-

activated protein kinase inhibitory proteins to phosphatidylinositol 4,5-bisphosphate in plasma membranes. Mol Cell Biol **22:**7953-7966.

74. **Liu, P., Rudick, M., Anderson, R.G. W.** 2002. Multiple functions of caveolin-1. J Biol. Chem **277:**41295-41298.

75. **Lu, Q., Hope, L.W., Brasch, M., Reinhard, C., Cohen, S.N.** 2003. TSG101 interaction with HRS mediates endosomal trafficking and receptor down-regulation. Proc. Natl. Acad. Sci. U.S.A. **100:**7626-7631.

76. **Luban, J.** 2007. Cyclophilin A, TRIM5, and resistance to human immunodeficiency virus type 1 infection. J Virol **81:**1054-1061.

77. **Luban, J., Bossolt, K.L., Franke, E.K., Kalpana, G.V., Goff, S.P.** 1993. Human immunodeficiency virus type 1 Gag protein binds to cyclophilins A and B. Cell **73:**1067-1078.

78. **Macias, M. J., Wiesner, S., Sudol, M.** 2002. WW and SH3 domains, two different scaffolds to recognize proline-rich ligands. FEBS Lett **513:**30-37.

79. **Mammano, F., Ohagen, A., Hoglund, S., Gottlinger, H.G.** 1994. Role of the major homology region of human immunodeficiency virus type 1 in virion morphogenesis. J Virol **68:**4927-4936.

80. **Marmor, M. D., Yarden, Y.** 2004. Role of protein ubiquitylation in regulating endocytosis of receptor tyrosine kinases. Oncogene **23:**2057-2070.

81. **Martin-Serrano, J., Bieniasz, P.D.** 2003. A bipartite late-budding domain in human immunodeficiency virus type 1. J Virol **77:**12373-12377.

82. **Martin-Serrano, J., Yarovoy, A., Perez-Caballero, D., Bieniaiz, P.D.** 2003. Divergent retroviral late-budding domains recruit vacuolar protein sorting factors

by using alternative adaptor proteins. Proc. Natl. Acad. Sci. U.S.A. **100:**12414-12419.

83. **Martin-Serrano, J., Zang, T., Bieniasz, P.D.** 2001. HIV-1 and Ebola virus encode small peptide motifs that recruit Tsg101 to sites of particle assembly to facilitate egress. Nat. Med. **7:**1313-1319.

84. **Mason, J. M., Morrison, D.J., Basson, M.A., Licht, J.D.** 2006. Sprouty proteins: multifaceted negative-feedback regulators of receptor tyrosine kinase signaling. Trends Cell Biol. **16:**45-54.

85. **Matsuo, H., Chevallier, J., Mayran, N., Le, B.I., Ferguson, C., Faure, J., Blanc, N. S., Matile, S., Dubochet, J., Sadoul, F., Parton, R.G., Vilbois, F., Gruenberg, J.** 2004. Role of LBPA and Alix in multivesicular liposome formation and endosome organization. Science **303:**531-534.

86. **McCutchan, F. E.** 2006. Global epidemiology of HIV. J Med. Virol **78:**S7-S12.

87. **McDonald, B., Martin-Serrano, J.** 2008. Regulation of Tsg101 expression by the steadiness box: a role of Tsg101 associated ligase. Mol. Biol. Cell **19:**754-763.

88. **Medina, G., Zhang, Y., Tang, Y., Gottwein, E., Vana, M.L., Bouamr, F., Leis, J., Carter, C.** 2005. The functionally exchangeable L domains in RSV and HIV-1 Gag direct particle release through pathways linked by Tsg101. Traffic **6:**880-894.

89. **Miller, M. D., Farnet, C., Bushman, F.D.** 1997. HIV-1 preintegration complexes: studies of organization and composition. J Virol **71:**5382-5390.

90. **Mizuno, E., Kawahata, K., Kato, M., Kitamura, N., Komada, M.** 2003. STAM proteins bind ubiquitinated proteins on the early endosome via the VHS domain and ubiquitin-interactin motif. Mol Biol Cell **14:**3675-3689.

91. **Morita, E., Sandrin, V., Alam, S.L., Eckert, D.M., Gygi, S.P., Sunquist, W.I.** 2007. Identification of human Mvb12 proteins as ESCRT-I subunits that function in HIV budding. Cell Host Microbe **2:**41-53.

92. **Morita, E., Sandrin, V., Chung, H.Y., Morham, S.G., Gygi, S.P., Rodesch, C.K., Sundquist, W.I.** 2007. Human ESCRT and ALIX proteins interact with proteins of the midbody and function in cytokinesis. EMBO J **26:**4215.

93. **Nalefski, E. A., Falke, J.J.** 1996. The C2 domain calcium-binding motif: structural and functional diversity. Protein Sci **5:**2375-2390.

94. **Nguyen, D. H., Hildreth, J.E.** 2000. Evidence for budding of human immunodeficiency virus type 1 selectively from glycolipid-enriched membrane lipid rafts. J Virol **74:**3264-3272.

95. **Nikko, E., Andre, B.** 2007. Split-ubiquitin two hybrid assay to analyze protein-protein interactions at the endosome: application to Saccharomyces cerevisiae Bro1 interacting with ESCRT complexes, the Doa4 ubiquitin hydrolase, and the Rsp5 ubiquitin ligase. Eukaryot cell **6:**1266-1277.

96. **Nonami, A., Taketomi, T., Kimura, A., Saeki, K., Takaki, H., Sanada, T., Taniguchi, K., Harada, M., Kato, R., Yoshimura, A.** 2005. The Sprouty-related protein, Spred-1, localizes in a lipid raft/caveola and inhibits ERK activation in collaboration with caveolin-1. Genes Cells **10:**887-895.

97. **Nydegger, S., Foti, M., Derdowski, A., Spearman, P., Thali, M.** 2003. HIV-1 egress is gated through late endosomal membranes. Traffic **4:**902-910.

98. **Odorizzi, G.** 2006. The multiple personalities of Alix. J Cell Sci **119:**3025-3032.

99. **Oestreich, A. J., Davies, B.A., Payne, J.A., Katzmann, D.J.** 2006. Mvb12 is a novel member of ESCRT-I involved in cargo selection by the multivesicular body pathway. Mol. Biol. Cell **18:**646-657.

100. **Oh, K. B., Stanton, M.J., West, W.W., Todd, G.L., Wagner, K.U.** 2007. Tsg101 is upregulated in a subset of invasive human breast cancers and its targeted overexpression in transgenic mice reveals weak oncogenic properties for mammary cancer initiation. Oncogene **26:**5950-5959.

101. **Ono, A., Ablan, S.D., Lockett, S.J., Nagashima, K., Freed, E.O.** 2004. Phosphatidylinositol (4,5) bisphosphate regulates HIV-1 Gag targeting to the plasma membrane. Proc. Natl. Acad. Sci. U.S.A. **101:**14889-14894.

102. **Ono, A., Freed, E.O.** 2004. Cell-type dependent targeting of human immunodeficiency virus type 1 assembly to the plasma membrane and the multivesicular body. J Virol **78:**1552-1563.

103. **Ono, A., Freed, E.O.** 2005. Role of lipid rafts in virus replication. Adv. Virus Res **64:**311-358.

104. **Parent, L. J., Bennet, R.P., Craven, R.C., Nelle, T.D., Krishna, N.K., Bowzard, J.B., Wilson, C.B., Puffer, B.A., Montelaro, R.C., Wills, J.W.** 1995. Positionally independent and exchangeable late budding functions of the Rous sarcoma virus and human immunodeficiency virus Gag proteins. J Virol **76:**2641-2647.

105. **Perez, M., Craven, R.C., de la Torre, J.C.** 2003. The small RING finger protein Z drives arenavirus budding: implications for antiviral strategies. Proc. Natl. Acad. Sci. U.S.A. **100:**12978-12983.

106. **Pickart, C. M.** 2001. Mechanisms underlying ubiquitination. Annu. Rev. Biochem **70:**503-533.

107. **Pietiainen, V. M., Marjomaki, V., Heino, J., Hyypia, T.** 2005. Viral entry, lipid rafts and caveosomes. Ann Med **37:**394-403.

108. **Pike, L. J., Casey, L.** 1996. Localization and turnover of phosphatidylinositol 4,5-bisphosphate in caveolin-enriched membrane domains. J Biol. Chem **271:**26453-26456.

109. **Ponting, C. P., Cai, Y.D., Bork, P.** 1997. The breast cancer gene product TSG101: a regulator of ubiquitination? J. Mol. Med. **75:**467-469.

110. **Provitera, P., Goff, A., Harenberg, A., Bouamr, F., Carter, C., Scarlata, S.** 2001. Role of the major homology region in assembly of HIV-1 Gag. Biochemistry **40:**5565-5572.

111. **Puffer, B. A., Parent, L., Wills, J.W., Montelaro, R.C.** 1997. Equine infectious anemia virus utilizes a YXXL motif within the late assembly domain of the Gag p9 protein. J Virol **71:**6541-6546.

112. **Quest, A. F., Leyton, L., Parraga, M.** 2004. Caveolins, caveolae, and lipid rafts in cellular transport, signaling, and disease. Biochem. Cell Biol **82:**129-144.

113. **Reeves, J. D., Doms, R.W.** 2002. Human Immunodeficiency virus type 2. J Gen. Virol. **83:**1253-1265.

114. **Rizo, J., Sudhof, T.C.** 1998. C2-domains, structure and function of a universal Ca^{2+} binding domain. J Biol. Chem **273:**15879-15882.

115. **Rubin, C., Litvak, V., Medvedovsky, H., Zwang, Y., Lev, S., Yarden, Y.** 2003. Sprouty fine-tunes EGF signaling through interlinked positive and negative loops. Curr. Biol **13:**297-307.

116. **Saad, J. S., Miller, J., Tai, J., Kim, A., Ghanam, R.H., Summers, M.F.** 2006. Structural basis for targeting HIV-1 Gag proteins to the plasma membrane for virus assembly. Proc. Natl. Acad. Sci. U.S.A. **103:**11364-11369.

117. **Sasaki, A., Taketomi, T., Kato, R., Saeki, K., Nonami, A., Sasaki, M., Kuriyama, M., Saito, N., Shibuya, M., Yoshimura, A.** 2003. Mammalian Sprouty4 suppresses Ras-independent ERK activation by binding to Raf1. Nat **5:**427-432.

118. **Scarlata, S., Carter, C.** 2003. Role of HIV-1 Gag domains in viral assembly. Biochim. Biophys. Acta **1614:**62-72.

119. **Schwarz, S. E., Rosa, J.L., Scheffner, M.** 1998. Characterization of human hect domain family members and their interaction with UbcH5 and UbcH7. J Biol. Chem **273:**12148-12154.

120. **Sharova, N., Swingler, S., Sharkey, M., Stevenson, M.** 2005. Macrophages archive HIV-1 virions for dissemination in *trans*. EMBO J **24:**2481-2489.

121. **Sherer, N. M., Lehmann, M.J., Jimenez-Soto, F.L., Ingmundson, A., Horner, S. M., Cicchetti, G ., Allen, P.G., Pypaert, M., Cunningham, J.M., Mothes, W.** 2003. Visualization of retroviral replication in living cells reveals budding into multivesicular bodies. Traffic **4:**785-801.

122. **Shioda, T., Shibuta, H.** 1990. Production of human immunodeficiency virus (HIV)-like particles from cells infected with recombinant vaccinia viruses carrying the gag gene of HIV. Virology **175:**139-148.

123. **Slagsvold, T., Aasland, R., Hirano, S., Bache, K.G., Raiborg, C.** 2005. Eap45 in mammalian ESCRT-II binds ubiquitin via a phosphoinositide-interacting GLUE domain. J Biol. Chem **280:**19600-19606.

124. **Staub, O., Yeger, H., Plant P.J., Kim, H., Ernst, S,A., Rotin, D.** 1997. Immunocolocalization of the ubiquitin-protein ligase Nedd4 in tissues expressing the epithelial Na^+ channel (ENaC). Am. J. Physiol **272:**1871-1880.

125. **Strack, B., Calistri, A., Craig, S., Popova, E., Gottlinger H.G.** 2003. AIP1/ALIX is a binding partner for HIV-1 p6 and EIAV p9 functioning in virus budding. Cell **114:**689-699.

126. **Sudol, M., Recinos, C., Abraczinskas, J., Humbert, J., Farooq, A.** 2005. WW or WoW: The WW domains in a union of bliss. IUBMB Life **57:**773-778.

127. **Sun , Z., Pan, J., Hope, X., Cohen, S.N., Balk, S.P.** 1999. Tumor susceptibility gene 101 protein represses androgen receptor transactivation and interacts with p300. Cancer **86:**689-696.

128. **Swanstrom, R., Will, J.W.** 1997. Synthesis, assembly, and processing of viral proteins. In: Coffin, JM, Hughes SH, Varmus, HE, editors. Retroviruses. New York: Cold Spring Harbor Laboratory Press**:**pp. 263-334.

129. **Thali, M., Bukovsky, A., Kondo, E., Rosenwirth, B., Walsh, C.T., Sodroski, J., Gottlinger, H.G.** 1994. Functional association of cyclophilin A with HIV-1 virions. Nature **372:**363-365.

130. **Usami, Y., Popov, S., Popova, E., Gottlinger, H.G.** 2008. Efficient and specif rescue of human immunodeficiency virus type 1 budding defects by a Nedd4-like ubiquitin ligase. J Virol **82:**4898-4907.

131. **van Rheenen, J., Song, X., van Roosmalen, W., Cammer, M., Chen, X., DesMarais, V., Yip, S.-C., Backer, J. M., Eddy, R. J. & Condeelis, J. S.** 2007. EGF-induced PIP2 hydrolysis releases and activates cofilin locally in carcinoma cells. J Cell Biol. **179:**1247-1259.

132. **Vana, M. L., Tang, Y., Chen, A., Medina, G., Carter, C., Leis, J.** 2004. Role of Nedd4 and ubiquitination of Rous sarcoma virus Gag in budding of virus-like particle from cells. J Virol **78:**13943-13953.

133. **VerPlank, L., Bouamr, F., La Grassa, T. J., Agresta, B., Kikonyogo, A, Leis, J., Carter, C.A** 2001. Tsg101, a homologue of ubiquitin-conjugating (E2) enzymes binds the L domain in HIV type 1 Pr55Gag. Proc. Natl. Acad. Sci. U.S.A. **98:**7724-7729.

134. **von Schwedler, U. K., Stuchell, M., Muller, B., Ward, D.M., Chung, H.Y., Morita, E., Wang, H.E., Davis, T., He, GP., Cimbora, D.N., Scott, A., Krausslich, H.G., Kaplan, J., Morham, S.G., Sunquist, W.I.** 2003. The protein network of HIV budding. Cell **114:**701-713.

135. **Wang, H., Machesky, N.J., Mansky, L.M.** 2004. Both the PPPY and PTAP motifs are involved in human T-cell leukemia virus type 1 particle release. J Virol **78:**1503-1512.

136. **Wang, H., Norris, K.M., Mansky, L.M.** 2002. Analysis of bovine leukemia virus gag membrane targeting and late domain function. J Virol **76:**8485-8493.

137. **Wang, S. W., Noonan, K., Aldovini, A.** 2004. Nucleocapsid-RNA interactions are essential to structural stability but not to assembly of retroviruses. J Virol **78:**716-723.

138. **Welsch, S., Habermann, A., Jager, S., Muller, B., Krijnse-Locker, J., Krausslich, HG.** 2006. Ultrastructural analysis of ESCRT proteins suggests a role of endosome-associated tubular-vesicular membranes in ESCRT function. Traffic **7:**1551-1566.

139. **Wills, J., Craven, R.C.** 1991. Form, function and use of retroviral Gag proteins. AIDS **5:**639-654.

140. **Wills, J. W., Cameron, C.E., Wilson, Y., Xiang, R., Bennet, R.P., Leis, J.** 1994. An assembly domain of the Rous sarcoma virus Gag protein required late in budding. . J. Virol **68:**6605-6618.

141. **Wong, E. S., Lim, J., Low, B.C., Chen, Q., Guy, G.R.** 2001. Evidence for direct interaction between Sprouty and Cbl. J Biol. Chem **276:**5866-5875.

142. **Xiang, Y., Cameron, C.E., Wills, J.W., Leis, J.** 1996. Fine mapping and characterization of the Rous sarcoma virus $Pr76^{gag}$ late assembly domain J. Virol **70:**5695-5700.

143. **Xie, W., Li, L., Cohen, S.N.** 1998. Cell cycle-dependent subcellular localization of the TSG101 protein and mitotic and nuclear abnormalities associated with Tsg101 deficiency. Proc. Natl. Acad. Sci. U.S.A. **95:**1595-1600.

144. **Yasuda, J., Hunter, E.** 1998. A proline rich motif (PPPY) in the Gag polyprotein of Mason-Pfizer monkey virus plays a maturation -independent role in virion release. J Virol **72:**4095-4103.

145. **Yuan, B., Campbell, S., Bacharach, E., Rein, A. Goff, S.P.** 2000. Infectivity of Moloney murine leukemia virus defective in late assembly events is restored by late assembly domains of other retroviruses. J Virol **74:**7250-7260.

146. **Yuan, B., Li, X., Goff, S.P.** 1999. Mutations altering the moloney murine leukemia virus p12 Gag protein affect virion production and early events of the virus life cycle. EMBO J **18:**4700-4710.

147. **Zhou, W., Resh, M.D.** 1996. Differential membrane binding of the human immunodeficiency virus type 1 matrix protein. J Virol. **70:**8540-8548.